ASSESSMENT OF THE IMPACT OF URBAN DEVELOPMENT ON FLOOD PEAKS IN THE ACACIA SUBURB, AREBBUSCH SUB-CATCHMENT WINDHOEK, NAMIBIA

A MINI THESIS SUBMITTED IN PARTIAL FULFILMENT

OF THE REQUIREMENTS FOR THE DEGREE OF

MASTER OF SCIENCE IN CIVIL ENGINEERING

OF

THE UNIVERSITY OF NAMIBIA

BY

DIRK JONES COETZEE

201046342

JULY, 2019

Main Supervisor: Dr Joachim. W. Lengricht

Co-Supervisor: Martin Hipondoka (PhD)

DECLARATION

I, **DIRK JONES COETZEE**, hereby declare that this study is my own work and is a true reflection of my research, and that this work, or any part thereof has not been submitted for a degree at any other University.

Date: _____

Signature: _____

The findings, interpretations and conclusions expressed in this study do neither reflect the views of the University of Namibia, Department of Civil Engineering nor of the individual members of the MSc Examination Committee, nor of their respective employers.

TABLE OF CONTENTS

LIST OF TABLES

LIST OF FIGURES

LIST OF ABBREVIATIONS

ALOS……Advanced Land Observing Satellite

ArcGIS…….Arc-Geographic Information System

ARF……..…….....Area Reduction Factor

ARM…….....Alternative Rational Method

CAD……..……....Computer Aided Drawing

COW……...…….....…….…..City Of Windhoek

DEM……...…...……..…Digital Elevation Model

FRACTAL…….……Future Resilience For African Cities And Lands

GPS…….……Global Positioning System

HEC-RAS…...…Hydrological Engineering Centre-River Analysis System

MAP……...…….Mean Annual Precipitation

MAWF…….……Ministry of Agriculture, Water and Forestry

RGB…….....…...….....Red, Green and Blue

SANRAL……South Africa National Roads Agency

SF……...……....Steady Flow

SRM…….Standard Rational Method

USF…….……...…Unsteady Flow

UTM…….……...….Universal Transverse Mercator

DEDICATION

This thesis is dedicated to my family, for their endless love and support. My parents, Herald and Elizabeth Coetzee, my two sisters Lizelle and Daphne Coetzee and my brother Lee-Roy Coetzee. I would also like to give a special dedication to my girlfriend and soon to be wife Charlotte Romeinchia Kisting for the love and motivation she gave me throughout the years as well as my Ray-Of-Sunshine daughter Alquecia Ruwada Feris.

ACKNOWLEDGEMENTS

Although the research was an individual work, it could never have been accomplished without the assistance, support, and efforts of some selfless people.

Firstly, I would like to thank Prof SJ van Vuuren for lecturing us in our first year of the master's program. Prof van Vuuren gave us new insights and perspectives not only limited to the scope of study but in general life teachings. Secondly, I would like to thank Dr Martin Hipondoka for introducing us to the topic of GIS and remote sensing, availing to us the true potential and power of this technology with regards to civil-water applications and analysis. I would also like to thank Dr Martin for assisting me with the thesis as my supervisor. I would also like to thank my main supervisor and Head of Department, Dr Joachim Lengricht for all the assistance with regards to writing letters to ask for data from the required institutions as well as his timeless support for my quest to become a civil engineer from my undergraduate years straight through the master's program; I am truly thankful. My gratitude also goes out to, Prof Frank PL Kavishe for his support throughout the master's program, Prof Kavishe treated us as his own children throughout the master's program and I'm truly grateful for the time and effort he spent on us.

I would also like to thank Mr Nicholas Walker from Aurecon Consulting engineers, Ms Silvia Leiriao from DHI consultants, Ms Vatera from MET services and Mr Samuel Kangootui from Ministry of Agriculture, Water and Forestry (MAWF) for granting me access to their research and consulting findings; as well as data required to carry out this research.

Special thanks to my friends, Mukendoyi Mutelo and Oriri Rukoro who persevered with me.

Lastly, I would like to thank our all mighty Father in heaven for all his grace, love and protection through these 4 years doing the master's programme.

ABSTRACT

Climate change is affecting global weather patterns, more so by exacerbating the sporadic nature of Namibia's rainfall patterns. This has negative consequences on urbanization as increased rainfall in certain rainy seasons coupled with increased urban development could lead to dangerous flooding in low-lying areas, as was the case with Acacia residential, Windhoek, in 2004. Increased urban development has the potential to increase runoff and flood peaks by 20% to 50% of those under natural conditions. This study investigated the urban development in the greater Arebbusch catchment, and its impact on the Acacia suburb. Employed methods and techniques comprised remote sensing, GIS, SANRAL Drainage manual and hydraulic modelling software (HEC-RAS). Landsat and Sentinel images were used to produce and determine land cover changes in the study area between 1989 and 2018, respectively. Furthermore, computer models of the Acacia River section, the steady and unsteady flow simulations and flood inundation area were carried out in the Acacia residential area and compared with the existing, regulatory 1:50-year flood line that the City of Windhoek uses as reference for urban development. Results indicate that the flood peaks in the study area increased by 13% over the past 30 years. This suggests that urban development influenced flood peaks in the study area, whilst the 1:50-year flood line remains static. It is therefore recommended that more assessment be done on the hydraulic flow of all constructions in close proximity to the 1:50-year flood line, whilst taking into greater consideration the accumulative effects of urban development on urban flood peaks.

Key words: Urban development, SANRAL, City of Windhoek, flood peaks, remote sensing.

1. INTRODUCTION

This chapter serves as an overview of the problem addressed in the study. It gives the background information, statement of the problem, objectives, hypothesis, significance and scope of the study.

1.1 Background of the study

Over the past century, extensive research has been carried out across the globe; to ascertain the causal relationship between urban development and rainfall runoff [1]. It has widely been established that urban development has the potential to substantially increase surface runoff and subsequently increase peak discharges in watercourses [2][3]. This realization has thus led to continuous research in the field, so as to apply the same principle to different geographical locations. Since Namibia gained its independence in 1990 urban development has increased sharply in the capital city, Windhoek; as more people flock to the capital for job opportunities they place immense pressure on its infrastructure capacity [4].

Acacia is a residential area in Windhoek's Dorado Park suburb, with an estimated coverage and number of households of 9 ha and 250 units, respectively. Acacia has been affected by floods since its early development in 2003, with recorded flooding in 2004, 2006 and 2009. According to Dentlinger [5], the final conclusion with regards to the nature of the floods, was that neither the Municipality nor the contractor was at fault and that it was a combination of various factors [5]. These include but are not limited to: extreme downpour intensity, antecedent soil moisture, storm-water canals constructed too narrow resulting in a bottleneck effect, building rubble dumping upstream resulting in a decrease

in river cross section [5].

Land-use changes have the potential to increase the size of flood peaks by 20% to 50% of those under natural conditions [2][3]. Therefore, this study was undertaken to assess the extent at which urban development in Windhoek may have affected rainfall runoff/ flood peaks in the Acacia sub-catchment and in return, how runoff/ flood peaks influenced the 1:50-year flood line for the residents living on the Acacia River banks.

1.2 Problem statement

Land use influences flood peaks by modifying how rainfall is stored on and run-off the surrounding area, i.e. construction of roads, buildings and other infrastructure remove vegetation and open soil areas by replacing them with impermeable surfaces that accelerate the rate of runoff thus increasing the peak discharges in the river courses [6]. This increase in built up areas coupled with man made changes to the natural river courses can lead to serious flash floods in low-lying areas as was the case in Acacia. The 1:100-year flood line was used prior to independence as the regulatory line above which development can take place but has since been changed to the 1:50-year flood line [5]. In addition, the re-adjustment to the 1:50-year flood line has not catered for the increased urban development that we see in the capital today. These two factors have the potential implications on the flood risk that may threaten residents of Acacia.

Hence, this study seeks to utilize computer-based models produced in HEC-RAS and ArcGIS, with input data like rainfall, soil moisture, river channel geometry and river roughness to ascertain the extent of which urban development in the Acacia sub-catchment/watershed has increased the peak discharges in the Arebbusch River.

1.3 Aim and objectives

The primary aim of this study is to ascertain the extent at which urban development has amplified flood peaks in the Acacia sub-catchment.

The specific objectives are to:

1. Utilize ArcGIS and the SANRAL and Namibian Drainage manuals as tools in characterizing the flood peaks for the two comparative years (land-use cover differential years).
2. Produce a model of the river course in HEC-RAS.
3. Produce a flow simulation in HEC-RAS using the obtained flood peaks.
4. Establish the 1-50-year flood line under current flow regime and relate it to the one employed in guiding the development of Acacia as a suburb.

1.4 Hypotheses

The study seeks to compare the peak discharge produced from the accumulation of rainfall runoff in the Acacia sub-catchment, from two years namely 1989 and 2018 where there is a clear distinction in urban development; so as to ascertain the effects of urban development on urban flood peaks.

Null Hypothesis (H_0): There is no significant difference in the flood peaks produced from the 2 varying urban developed catchments; 1989 vs. 2018 (95% confidence level).

Alternative Hypothesis (H_1): There is significant difference in the flood peaks produced from the 2 varying urban developed catchments; 1989 vs. 2018 (5% significance level).

1.5 Significance of the study

The study contributes to our understanding with regards to hydraulics and hydrology, in terms of the relationship between urban development and rainfall runoff in urban areas. The study also has various significance for the City of Windhoek (COW) Municipality as the results may assist in decision making as well as future developments around the river courses, such as with the newly proposed Windhoek River walk Project.

1.6 Limitations of the study

Owing to the lack of freely available satellite images in the 1980's, the Landsat images used was limited to a spatial resolution of 30 m. Spot data with relatively higher spatial resolutions, are commercially available for the 1980's, but financial constraints limited the study to free Landsat and Sentinel data, the latter with a spatial resolution ranging between 10 to 20 m. This limitation has the potential to slightly distort some of the findings

as higher resolution data sets would have been ideal.

1.7 Delimitations of the study

Only a section of the Arebbusch River was taken into consideration due to financial and time constraints. This section flows around the eastern side of Acacia, roughly 500 m on both sides of the Acacia bridge; resulting in a 1 km stretch of river that was taken into consideration. River cross sections were also minimized to 100 m. The study was further limited to the Acacia suburb as this is the chosen study area. No other modelling software except for HEC-RAS and ArcGIS was used in the study.

2. LITERATURE REVIEW

The following chapter serves as an overview of the various terminologies, definitions, findings, assumptions and conclusions produced around the world to better the understanding of rainfall run-off and its critical relationship with urban development.

2.1 Overview of urban drainage terminology

Surface runoff (Rainfall runoff/ overland flow) can be described as the flow of water that flows over the ground surface due to the fact that the ground is either fully saturated meaning no more infiltration can take place, or flow over impervious areas (pavements, roofs and gutters). This runoff that is generated within a catchment through precipitation has the potential to cause flash flooding in urban areas [2][3].

Floods can be described as the river discharge that has the kinematic energy to cause damage to urban structures in low lying areas (areas closer to the river and in compromised flood zones). From an ecological point of view, floods form part of the natural river process and the lack of this natural flooding due to urban development has various negative effects on the ecology of the flora and fauna in the water course [7]. Flooding events can be separated into 3 main categories, these are: 1. Coastal floods; 2. fluvial floods and 3. Pluvial floods. The most common are the fluvial floods occurring when rivers flood their banks, but the floods most important to urban developers are that of pluvial floods flooding urban areas. They are difficult to properly predict stemming from their smaller temporal and spatial scale when compared to fluvial floods [2][3][8].

Flood hydrograph is a graphical representation of the flood peak as it travels in a wave like motion through the river course from the time of commencement of the flood until the discharge returns to normal below given flood line levels. The flood hydrograph is characterized by 3 points mainly its peak, shape and volume [1][2][3].

Floodplain can be described as the area of land adjacent to the river that has the potential to be inundated by water, should a large enough flood peak be produced from rainfall runoff. In urban areas floodplains have often become prime real-estate sites for industrial, residential and informal settlements [9]. It should be noted though that all development on a floodplain is vulnerable to flood damage as larger return period floods like 1:100 and 1:150 are more likely to prevail with climate change spearing the shift in global climate patterns as the recent El Nino and La Nino effects have proven [8].

Probabilities in hydrological analysis often only take into consideration the largest peak discharge in each hydrological year, resulting in the forbearance of other flood peaks during the year that are not larger than the largest peak; even if these peaks might have been larger than other maxima recorded for other years [1][2][3]. This means that if records were kept for 50 years then 50 annual maxima would have been identified and used in the analysis. The results of the analysis are expressed as the relationship between the peak discharge at a given location and the probability that this discharge will be exceeded in any one year [1][2][3]. This is referred to as the Annual Exceedance Probability (AEP) and is written as 1:20 years, 1:100 years, etc. This means that the calculated peak discharge has a 5% and 1% probability of being exceeded in any one year for the aforementioned examples of the 1:20 and 1:100-year floods, respectively [1][2][3].

Risk of failure of a structure exposed to floods differs from exceedance probability of a flood, as the former is a function of the structure's resistance to failure and its design characteristics [1][2][3][10]. Consequently, the risk of failure of a structure is due primarily to the design flood which is always less than the exceedance probability of the design flood [2][3].

Flood lines are used to control development on floodplains or river banks and Acacia has been constructed between the 1:50-year and 1:100-year floodplain as was indicated in section 1.2. They are contour lines on a map showing the water levels likely to be reached by a flood having a specified exceedance probability [11].

2.2 Rainfall runoff

According to SANRAL [2] the potential floods damage to urban structures can be related to the following parameters:

- High flood level (HFL) – the maximum water level reached at a given point during the flood.
- Peak discharge (Q_p) – the maximum flow rate during the flood.
- Maximum flow velocity (V_{max}) – the maximum calculated flow velocity associated with a given flow rate.
- Flood volume – the volume of the water that is released from the catchment, responding to a given storm event and the catchment characteristics.
- Flood duration – the period of time during which the discharge does not drop below a given limit.

- Time of concentration (T_c) – is the measure of the catchment response time. This is the time it takes for the surface runoff from the catchments hydraulically most distant part, to reach the main water course of the catchment.
- PMF – is the Probable Maximum Flood with a return period of about 10 000 years for which the possibility of occurrence in any one year is very low or unlikely.
- RMF – is the Regional Maximum Flood which is the expected highest recorded flood in a specified region, based on a procedure developed by Francou-Roudier and calibrated for Namibia by Zoltan Kovacs [1][2][3][12].

From the various parameters listed above it should be noted that peak discharge is by far the most important parameter in estimating the required cross-sectional area that can accommodate a specified flood event as well as determining the backwater effect of structures that cause blockage in the line of flow [2][3]. Peak discharge is directly proportional to the characteristics of the storm event as well as the catchment area. Once the peak discharge has been calculated, the high-flood level (flood line) and associated flow velocities can be determined by means of hydraulic calculations. Flood volume and temporal variance of flow rate can be derived from a hydrograph. An example taken from SANRAL can be seen below.

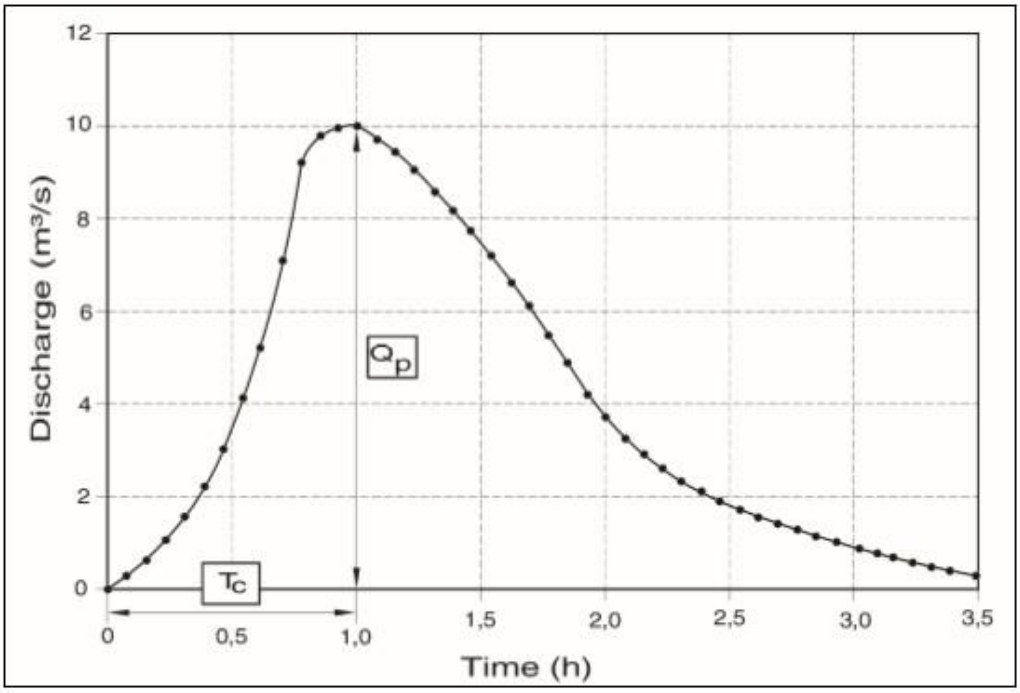

Figure 2-1 Example of flood hydrograph (Source: [2])

2.3 Factors affecting runoff

It is essential in flood hydrology to firstly understand how various environmental factors affect rainfall run-off in a catchment; before any hydrological calculations are undertaken.

There are 4 main factors that influence rainfall-runoff ([1][2][3][7][8]):

1. Physiographic factors (Area of the catchment, Catchment shape and slope, Stream patterns, Infiltration, Soil type and geology, Seasonal effects of vegetation);
2. Antecedent soil moisture conditions (Temporal storage);
3. Urban developmental influences (Land use/urbanization); and
4. Climatological variables (Climate, Rainfall, Time and area distribution of rain storms)

Each of the aforementioned factors can be further elaborated on in detail, but only the points specific to this research are discussed further as follows.

Physiographic factors:

- Area of the catchment: affects the rainfall/runoff relationship of the storm event and subsequently defines the suitability of the calculation method chosen. In larger catchments the determining relationship is that of quantity of rainfall vs. water storage capacity of the ground; while in smaller catchments its more focused on the rainfall intensity vs. the infiltration rate [2][3].
- Catchment shape and slope: The specific shape of the catchment affects its subsequent flood discharge. This phenomenon is proven when 2 catchments of the same size, but having differing shapes; produce different peak discharges as is indicated in Figure 2-2. This is attributed to the time of concentration; a circular catchment takes less time for concentration compared to an elongated catchment.

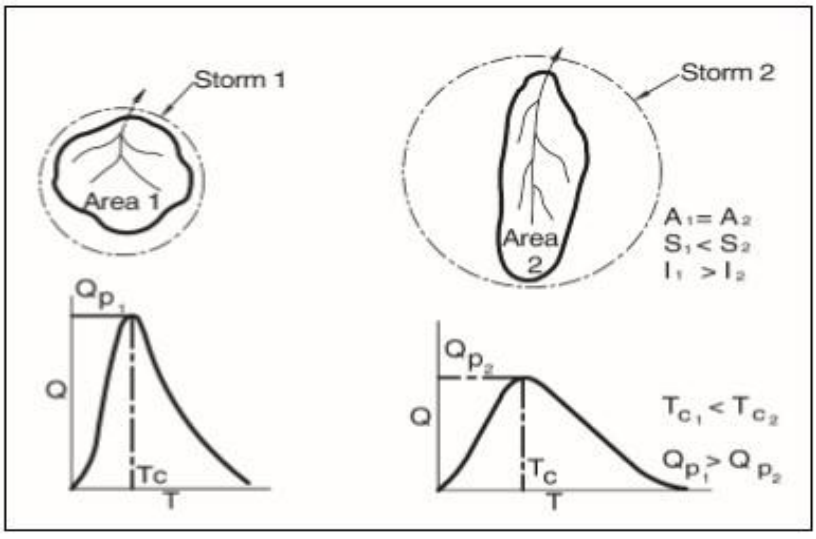

Figure 2-2: Same-sized catchments producing different peak flows (Source: [2])

- Slope of the catchment: The catchment slope is related to the velocity of the surface runoff produced during a storm event and is used in the determination of the rainfall runoff coefficients. Catchments having steep slopes have less vegetation coverage, soil layers are shallower and there are fewer depressions for rainfall to collect. This results in rainfall to runoff more rapidly, reducing infiltration and time taken to reach the main river stream and subsequently leading to higher flood peaks [2][3].
- Infiltration rate of the catchment: The catchment soils infiltration rate affects the flood discharge by determining how much overland flow occurs. It is the measure of the rate at which soil is able to absorb the rainfall. The rate decrease as the soil becomes saturated; if the rainfall rate exceeds the infiltration rate runoff will be observed [2][3].

Urban developmental factors:

- Land use: Urbanization, which is the conversion of other types of land to uses associated with the growth of population and economy, is a significant land-use and land-cover change especially in recent human history [8]. This might be the most important factor affecting rainfall runoff and subsequent flood peaks in urban areas as was mentioned briefly in section 1.1. The effect of urbanization on rainfall runoff is related to the amount of surface area that is made impermeable by the introduction of urban roofs, parking lots, roads and pavements. This is further coupled with storm water systems which transport surface runoff to the river streams at an increased rate. This phenomenon can be observed in the figure below, indicating the influence of urban development on peak discharge as a function of the impermeable surface area, return period and percentage area having storm water

drainage in the catchment [2][3][13][14].

Table 2-1: Impermeable urban area %, influence on peak flow (Source: *[2]*)

Return period (years)	Percentage area consisting of man-made impermeable surfaces				
	1	10	25	50	80
2	1,0	1,8	2,2	2,6	3,0
5	1,0	1,6	2,0	2,4	2,6
10	1,0	1,6	1,9	2,2	2,4
25	1,0	1,5	1,8	2,0	2,2
50	1,0	1,4	1,7	1,9	2,0
100	1,0	1,4	1,6	1,7	1,8

Table 2-2: Impermeable urban area % with drainage, influence on peak flow

(Source: *[2]*)

Percentage area with storm water drainage	Percentage of impermeable surface area					
	0	20	40	60	80	100
0	1,0	1,3	1,5	1,8	2,0	2,4
20	1,3	1,5	2,1	2,5	2,9	3,7
40	1,4	2,1	2,5	2,9	3,7	4,7
60	1,5	2,2	2,8	3,6	4,5	5,5
80	1,6	2,3	3,0	4,2	5,0	6,2
100	1,7	2,4	3,2	4,4	5,6	6,8

It should be noted though that this effect of urbanization varies according to the size of the flood; as the flood size increases and its recurrence interval increases, the subsequent effect of urbanization decreases [15].

Climatological variables:

- Climate: Climate plays an important role on the factors that influence runoff. Vegetation and soil formation are directly related to rainfall and temperature.

Generally speaking, wetter parts of the country experience higher rainfall intensities, which subsequently mean these areas have wetter antecedent soil moisture conditions leading to higher run-off from storm events [2][3].

- Time and area distribution of storm events: During an interview conducted on the 16th of March 2018, Mr C. Van Der Merwe who acts as the section engineer of planning and design at the COW municipality; pointed out that rainfall runoff is quite complex to pin down to a few factors and should rather be described as a combination of various factors working in tandem and resulting in the so called "perfect storm" [16]. This perfect storm he concluded was the cause to the 2004 Acacia flooding which he attributed to heavy rain pour moving from the South of Windhoek over the city to the North and then back down South again, indicating that the soil was wetted in the first distribution of rainfall and then when the rain pour moved back South the overflow rate was almost 100%. This phenomena coincides with prominent factors identified by SANRAL that affect the runoff in a catchment, which includes duration of the storm event, magnitude, uniformity, velocity and direction of the storm passing over the catchment [2][3]. The differences in area and time distribution of rainfall depend in turn on the type of rain i.e. orographic, convection, frontal or cyclonic rainfall. Namibia receives mostly convection rainfall that occurs in the form of thunderstorms and tends to be extremely uneven and unpredictable [4][17][18][19].

2.4 Flood peak calculation methods

Various methods have been developed across the globe as urban drainage and road drainage are very important civil design aspects that need to be taken into consideration for the safe utilization by the public. The methods are based mainly on 3 sectors:

1. Measured physical basis
2. Deterministic basis
3. Empirical basis

The most used methods in Southern Africa has been identified by SANRAL as:

- Statistical methods
- Rational method
- Alternative Rational method
- Unit hydrograph method
- Standard Design Flood (SDF) method
- Empirical method

Table 2-3 indicates the various methods and their application limitations in terms of recommended maximum catchment area, input data required and flood return period determination.

Table 2-3: Application summary of flood calculation methods (Source: *[3]*)

Method	Input data	Recommended maximum area (km²)	Return period of floods that could be determined (years)	Reference paragraph
Statistical method	Historical flood peak records	No limitation (larger areas)	2 – 200 (depending on the record length)	3.4
Rational method	Catchment area, watercourse length, average slope, catchment characteristics, rainfall intensity	< 15	2 – 100, PMF	3.5.1
Alternative Rational method		No limitation	2 – 200, PMF	3.5.2
Synthetic Hydrograph method	Catchment area, watercourse length, length to catchment centroid (centre), mean annual rainfall, veld type and synthetic regional unit hydrographs	15 to 5000	2 – 100	3.5.3
Standard Design Flood method	Catchment area, slope and SDF basin number	No limitation	2 – 200	3.5.4
Empirical methods	Catchment area, watercourse length, distance to catchment centroid, mean annual rainfall	No limitation (larger areas)	10 – 100, RMF	3.6

Statistical methods involve the use of historical data to determine a flood with a given return period. Utilization of this method is limited to catchments that have extensive flood records or have records from nearby catchments that have comparable traits. Statistical methods are quite useful in determining flood peaks with long return periods, provided that they have accurate records covering long periods of recorded data [2][3].

Rational method is based on a simplified representation of the law of conservation of mass. Runoff coefficients of various surfaces, rainfall intensity and catchment area are the three main factors influencing the calculation of the peak discharge via the rational method. The method is usually only utilized in catchments that are smaller than 15 km^2 due to the fact that uniform aerial and time distributions of rainfall have to be assumed for this method [2][3].

Alternative Rational method can be described as having a slight modification to the standard rational method, in that the rational method makes use of the depth-duration frequency diagram to determine point rainfall; while the alternative rational method uses the modified recalibrated Hershfield equation as proposed by Alexander for storm durations lasting up to 6 hours. Furthermore, it makes use of the South African Department of Water Affairs technical report TR102 for durations lasting more than 1 day up to 7days [1][2][3][19].

Unit Hydrograph method is based primarily on regional analysis of historical data resulting in reliable results in the determination of flood peaks as well as hydrographs in medium rural catchments (15-5000km^2); albeit some natural variability in the specified catchments hydrological properties can be lost due to broad generalizations of averaged hydrographs, this is true with catchments smaller than 100km^2 [1][2][3].

Standard Design Flood (SDF) method was developed by Alexander. The method provides a uniform approach to flood calculations in that it is based on a calibrated discharge coefficient for recurrence periods of 2 to 100 years. Calibrated discharge parameters are based on historical data which are determined for various basins in Namibia and South Africa [2][3][20].

Empirical methods make use of a combination of historical data, results of other methods and prior experience. These methods are therefore more suited for cross referencing the order of magnitude of the results obtained from the other methods. The peak discharges determined according to these methods are thus likely to be less accurate than those obtained using statistical or deterministic methods [1][2][3].

The ARM is a robust and simple to use method that is applicable to catchments with various sizes and return periods of up to 200. The SRM is limited by catchment size as the study area is larger than said limitation. The input data required by the ARM is fairly simple to gather and its easy and simpler to use in comparison to the other methods [2][21]. This is why the ARM has been chosen as the method of choice for determining the flood peaks.

2.5 Overview of probabilities in relation to flood return frequencies

It is necessary to calculate the probability of a flood event or any event that could potentially cause damage to infrastructure, from occurring or returning; as this has important economic, social and ecological implications. Even more so in densely populated urban areas where rivers usually run through cities. The return period (T) is described as being the average period over a certain amount of years during which a flood event repeats or exceeds itself [1][2][3][22]. The annual probability of the occurrence of an event having a T-year return period equals:

$$P = (\frac{1}{T}) \quad \text{(Eq. 1)}$$

The probability of an event with a return period of T to occur over a given design life of *n* years is determined by:

$$P_1 = 1 - (1 - \frac{1}{T})^n \quad \text{(Eq. 2)}$$

Where: P_1 = probability of at least one exceedance during the design life

n = design life in years

T = return period in years

Table 2-4, extracted from the SANRAL drainage manual gives an overview of the design return periods required in order not to exceed an allowable risk of occurrence.

Table 2-4: Required return periods in order not to exceed occurrence (Source: *[2]*)

Probability of occurrence (%)	Life of project (years)				
	1	10	25	50	100
1	100	910	2 440	5 260	9 100
10	10	95	238	460	940
25	4	35	87	175	345
50	2	15	37	72	145
75	1,3	8	18	37	72
99	1,01	2,7	6	11	22

2.6 Overview of the Alternative Rational Method (ARM)

The Acacia sub-catchment, located in the greater Arebbusch catchment, has an approximate area of 19km^2 and therefore needs to make use of a calculation method that caters for its medium sized catchment. We can see from Table 2-3 that the Alternative Rational method meets these requirements and is quite simple to compute. The calculation of the following parameters is the same as that of the standard rational method:

- Catchment area (A)
- Catchment slope (S)
- Time of concentration (T_c)
- Area Reduction Factor (ARF)

Further calculation requirements for ARM include:

- Watercourse length

- Catchment characteristics
- Rainfall intensity

ARM has no limitation to its recommended area and can be used to predict 2-200-year flood return periods. The Rational Formula is based on the conservation of mass and the hypothesis that the flow rate is directly proportional to the size of the contributing area, rainfall intensity and the runoff coefficient. Peak flow can therefore be calculated as:

$$Q = \frac{CIA}{3.6} \quad \text{(Eq. 3)}$$

Where:

Q = flood peak at catchment exit (m^3/s)

C = the Rational runoff coefficient (dimensionless)

I = the average rainfall intensity over the whole catchment (mm/h)

A = catchment area (km^2)

It should be noted that a few assumptions are made in the simplification of the calculations, and are approximately identical to most of the runoff methods. Both the standard rational and ARM make use of these assumptions [1][2][3][21].

- The relationship between rainfall intensity and rate of runoff, C, is a constant for a specified catchment;
- The peak discharge occurs when the total catchment contributes to the flow, this happens at the time of concentration (T_c);

- The return period of the peak flow, T, is the same as that of the rainfall intensity;
- The design storm produces a uniform rainfall intensity over the entire catchment;
- The rainfall has a uniform time distribution for at least a duration equal to the time of concentration (T_c);

Rainfall intensity (I) ARM calculations:

Similar to that of the SRM, the intensity of the design storm is directly proportional to that of the return period and inversely proportional to the duration of the storm event. Therefore, the time of concentration is based on the average catchment slope and distance that the water particles have to travel.

The intensity of the rainfall is related to the mean annual rainfall and to the specific rainfall region. As aforementioned the modified recalibrated Hershfield relationship is used to determine point rainfall, which is then converted to intensity by dividing the point rainfall by the time of concentration, for storm durations of up to 6 hours using the following equation:

$$P_{t,} = 1.13(0.41 + 0.64lnT)(-0.11 + 0.27lnt)(0.79M^{0.69}R^{0.20}) \quad \text{(Eq. 4)}$$

Where:

$P_{t,T}$ = precipitation depth for a duration of *t* minutes and a return period of T years

t = duration in minutes

T = return period

M = 2-year return period daily rainfall from TR102

R = average number of days per year on which thunder was heard (South African Weather Service has upper-air sounding data recorded since 1961) [1][2][18].

It should be noted that for storm durations between 6 and 24 hours, linear interpolation is used between the calculated point rainfall from the above equation and that of the 1-day point rainfall from the TR102 manual [2][3][19].

Area Reduction factor calculations:

The ARF can be calculated by either making use of the graphical relationship as proposed by Alexander, or by utilizing the following equation which is based on the UK Flood Studies Report [2][20]:

$$= 9000 - 12800lnA + 9830(60T_c)^{0.4} \quad \text{(Eq. 5)}$$

Where:

ARF = area reduction factor as a percentage (> 100%)

A = catchment area (km^2)

T_c = time of concentration (hours)

Figure 2-3 indicates the graphical relationship that can be utilized to gain the ARF without the need for the above calculation.

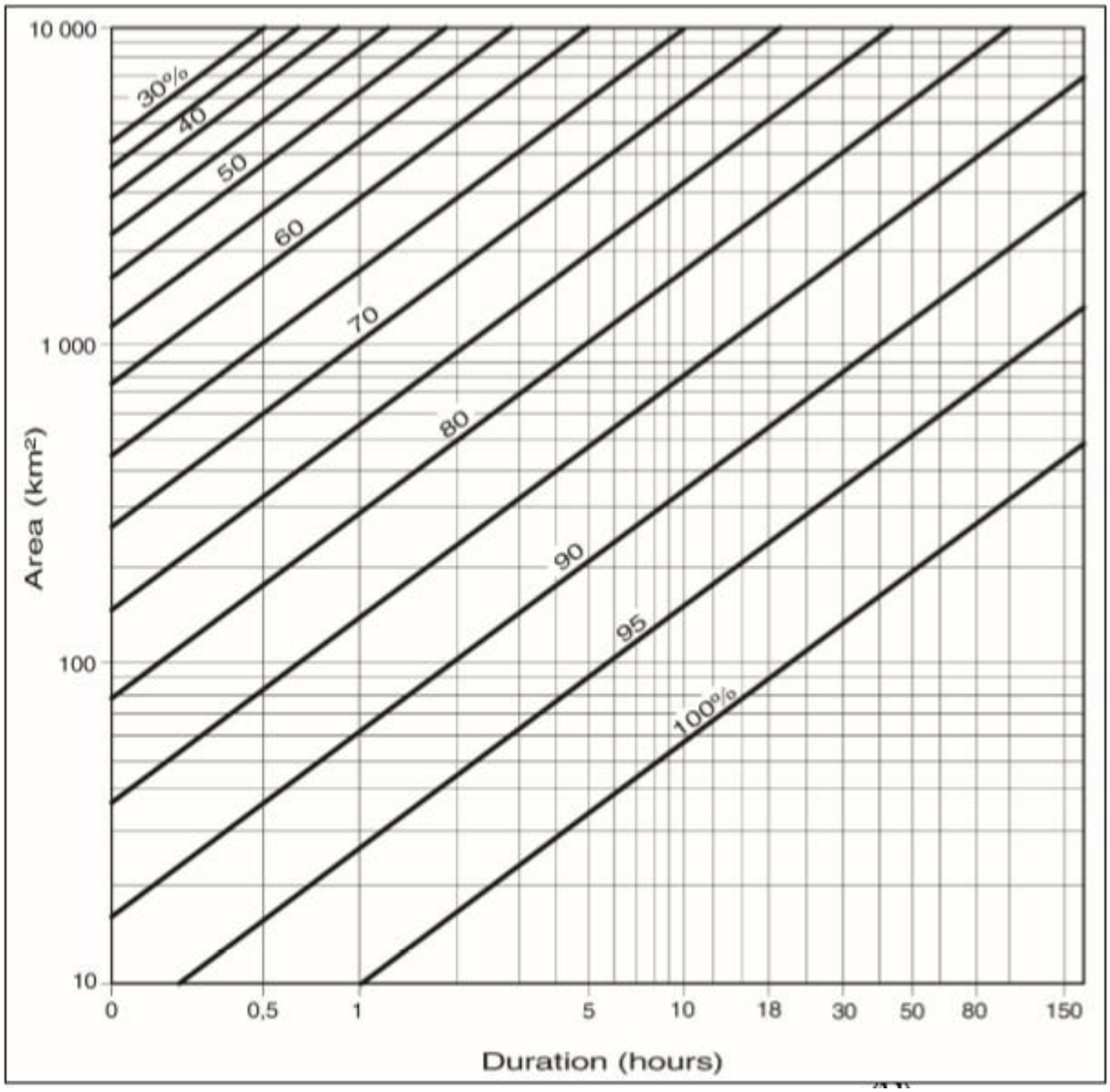

Figure 2-3: Area reduction factors (Source: [2]*)*

Time of concentration calculations using the Kirpich Formula:

$$T_C = \left(\frac{0.87L^2}{1000S}\right)^{0.385} \quad \text{(Eq. 6)}$$

Where:

T_C = time of concentration (hours)

L = hydraulic length of catchment (km)

S = channel gradient (m/m)

Catchment slope:

The Namibian drainage manual advocates the use of the 10-85 slope, developed by the United States Geological Survey for the derivation of the main channel slope. Figure 2-4 defines the slope characteristics.

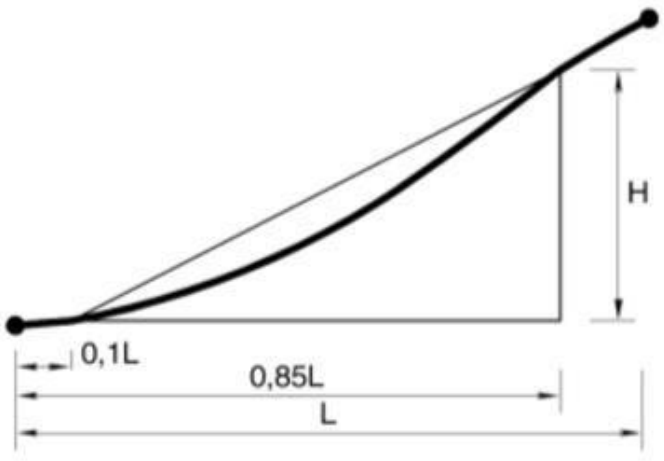

Figure 2-4: 1085-Slope from "US Geological Survey" (Source: [2]*)*

The following formula can be used in tandem with Figure 2-4:

$$S = \frac{H_{0.85L} - H_{0.10L}}{(1000)(0.75L)} \quad \text{(Eq. 7)}$$

Where:

S = channel gradient (m/m)

$H_{0.10L}$ = elevation height at 10% of the length of the watercourse (m)

$H_{0.85L}$ = elevation height at 85% of the length of the watercourse (m)

L = length of watercourse (km)

2.7 Hydraulic calculation considerations

Hydraulic calculations are taken into consideration due to the fact that the river section can be classified as open channel flow and making use of these calculations; values of variables that describe flow conditions can be determined. Furthermore, the chosen hydraulic modelling software HEC-RAS makes use of these calculations in its simulations and so some of the calculations it uses are to be elaborated on [8]. Three fundamental laws govern the application of hydraulic calculations; these are [1][2][3]:

1. Conservation of mass (continuity principle);
2. Conservation of energy;
3. Conservation of momentum.

Almost all hydraulic calculations involve the law of conservation of mass. The law of conservation of momentum is used to calculate forces and flow conditions where all the forces

that act upon a body of water can be quantified. The law of conservation of energy is used where energy losses can be calculated or omitted when small enough [2].

Over the last few decades the performance of hydraulic modelling software has increased extensively resulting from more computationally capable computer systems that can run complicated algorithms such as HEC-RAS, SWIMM5, Flood Modeller, Mike 11 and SOBEK 1DFlow [8][10][15]. HEC-RAS was developed by the US Department of Defence, Army Corps of Engineers and made public/free to use in 1995; and hence its free-to-use policy it will be utilized as the sole modelling software for this mini research.

HEC-RAS is capable of modelling hydraulic water flow through rivers and other conduits by making use of the law of conservation of energy equation; derived from Newton's second law of motion. This law states that the total energy of an isolated system remains constant over time [2][3]. In its complete form this equation is represented below as:

$$\frac{\alpha_1 \overline{V}_1{}^2}{2g} + y_1 \cos\theta_1 + z_1 = \frac{\alpha_2 \overline{V}_2{}^2}{2g} + y_2 \cos\theta_2 + z_2 + \sum h_{f_{1-2}} + \sum h_{1_{1-2}} \qquad \text{(Eq. 8)}$$

Where:

α_i = coefficient compensating for variations in velocity across a section

$\overline{V}_i{}^2$ = average velocity across a section (m/s)

g = acceleration due to gravity (9.81 m/s^2)

y_i = depth of flow measured perpendicular to the streambed (m)

θ_i = Longitudinal bed slope angle (^{o})

z_i = bed level at point where depth of flow = y_i (m)

$\sum h_{f_{1-2}}$ = friction losses between sections 1 and 2 (m)

$\sum h_{1_{1-2}}$ = sum of transition losses between 1 and 2 (m)

Note: Subscript 1 and 2 refers to the upstream and downstream sections respectively.

The various energy components can be seen below in Figure 2-5.

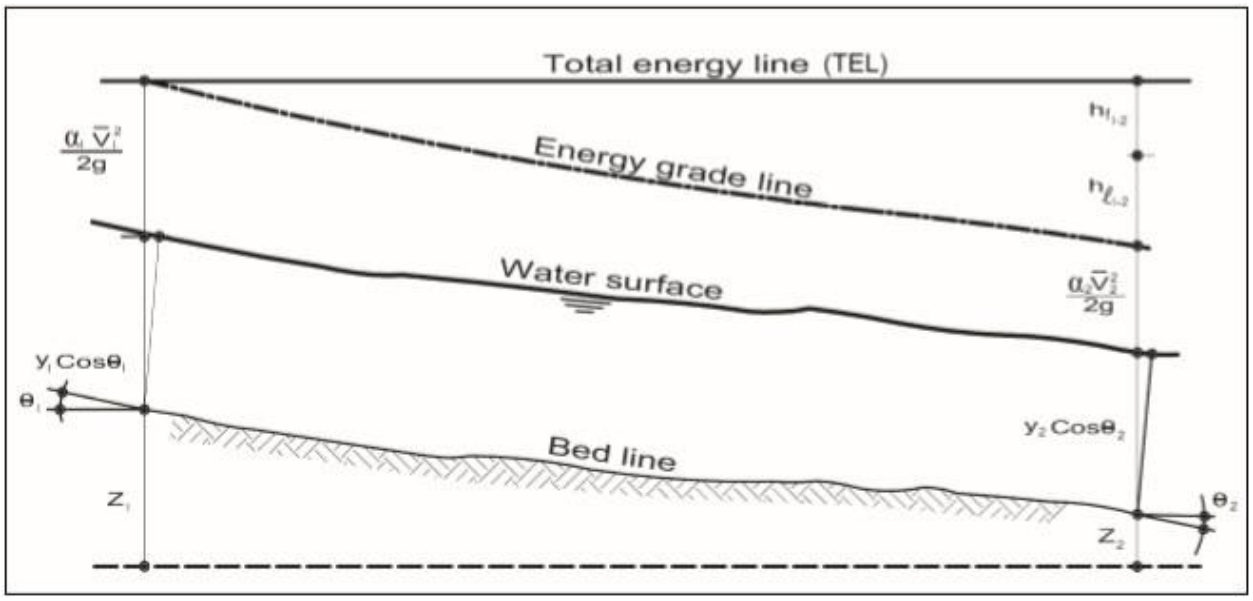

Figure 2-5: Longitudinal section along flow path (Source: [2][3]*)*

Conveyance and friction loss calculations are performed by HEC-RAS as well in conjunction with the aforementioned energy conservation law. The conveyance equation derived from the Manning Equation can be described as:

$$Q = \frac{1}{n} R_h^{\frac{2}{3}} A S_f^{\frac{1}{2}} \quad \text{(Eq. 9)}$$

$$K = \frac{1}{n} R_h^{\frac{2}{3}} A \quad \text{(Eq. 10)}$$

$$Q = K S_f^{\frac{1}{2}} \quad \text{(Eq. 11)}$$

Where:

Q = flow

n = Manning's coefficient

A = cross sectional area

R_h = hydraulic radius

S_f = friction slope

K = conveyance

Before friction losses can be elaborated on; a distinction needs to be made between the 3 main flow types categorized according to the Reynolds number, mainly:

- Lamina flow ($R_e \leq 500$)
- Transition flow ($500 < R_e \leq 5000$)
- Turbulent flow ($R_e \geq 5000$)

The Reynolds number can be calculated as follows:

$$R_e = \frac{\bar{v} R}{v} \quad \text{(Eq. 12)}$$

Where:

$\overline{v}$ = average flow velocity (m/s)

R = hydraulic radius (m)

v = kinematic viscosity (≈1.14 x 10^{-6} m^2/s)

Most pluvial floods occur under turbulent flow therefore only this type of flow will be elaborated on in terms of friction loss calculations. According to the SANRAL drainage manual the following equation best represents the friction losses under turbulent flow:

$$\overline{v} = 5.75\sqrt{gRS}\ log\frac{12R}{k_s\frac{3.3v}{\sqrt{gRS}}} \quad \text{(Eq. 13)}$$

Where:

$\overline{v}$ = average flow velocity (m/s)

R = hydraulic radius (m)

S = energy slope, which is equal to bed slope only when flow is uniform (m/m)

k_s = roughness coefficient (size of irregularities on bed and sides) (m)

v = kinematic viscosity (≈1.14 x 10^{-6} m^2/s)

It should also be noted that the simplified Manning's equation is utilized as well:

$$\overline{v} = \frac{R^{\frac{2}{3}}S^{\frac{1}{2}}}{n} \quad \text{(Eq. 14)}$$

Where:

n = roughness coefficient ($s/m^{1/3}$)

The roughness coefficient n varies in roughness with the change in hydraulic radius.

2.8 GIS and Remote Sensing

Over the past 3 decades an explosion of progress has taken place in the field of GIS, in both expanding of literature and development in GIS infrastructure [23]. Geographic Information Systems can be described as computer programs that are used to store, capture, retrieve, analyse and display spatial data. Spatial data is data that identifies the geographic location of features and boundaries on Earth [7][15][23].

Vector data comprises of vertices and paths while raster data on the other hand is made up of a grid of pixels. Vector data consists of points, lines and polygons (indicating areas). Vector points are latitude and longitude coordinates on a spatial reference frame. Vector lines connect points/vertices which become vector lines and these usually represent paths on maps like roads, rivers or pipelines. Furthermore, polygons are created when vertices are further connected to produce a closed path which results in a vector polygon; these indicate boundaries and areas like buildings, agriculture fields or bodies of water [24].

Raster data are regularly-spaced and square in most cases. Two main sections, discrete and continuous, exist in raster data set. Discrete raster's have distinct values meaning one grid cell represents a land cover class or a soil type. It is therefore possible to distinguish each thematic class on a land use/land cover map. Continuous raster's have gradual change meaning they have gradually changing data such as elevations or temperature. A

continuous raster surface can be derived from a fixed registration point, i.e. digital elevation models use sea level as a datum, with each cell representing a value above or below sea level [24].

Image classification: Image classification is used in this research to gain the distribution of land cover over the catchment area which is a requirement for the run off coefficients calculations. Image classification can be defined as the task of extracting information classes from a multiband raster image. The resulting raster can then be used to create thematic maps where cells of similar colour spectrums are counted together giving overall cell count which can then be multiplied with the cell size to gain area coverage of certain land types like urban, rural, forest or water bodies. Figure 2-7 gives a schematic of the image classification process [24].

It should be noted that due to the fact that the Sentinel and Landsat images are of different cell sizes, their corresponding classified images will have differing cell sizes as well. This has an impact on the area calculations and as such resampling techniques will have to be employed to get the classified images to the same sizes. Four different resampling techniques are employed by Arc Map these are [25]:

- Nearest— The fastest resampling method; it minimizes changes to pixel values. Suitable for discrete data, such as land cover.
- Bilinear— calculates the value of each pixel by averaging (weighted for distance) the values of the surrounding 4 pixels. Suitable for continuous data.
- Cubic— calculates the value of each pixel by fitting a smooth curve based on the

surrounding 16 pixels. Produces the smoothest image but can create values outside of the range found in the source data. Suitable for continuous data.

- Majority— determines the value of each pixel based on the most popular value within a 3 by 3 window. Suitable for discrete data.

Post-classification processes indicated in Figure 2-7 includes the accuracy assessment of the classified images and is an integral part of the classification process as it is necessary to quantitatively determine the effectiveness by which pixels were grouped into correct land cover classes. It can never be assumed that a classified image created from remote sensing data is completely accurate as errors originate from various sources, these include but are not limited to [26][27]:

- Misidentification of parcels
- Excessive generalization of pixels
- Errors in algorithm registration of pixels

Two main accuracy assessments are in practice, these being non-site-specific and site-specific accuracy with the main difference being that site-specific assessment employs the confusion matrix while the later does not. The accuracy assessment compares the pixels from the classified images to that of ground reference test points identified on higher resolution images or physical field verifications; if said classified pixels corresponds closely to that of the reference points the classified images are said to be accurate (in relation to the statistical measures imposed), i.e. high accuracy indicates a low level of bias in the results [26][27][28].

The results of the accuracy assessment are tabulated and assessed empirically in a square matrix also referred to as a confusion matrix. The numbers of sampled reference points are related to the binomial probability algorithm which equates to:

$$n = z^2 \frac{pq}{e^2} \quad \text{(Eq. 15)}$$

Where:

n = number of samples

p = expected percent accuracy

q = 100 – p

e = allowable error

z = 2 (from the standard normal deviate of 1.96 for the 95% two-sided confidence level)

Once the number of samples have been determined various sampling methods can be employed these include: simple random, stratified random, systematic, systematic non-aligned or cluster sampling. Figure 2-6 gives a depiction of the sampling techniques.

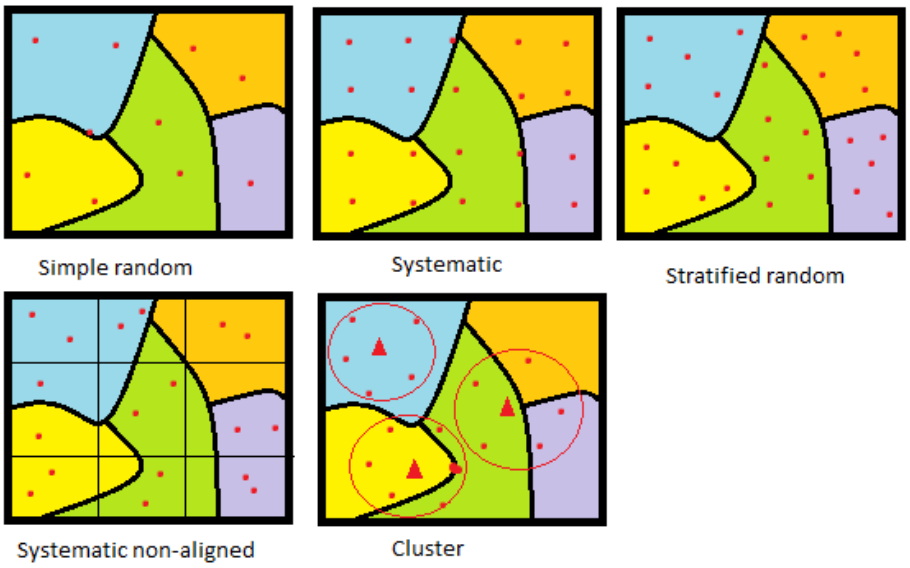

Figure 2-6: Reference points sampling techniques (29).

- Simple random: Random selection of observations and each point has equal probability of selection.
- Systematic: Involves a random start and the proceeds with the selection of every n^{th} element.
- Stratified random: A minimum number of observations are randomly placed in each class/category.
- Systematic non-aligned: Region is divided into equally spaced cells, which allows for an even distribution of randomly placed observations in each grid cell.
- Cluster sampling: Observations are collected randomly or systematically around a centroid of the cluster [29].

Four main accuracy indicators are made use of in the assessment, which are derived from the confusion matrix itself. These are the overall accuracy, producer's accuracy, the user's accuracy and the Kappa analysis [29].

- The Overall accuracy is obtained by comparing the overall accuracy of the classified image to that of the reference data. The following equation is made use of:

  $$OA = \frac{1}{N} \sum_{i=1}^{r} n_i \quad \text{(Eq. 16)}$$

  Where:

  N = total number of pixels

  r = number of classes

  n = correctly identified pixels in each class

- The user's accuracy is a statistic that specifies the probability of a ground reference datum being correctly classified and it is a measure of the omission error. This statistic is calculated because the producer may want to know how well an area can be classified [28][29].
- The producer's accuracy is calculated by dividing the diagonal number from a class's column by the sum of the entire column including the number found within the diagonal. The user's accuracy is a measure of the commission error. This statistic indicates the probability of how well the classified sample represents what is found on the ground. This measure is calculated by dividing the diagonal of a class by the sum of the numbers within the row of that class [28][29].

- The Kappa analysis is a discrete multivariate technique that produces a K-value, which is an estimate of Kappa. This statistic is a measure of how well a classification map and the associated reference data agree with each other. This agreement is based on the major diagonal of the error matrix and a chance agreement (row and column values). Strong agreement occurs if the K is greater than 0.80. Moderate agreement occurs when K values fall between 0.40 and 0.80 and poor agreement occurs with K values less than 0.40 [28][29]. The kappa coefficient is calculated by making use of the following equation.

$$\hat{K} = \frac{M\sum_{i=j=1}^{r} n_{ij} - \sum_{i=j=1}^{r} n_i n_j}{M^2 - \sum_{i=j=1}^{r} n_i n_j} \qquad \text{(Eq. 17)}$$

Where:

r = number of rows in error matrix

n_{ij} = number of observations in row i, column j

n_i = total number of observations in row i

n_j = total number of observations in column j

M = total number of observations in matrix

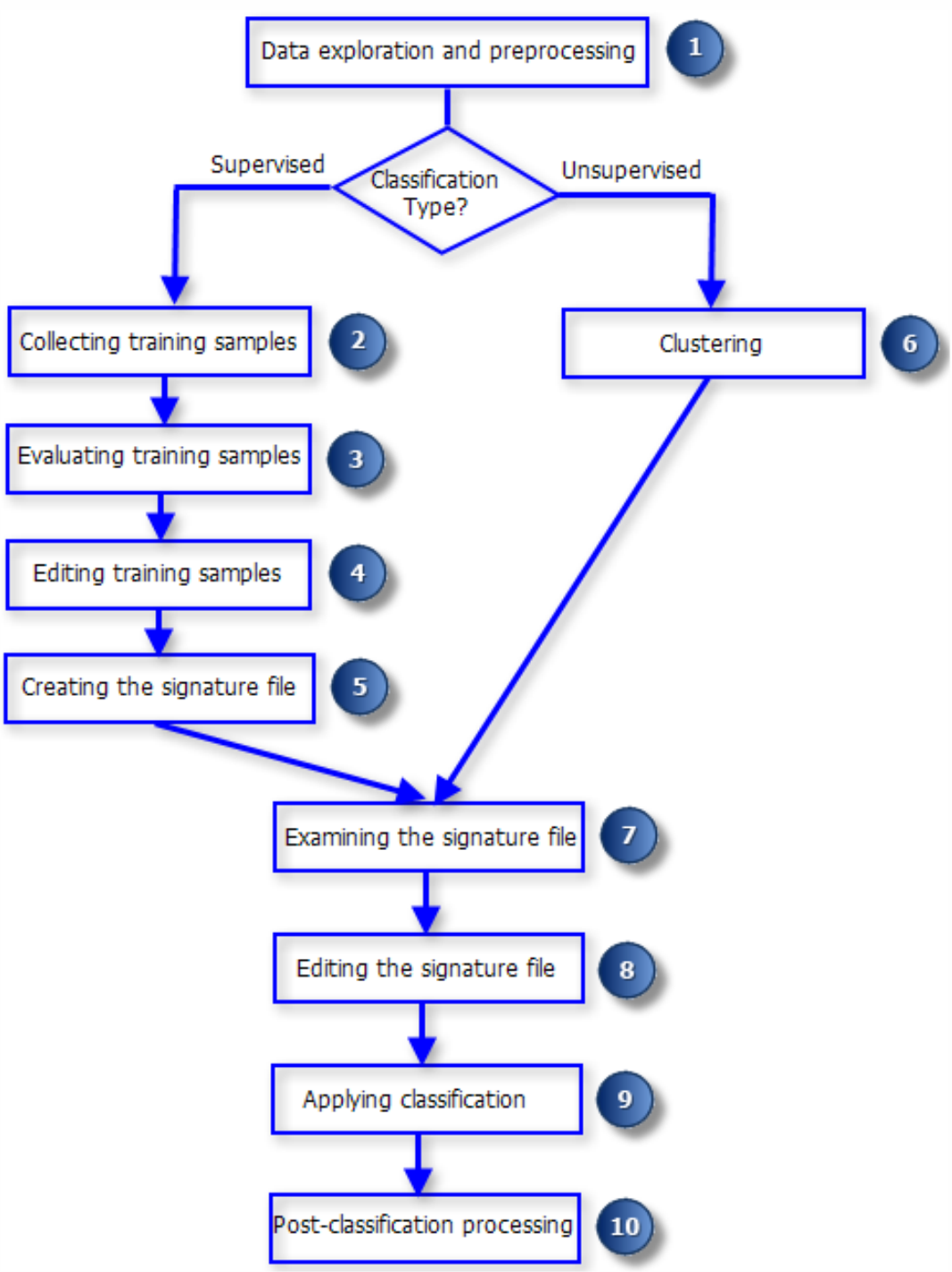

Figure 2-7: Image classification workflow schematic (Source: [24])

3. METHODOLOGY

3.1 Overview of the study area

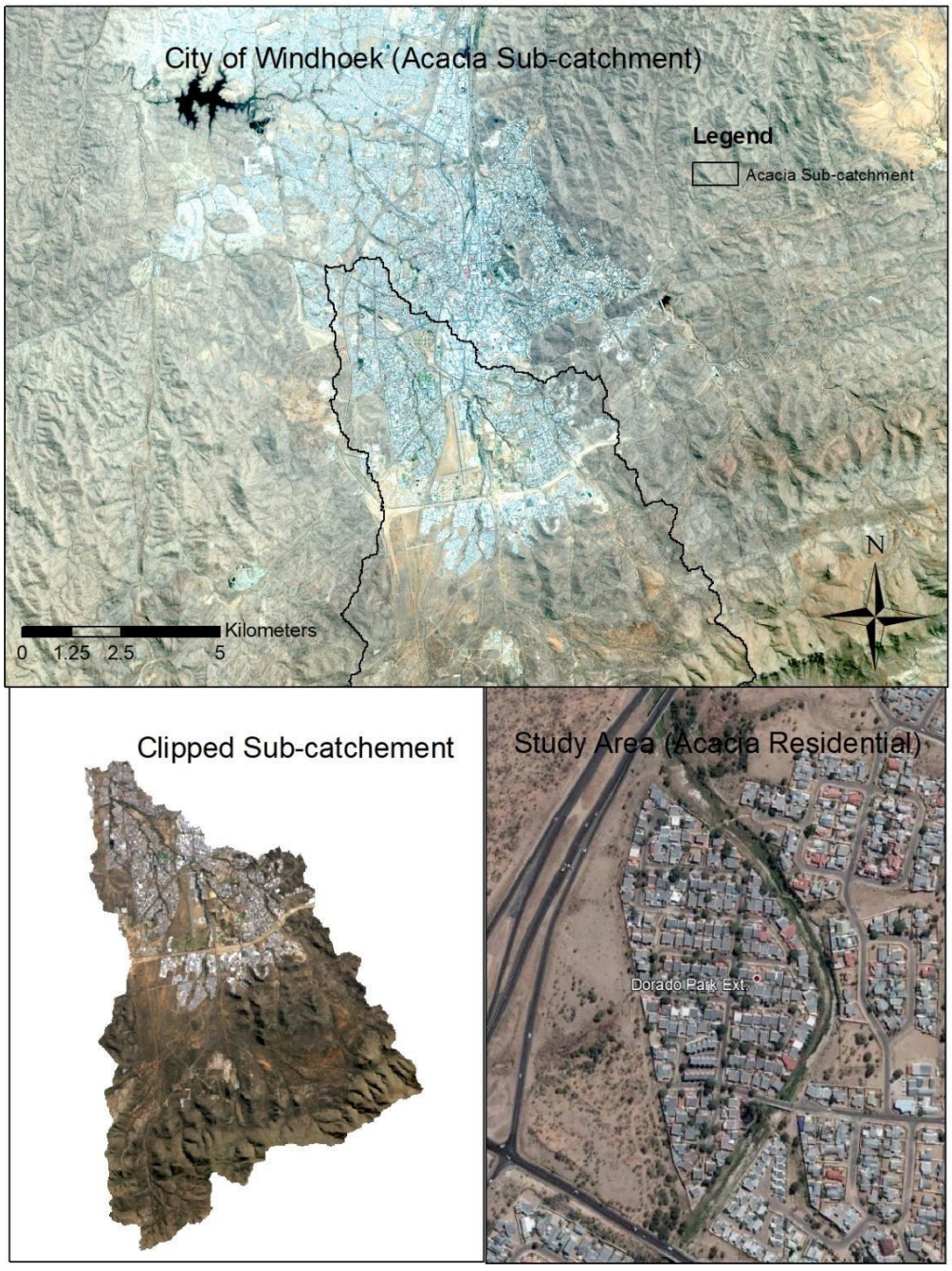

Figure 3-1: Study area.

The Arebbusch River runs all through Windhoek City starting in the South at the Kleine Kuppe Mountains and ending in the North-West at the Goreangab Reservoir. As of the 2011 population census, Windhoek has been home to around 325 858 inhabitants but this number has since grown with the influx of urbanization as people from rural towns look for improved job opportunities and living conditions in the capital [4]. Windhoek is located on the Khomas Highland plateau at around 1700 meters above sea level. Figure 3-2 indicates a range between 2331 and 1556 meters above sea level spanning over the Arebbusch catchment with the highest elevation in the South Auas Mountains and the lowest elevation at the Goreangab dam. Acacia is centrally located on the Western side of Windhoek. It is a small residential area with around 250 housing units and an approximate area of 9 ha. The Acacia River runs all around the Eastern side of the area and it has only one access/exit point being the Acacia Bridge. The city of Windhoek experiences a varied inter-annual rainfall with a Mean Annual Precipitation (MAP) of around 360 mm [17][19][30]. According to Koppen climate classification, the city; experiences a hot semi-arid climate as its annual average temperature is above 18 ^{o}C. Figures 3-2 and 3-3 indicate the Arebbusch and Acacia catchments having coverage areas of 141 km^2 and 93 km^2 respectfully. The objectives of the study is obtained by making use of a comparative study of two years (1989 and 2018), i.e. when urban development was relatively low against the present, by utilizing corresponding satellite images as well as satellite derived digital elevation models (DEM) as input for simulating rainfall runoffs. In conjunction with the SARAL and Namibian Drainage manuals, flood peaks can be calculated for the sub catchment and used with HEC-RAS and ArcGIS to simulate rainfall runoff and thus produce inundation maps.

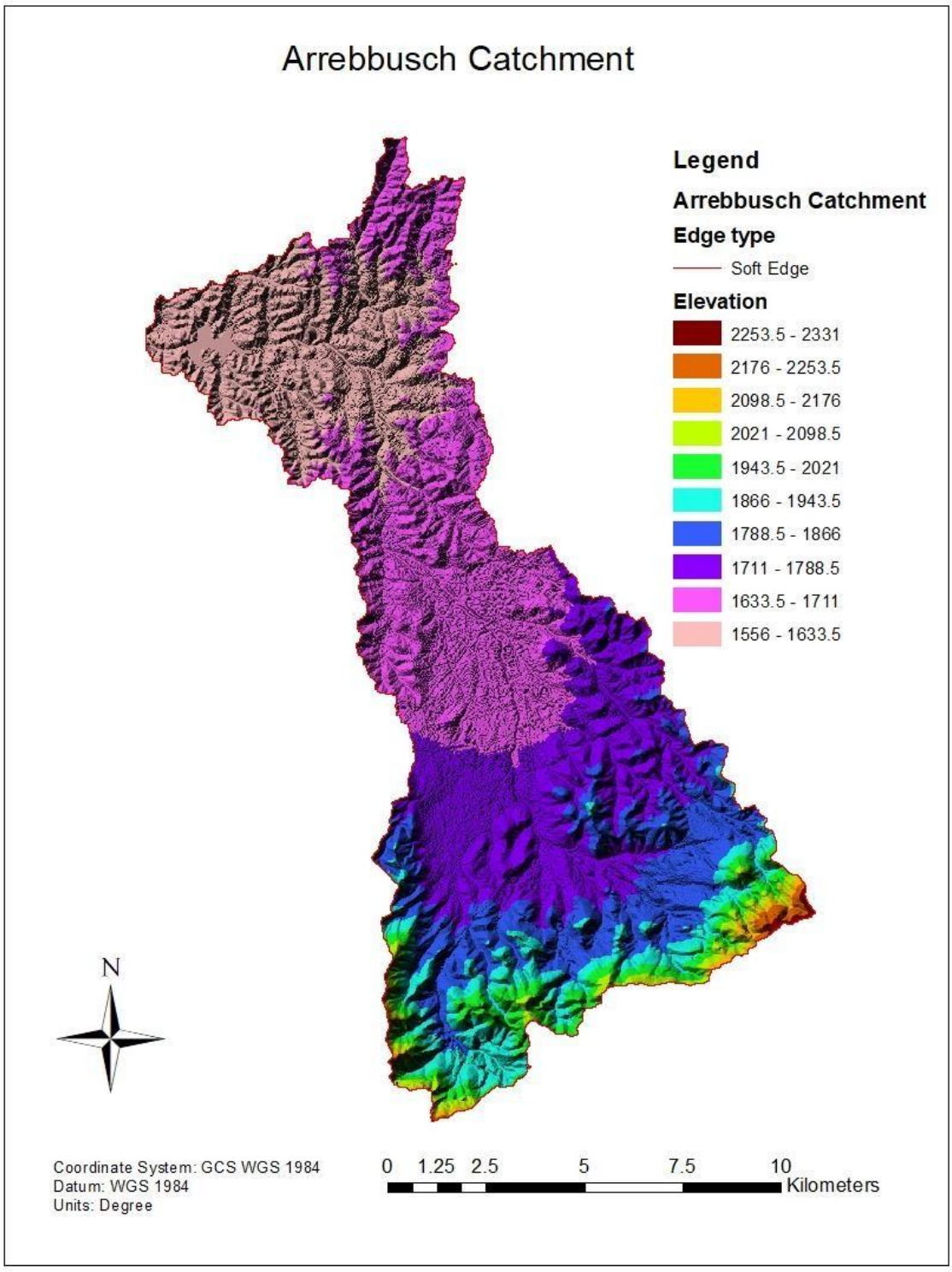

Figure 3-2: Elevation map of Arebbusch catchment

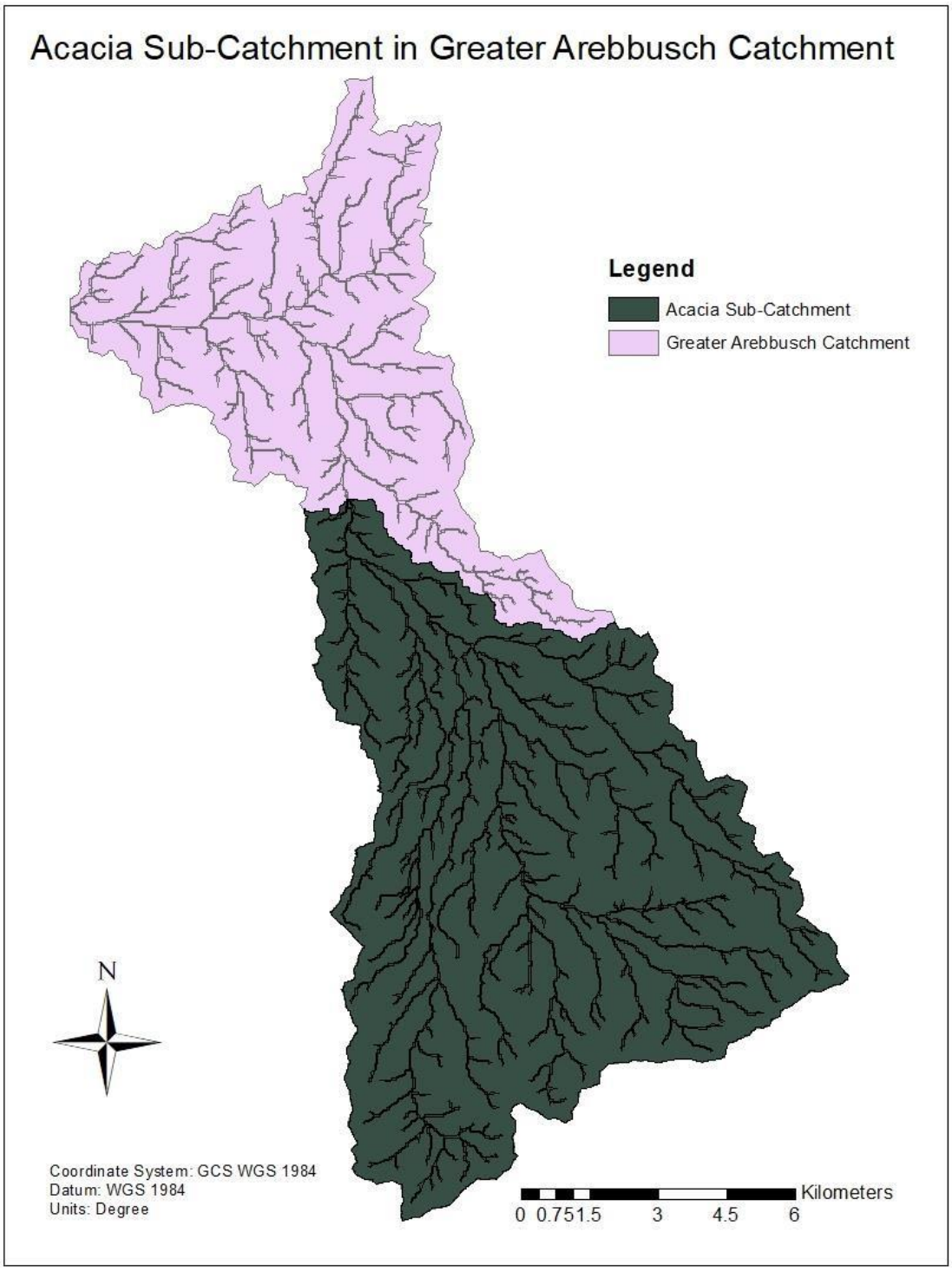

Figure 3-3: Acacia and Arebbusch catchments with stream paths

The catchment characteristics were determined by making use of the digital elevation model downloaded from ALOS (Advanced Land Observing Satellite) which has a resolution of 1 arc-second, equating to 30m.

Figure 3-4: Image of Acacia River upstream section.

3.2 Alternative Rational Method Calculation Steps

The following 10 steps have been extracted from the SANRAL and Namibian drainage manuals and are guidelines in helping to determine the aims and objectives set out by this research. The steps are applied to both 1989 and 2018 scenarios.

Step 1: Determine the catchment area (km^2). The area can either be obtained manually by looking at 1:50 000 scale topographical maps and/or 1:10 000 scale Ortho-photos; or digitally by making use of ArcGIS software. ArcMap 10.4.1 was

made use of in this Research. The *Watershed* tool containing the *Hydrology* toolset of the *Spatial Analyst Tools* toolbox (Figure 3-5) was used to identify catchment areas for specified pour points representative of the catchment outlet. Both catchment areas were obtained as indicated in Table 3-1.

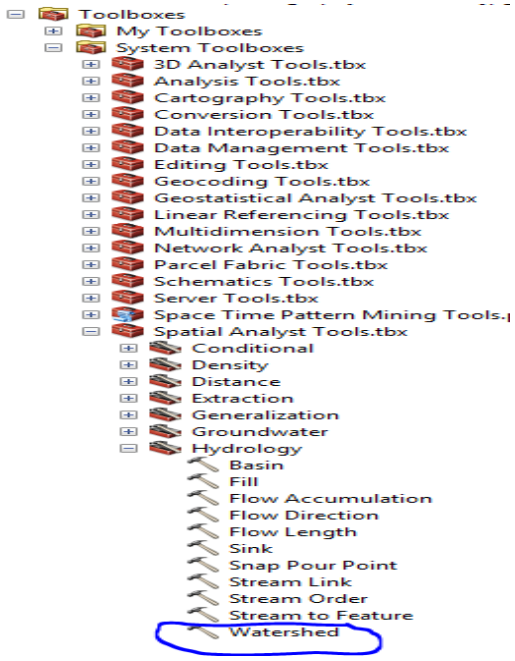

Figure 3-5: ArcMap toolbox snipped image.

Step 2: Determine the length of the longest watercourse (km). This was done by making use of the DEM file that was obtained from ALOS. The same *Spatial Analyst Tools* toolbox was used. The following tools were made use of on the DEM in the following order: *Fill, Flow Direction, Flow Accumulation, Flow length, Snap Pour Point, Stream link, Stream order* then the *Raster Calculator* was used to produce the individual streams in the catchment. The stream-order file attribute table can then be opened and a new column/field can be added to calculate the length of the water courses by using the

Calculate Geometry option.

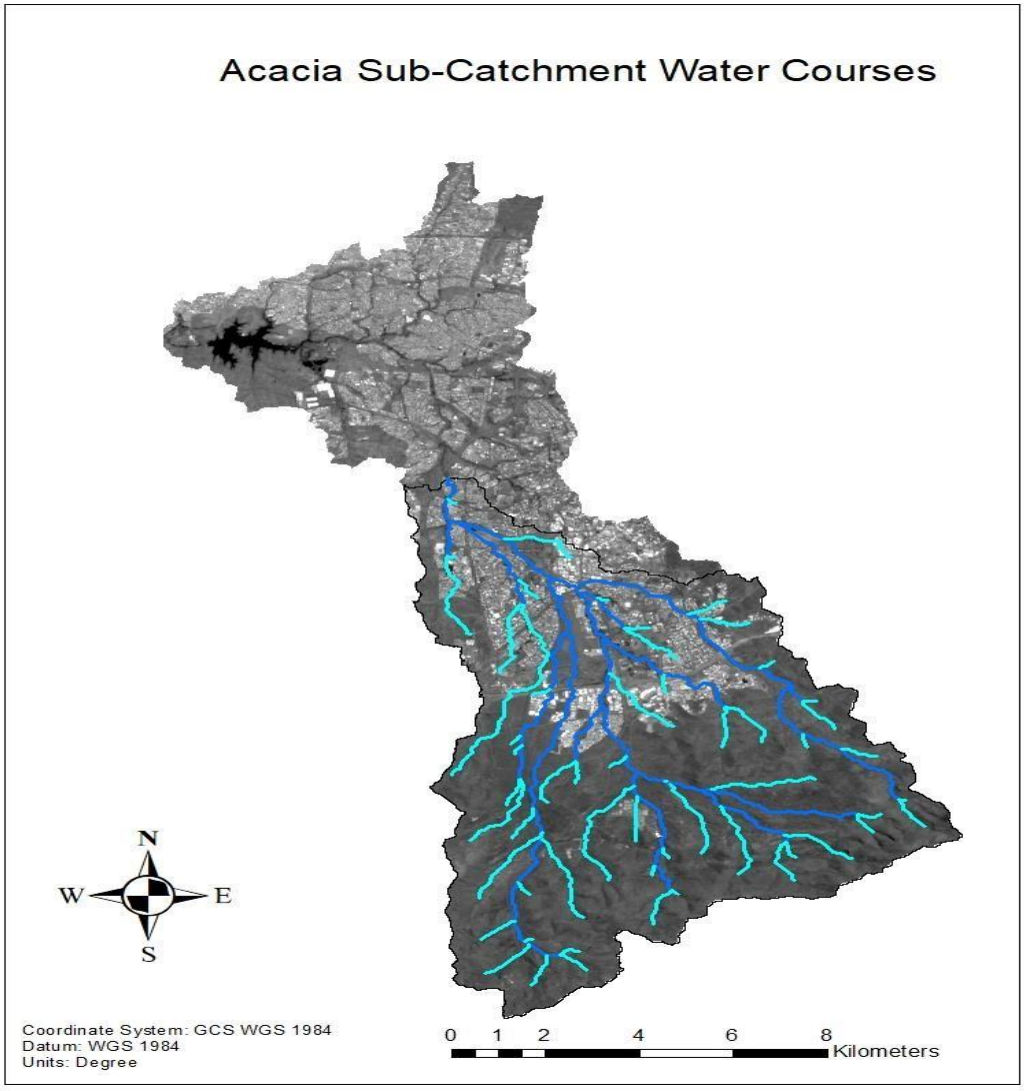

Figure 3-6: Acacia sub-catchment water courses longest path layout.

Step 3: Determine the average slope of the longest watercourse. Utilizing the 1085-slope method as developed by the Geological Survey, and tested by the UK Institute of Hydrology the average slope was calculated using Eq. 7; with the $H_{0.85L}$ = 1844m and $H_{0.10L}$ = 1654m.

Step 4: Calculate the time of concentration from the catchment characteristics. Using the recommended empirical formula developed by the US Soil Conservation Services; T_c can be calculated using Eq. 6.

Step 5: Identify the catchment characteristics to determine the run-off coefficient. In Figure 3-6 it is fairly clear to see that the Acacia sub-catchment consists of both rural and urban land cover; rural in this case attributed by land that is clear of urban development. The geological characteristics of the study area should also be observed and in the case of Windhoek it is situated in unconsolidated superficial deposits consisting mostly of the metamorphic rock mica schist, containing quartz and mica resembling slates and fairly easy to split [30]. The average soil type can also be described as semi-impermeable with moderately high storm flow potential [30]. Figure 3-7 gives a simplified geological map of Namibia taken from the Namibian Drainage Manual.

The runoff coefficient for both 1989 and 2018 catchments which covers both rural and urban land should be determined on the weighted average bases, considering the relative size of the urban and rural areas and their applicable runoff coefficients; by making use of runoff coefficient tables as well as the following equation:

$$C = \propto C_1 + \beta C_2 \quad \text{(Eq. 18)}$$

Where:

C = weighted runoff coefficient for the catchment

C_1 = runoff coefficient for rural areas (then $C_1 = C_{1A} * C_{1B}$) (Eq. 19)

C_2 = runoff coefficient for urban areas

α = percentage of catchment defined as rural area

β = percentage of catchment defined as urban area.

C_{1A} = Catchment cover factor

C_{1B} = Catchment size factor

Table 3-1: Runoff coefficient for urban areas (Source: *[3]*)

Urban areas		
Land use	**Condition**	**Range of C_2 values**
Lawns	Sandy soil, flat < 2%	0.05 – 0.10
	Sandy soil, steep> 7%	0.15 – 0.20
	Heavy soil, flat < 2%	0.13 – 0.17
	Heavy soil, steep> 7%	0.25 – 0.35
Residential	Single - Family areas	0.30 – 0.50
	Apartment dwelling areas	0.50 – 0.70
Industrial	Light areas	0.50 – 0.80
	Heavy areas	0.60 – 0.90
Business	Downtown areas	0.70 – 0.95
	Neighbourhood areas	0.50 – 0.70
Streets	Asphaltic	0.70 – 0.95
	Concrete	0.80 – 0.95
	Brick	0.70 – 0.85
Roofs		0.75 – 0.95

Table 3-2: Runoff coefficient rural areas-Catchment cover factor (C_{1A}) (Source: *[3]*)

Vegetation		Slope		
		Flat <1%	Undulating 1% to 5%	Steep > 5%
Cultivated land	Properly contoured	0.25	0.30	0.35
	Not contoured, no erosion	0.40	0.50	0.60
	Eroded	0.60	0.65	0.75
Grass veld	Dense growth, complete coverage	0.30	0.35	0.45
	Tread out, over-grazed	0.40	0.45	0.50
	Barren, eroded, dongas	0.60	0.65	0.75
Karoo	Dense growth, complete coverage	0.40	0.50	0.60
	Tread out, over-grazed	0.50	0.60	0.70
	Barren, eroded, dongas	0.60	0.65	0.75
Wood lands	Virgin forest, brushwood	0.15	0.18	0.20

Table 3-3: Runoff coefficient rural areas-Catchment size factor (C_{1B}) (Source: *[3]*)

Catchment area (km^2)	Coefficient C_{1B}
< 5	1.0
5 to 15	0.9
15 to 50	0.8
50 to 150	0.7
150 to 500	0.6
500 to 1000	0.5

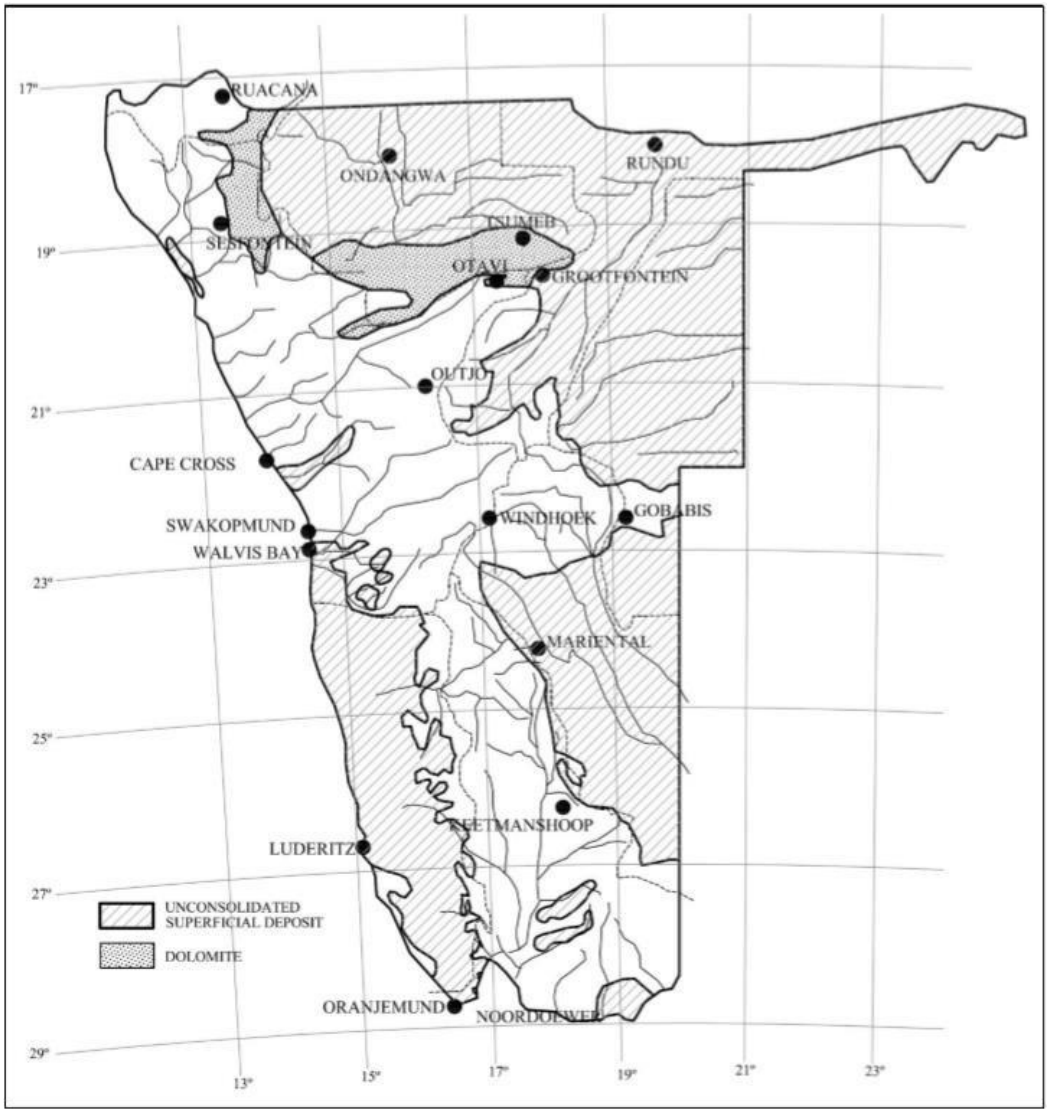

Figure 3-7: Simplified geological map of Namibia (Source: [3])

From the above listed figures, the following values have been abstracted as inputs for Eq. 18: 2018: C_{1A} =0.45; C_{1B} = 0.7; C_1 = 0.315; C2 = 0.65; α = 69%; β =31%

1989: C_{1A} =0.45; C_{1B} = 0.7; C_1 = 0.315; C2 = 0.65; α = 82%; β =18%

Therefore, the overall runoff coefficient for the Acacia sub-catchment 2018 is: C = 0.419

Overall runoff coefficient for Acacia sub-catchment 1989 is: C = 0.375

Step 6: Determine the representative rainfall/design rainfall by making use of the TR102 document. The design rainfall is a very important parameter of the deterministic methods and various researches has been carried out to assist engineers in ascertaining this value. Adamson, Pitman and Alexander have all contributed to this endeavour for the assessment of southern African countries as they share approximate natural conditions. The design rainfall is linked to a specific recurrence interval and a critical storm duration [1][2][19]. The 1:50 year one day design point rainfall has been obtained from Figure 3-12(c) of the Namibian Drainage Manual. Figure 3-8 gives an example of the co-axial diagram used, to obtain the design point rainfall depth. In this case with Windhoek being an inland settlement, the calculated time of concentration of 3 hr., return period of 50 years and mean annual precipitation of 360 mm.

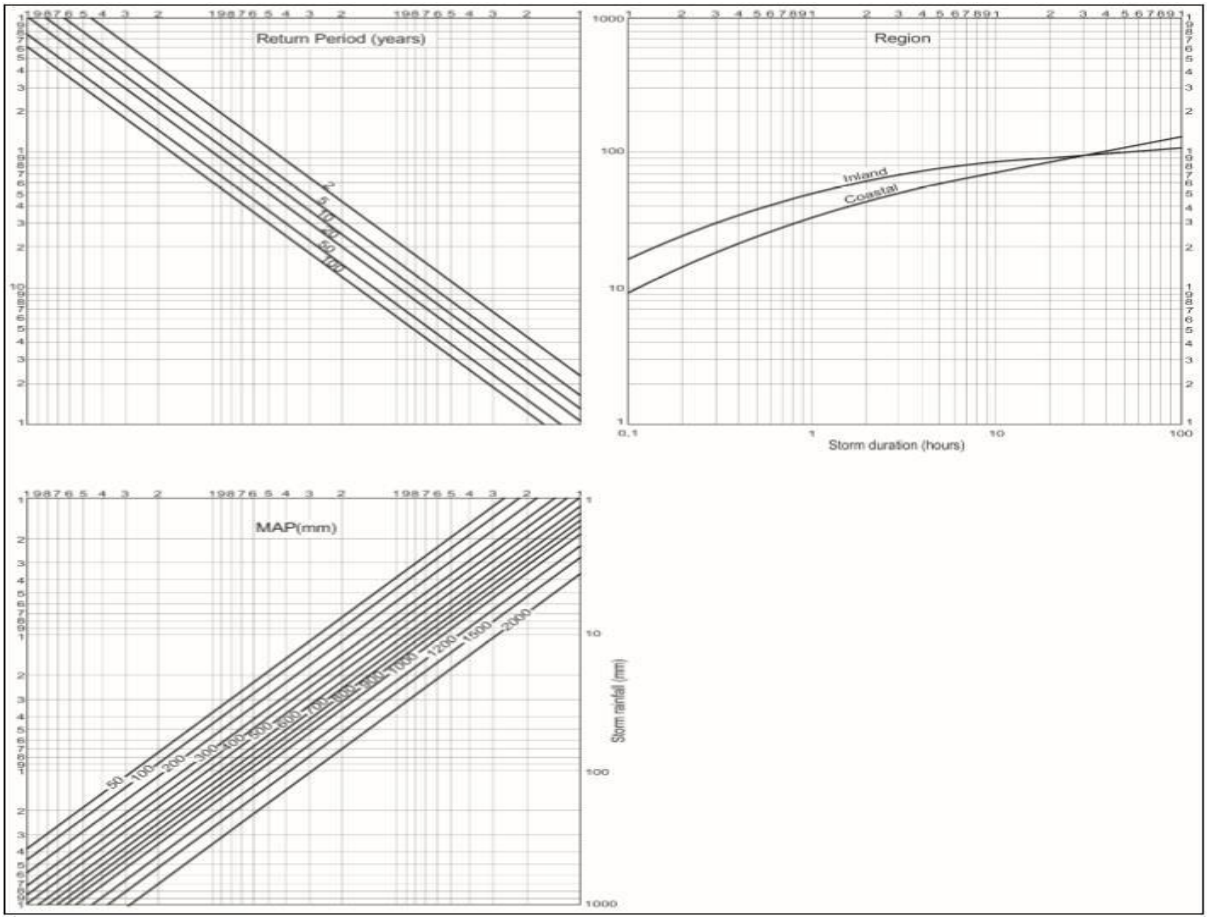

Figure 3-8: Depth-Duration-Frequency diagram for point rainfall (Source: [1][2])

Step 7: Calculate the point intensity (mm/hour). This is determined by dividing the point rainfall with the time of concentration.

$$P_{iT} = \frac{P_{tT}}{T_C} \quad \text{(Eq. 20)}$$

Where:

P_{iT} = point intensity for the different return periods (mm/h)

P_{tT} = precipitation depth for a duration of t minutes and a return period of T years (mm)

T_C = time of concentration (hours)

Step 8: Determine the ARF for the different return periods using Eq. 5 coupled with a catchment area of 93 km^2 and time of concentration of 3 hrs. The ARF value was determined as 83.5%.

Step 9: Determine the average rainfall intensity or effective catchment precipitation by utilizing the following equation:

$$I_T = P_{iT} \frac{ARF_T}{100} \quad \text{(Eq. 21)}$$

Where:

I_T = rainfall intensity averaged over the catchment (mm/h) for the return period T.

ARF_T = area reduction factor as a percentage for the return period T.

P_{It} = point intensities for the different return periods (mm/h)

Step 10: Determine the peak flow for each of the required return periods.

$$Q_{50} = \frac{C_{50} I_{50} A}{3.6} \quad \text{(Eq. 22)}$$

Where:

Q_{50} = peak flow rate for 50-year return period (m3/s)

C_{50} = combined runoff coefficient for 50-year return period

I_{50} = average rainfall intensity over the catchment for 50-year return period (mm/h)

A = effective area of catchment (km^2)

3.6 = conversion factor

In Eq. 22, it can be deduced that the determining variable is that of the runoff coefficient C as the rainfall intensity value I, and the catchment area A; remains constant for both study years (1989 and 2018).

3.3 HEC-RAS and RAS-Mapper usage

The following sub-chapter outlines the steps taken to produce river cross section data of the Acacia River by making use of HEC-RAS version 5.0.5 GIS component named RAS-Mapper. Floodplain analysis is one of the primary functions of the U.S. Army Corps of Engineers Hydrologic Engineering Centre's HEC-RAS software program. RAS Mapper allows the modeller to quickly view floodplain extents without using another GIS or CAD program. This results in more easily identification of issues with model results so as to make improvements on the ready. In the past an inter-connected usage of HEC-RAS and ArcMap had to be made use of so as to gain the georeferencing/spatial referencing that ArcMap provided, but since the release of HEC-RAS version 5+ the RAS developers have since incorporated its own georeferencing algorithms into the software.

Visualization of hydraulic results is extremely useful for model reviews, presentation reports and submittals. RAS Mapper allows for the display of water surface elevations (Traditional floodplain mapping), floodplain depths, floodplain boundary and flow

velocities. This allows for very specialized presentation of hydraulic results for almost every type of hydraulic analysis.

Before any work can commence on the HEC-RAS software, a projection setup needs to be done firstly so as to assign a desired co-ordinate system and projection to be used. The projection file has the extension *.prj and can be downloaded from http://spatialreference.org/ website. The Universal Transverse Mercator (UTM) conformal projection system, zone33 South was used.

Once the projection file has been incorporated into RAS-Mapper, adding web-imagery can then be done to check if all the data has been correctly incorporated. A new layer can then be created in the Geometries Tab and named 1D Geometries which will include the River flow line, Cross sections, Bank lines and Flow paths. Once these features have been made by using the Edit toolbar they will automatically be transferred to the Geometric Data window as cross sections.

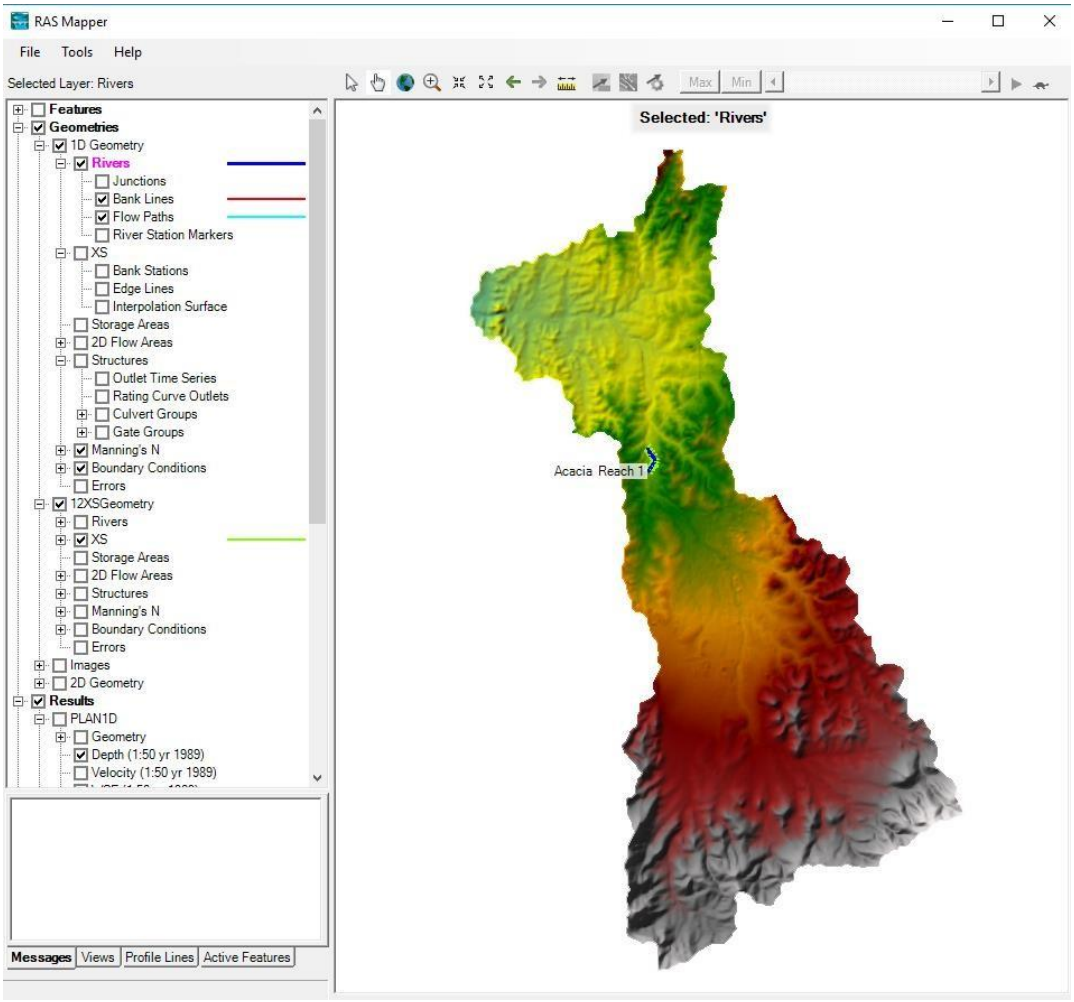

Figure 3-9: Acacia River section in greater Arebbusch catchment DEM.

A total of 12 cross sections have been delineated for the Acacia River reach with station numbers ranging from 85 on the upstream side to station number 30 on the downstream side. A bridge has been inserted between cross sections 70 and 65 and has been marked as station 68 (indicating the Acacia Bridge). The bridge section data has been entered by making use of the Bridge/Culvert icon in the Geometric Data window. Here the Deck/Roadway, Pier and Bridge Modelling Approach data is entered by making use of each of the icons in the newly opened Bridge/Culvert window.

HEC-RAS computes energy losses caused by structures such as bridges and culverts in three parts, and these include [31][32]:

1. Losses that occur in the reach immediately downstream from the structure where expansion of flow takes place.
2. Losses at the structure itself, which can be modelled with several different methods.
3. Losses that occur in the reach immediately upstream of the structure where flow is contracting to get through underneath the bridge openings.

To set up the bridge correctly 4 defined cross sections need to be established, these can be described as follows:

1. Cross section 1 which is located sufficiently downstream from the bridge so that flow is not affected by the structure (i.e. enough space given for the flow to fully expand).
2. Cross section 2 which is located immediately downstream from the bridge, representing the natural ground just outside the bridge.
3. Cross section 3 which is located just upstream of the bridge, reflecting the length required for the abrupt acceleration and contraction of the flow occurring in the immediate area of the opening.
4. Cross section 4 which is an upstream cross section where flow lines are approximately parallel and the cross section is fully effective [1][2][3][32].

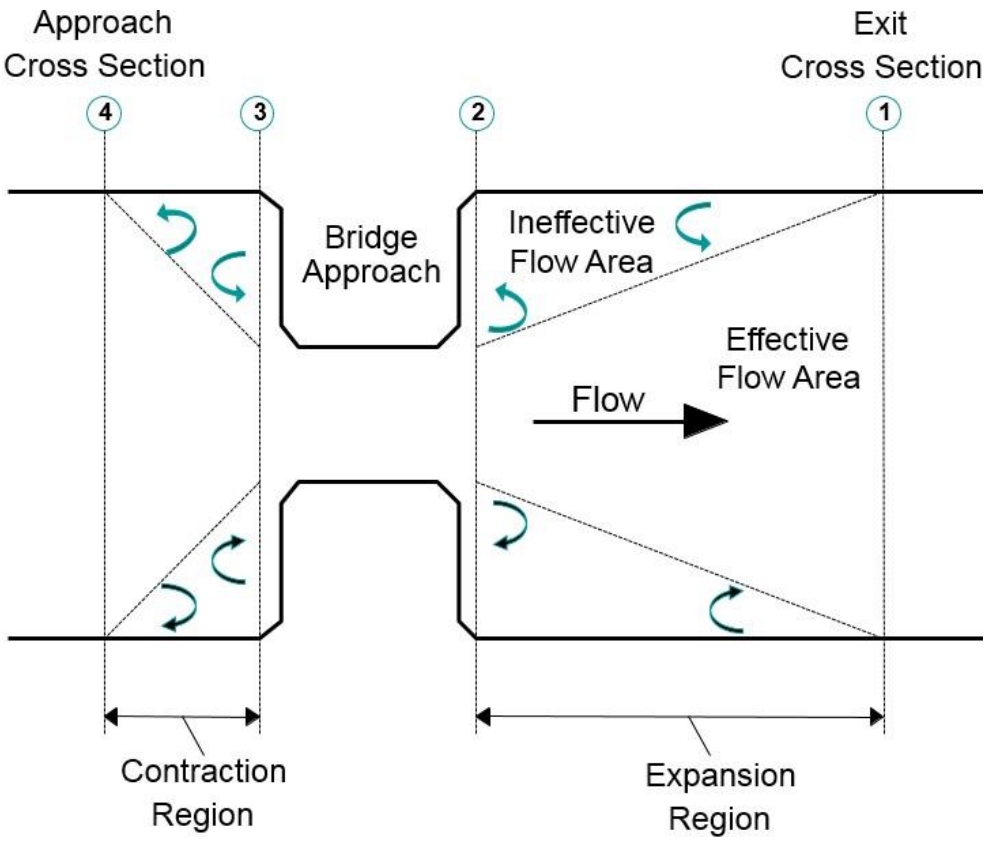

Figure 3-10: Bridge flow contraction and expansion regions (Source: [32])

The bridge dimensions used are summarized in Figure 3-11 and Figure 3-12.

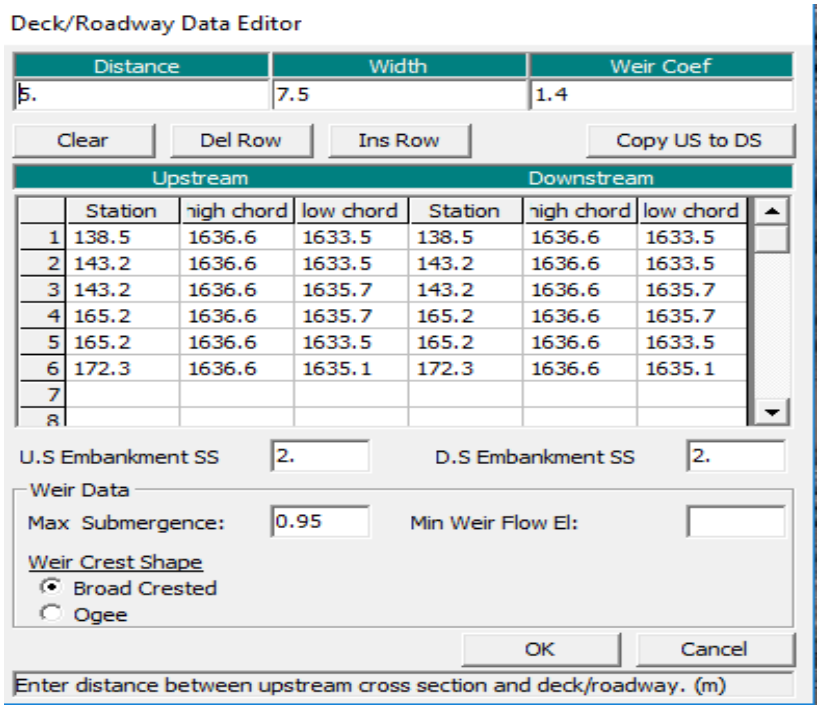

Figure 3-11: Bridge deck HEC-RAS input dimensions

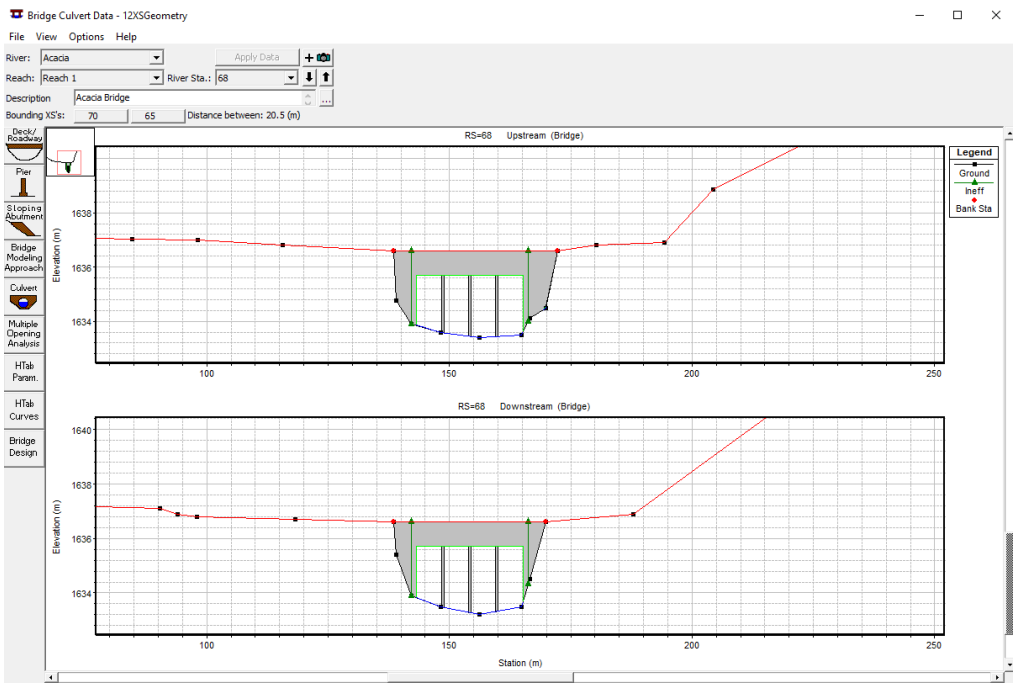

Figure 3-12: Acacia Bridge cross section profile.

The bridge length spans 22 m long with a deck/roadway thickness of 0.9 m. The bridge has three rectangular shaped piers supporting it with thickness of 0.5 m and spaced 5.5 m apart.

3.4 HEC-RAS Steady and Unsteady flow analysis

Once cross section and bridge data have been obtained and entered into HEC-RAS, steady and unsteady flow simulations can then be carried out. From the HEC-RAS main window the Unsteady or Steady Flow Analysis options can be selected from the Run menu, or alternatively from the icons themselves in the window. The main difference between steady and unsteady flow is that the flow parameters such as velocity, pressure, and density of a flow for each point are independent of time in a steady flow whereas they depend on time in unsteady flow [1][13][31][33]. In HEC-RAS flow simulations steady flow analysis only requires the slope/normal/friction depth of the main channel whereas in unsteady flow the boundary conditions require a stage hydrograph and the friction slope and for its initial conditions it requires an initial flow from the upstream station.

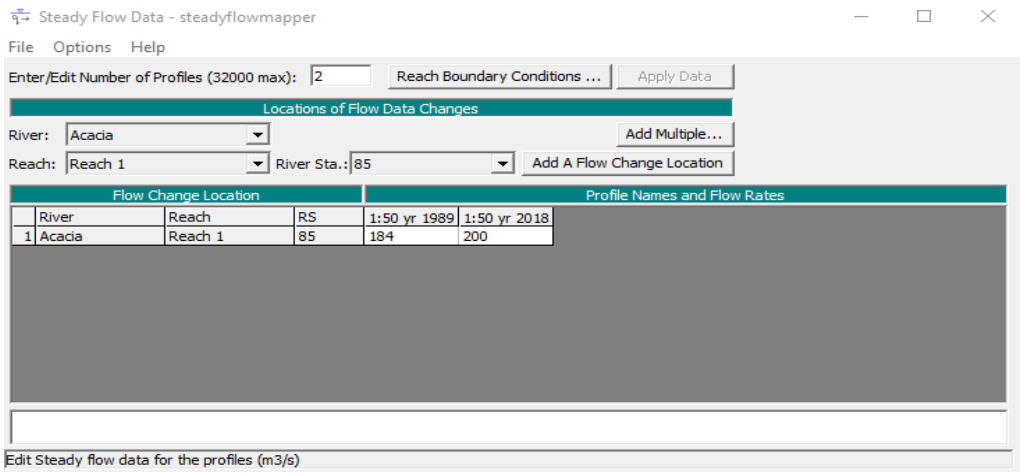

Figure 3-13: Steady flow data input window.

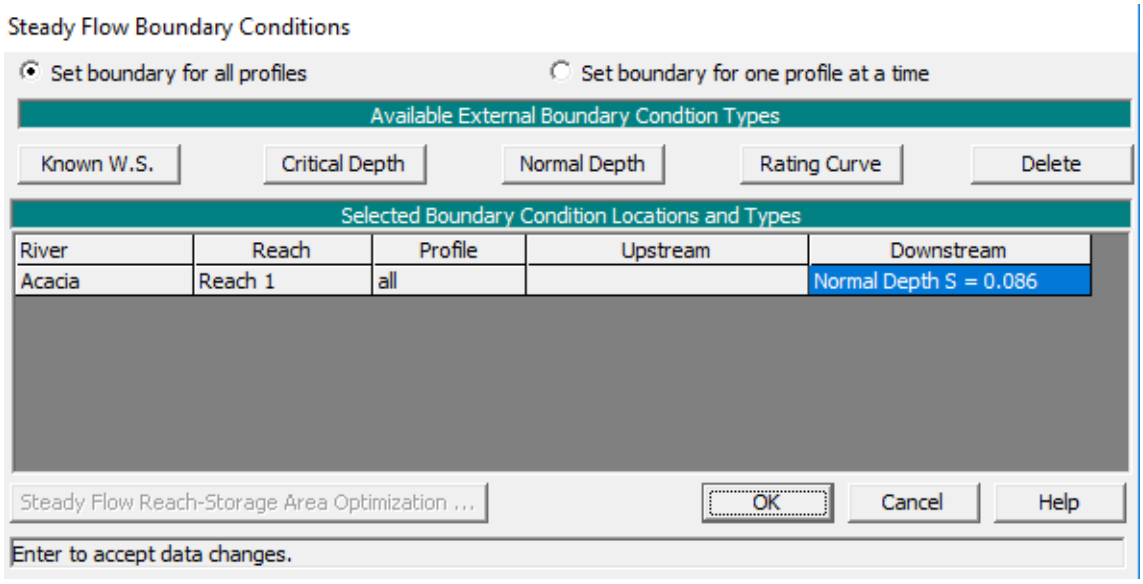

Figure 3-14: Steady flow boundary conditions input window.

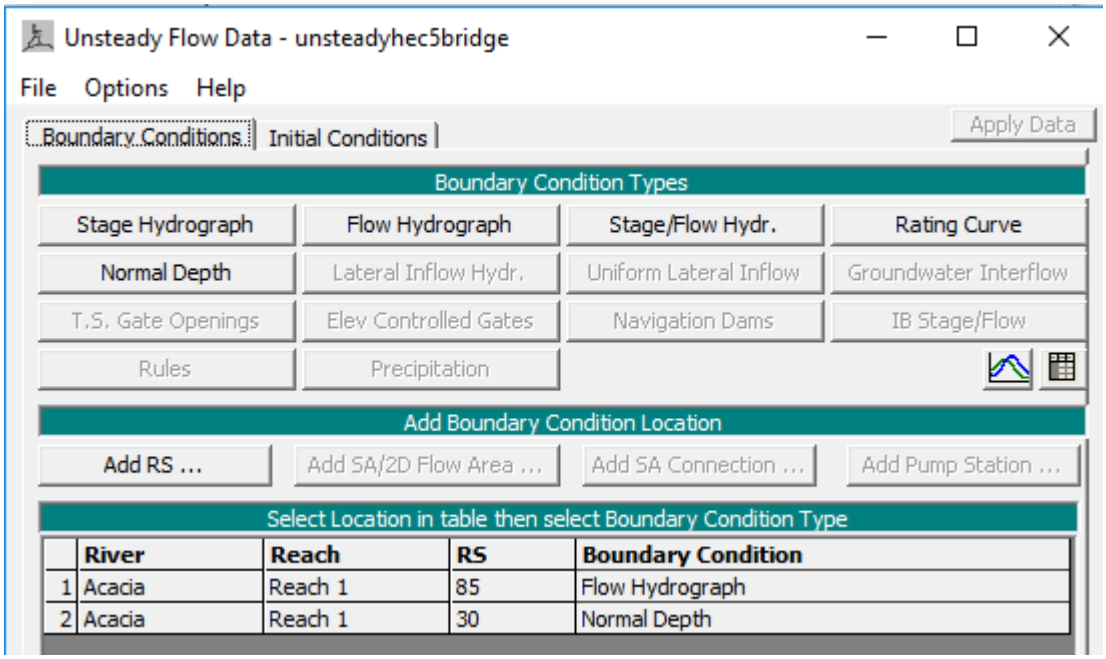

Figure 3-15: Unsteady flow boundary conditions input window.

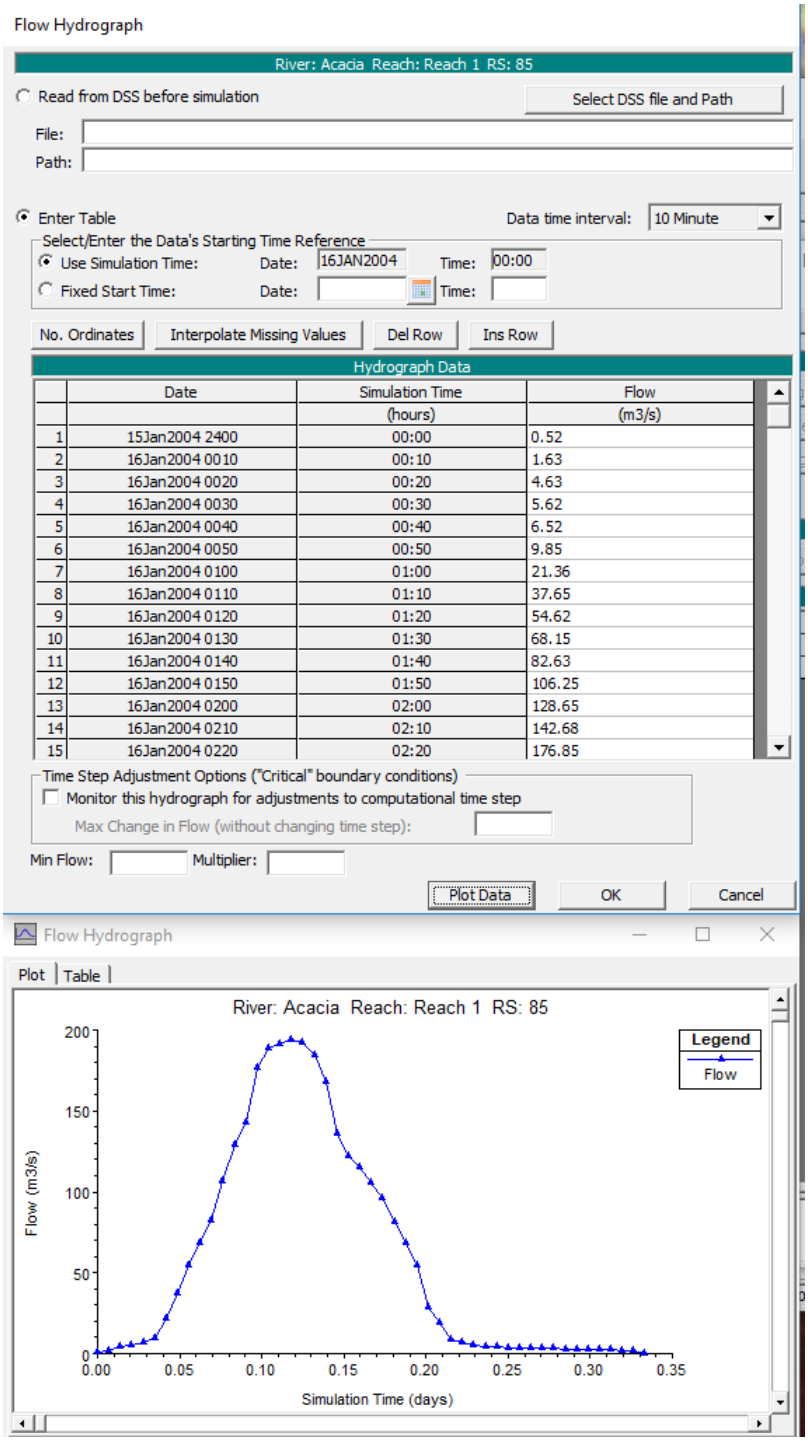

Figure 3-16: Unsteady flow, hydrograph input table and graphical plot.

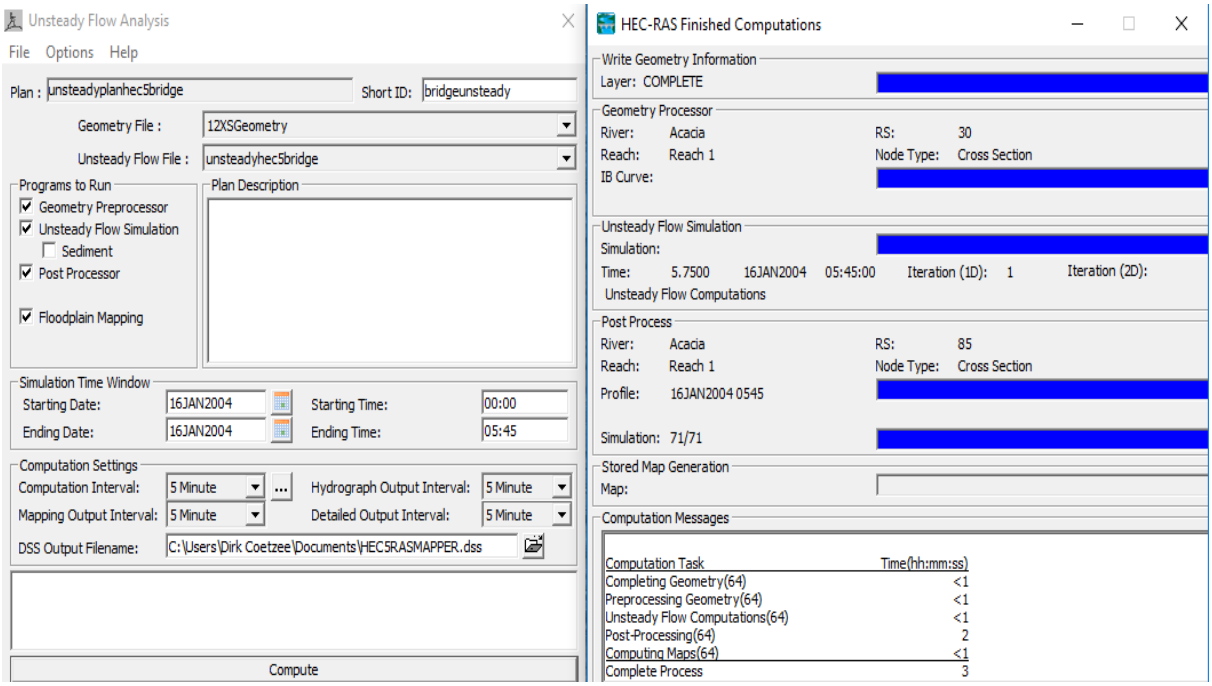

Figure 3-17: Unsteady flow simulation run input window.

3.5 Remote sensing

The Landsat and Sentinel land cover images were downloaded from the USGS EarthExplorer website and contain various colour spectrum bands; which alludes that the important bands for work had to be combined to make a composite image. Landsat 5 had the data for the 1989 (30 m cell size) land cover while more precise imaging was obtained through the Sentinel 2A data for 2018 (10 m cell size). The RGB spectrum was used for both images, meaning that composite band images were made for both years by only making use of the RED, Green and Blue colour spectrums. This process was made possible by using the System Toolboxes of ArcMap with the following sequence: System Toolboxes> Data Management Tools> Raster> Raster Processing> Composite Bands.

Once the composite images were produced, supervised and unsupervised classification was made use of to classify the land cover of the 1989 and 2018 Acacia sub catchments.

Using the Image Classification tool bar, the 1989 Landsat 5 image was used to firstly create training samples which give the programs algorithm some grouping mechanism for classifying different coloured pixels. The training samples are then saved in a signature file and then Maximum Likelihood Classification is run on the image. The same process was carried out on the 2018 Sentinel 2A image. Both 2018 classified Sentinel images were resampled to 30x30 m so as to make them identical to that of the Landsat 5 images size. Nearest resampling was chosen as it applies to land cover data.

Once resampling was done the next step was to calculate the areas of the various land cover classes. This was made possible by analysing the Attribute tables of the each of the four classified images in ArcMap. The Attribute Tables of the images lists the number of pixels assigned to each land cover class. A simple conversion from pixels to kilometres squared is possible by multiplying each pixel with the cell size which in both image classes is 30x30 m now that the images have been resampled.

The next process to follow is the accuracy assessment of the classified images. This process consists of 4 sub sections:

- Calculation of sample size,
- Selection and distribution of samples/reference points on both original Landsat and Sentinel images,
- Production of confusion matrices (ArcMap to excel exports),

- Calculation of accuracy indicators.

Calculation of sample size is carried out by either making use of the rule of thumb that the samples size should be at least 20 to 100 samples per class [34] or by making use of Eq. 15. Selection of appropriate sampling and distribution techniques is obtained through literature review. Different sampling allocations favour different estimation objectives, i.e. equal sample size favours estimation of user's accuracy, while proportional allocation usually results in smaller standard errors for producer's and overall accuracy. As a compromise, it is suggested to use a sample allocation somewhere in between same and proportional allocation, taking into account a minimum sample size per stratum. For land cover maps it is recommended to use stratified random sampling [35].

By making use of ArcMap's System Toolboxes random points can be created over the study area. System Toolboxes>Data Management Tools>Sampling>Create Random Points. Once the random points have been produced the next step is to use ArcMap's Add Base map option to import Google Earth imagery which can depict the study area in higher detail. This base map along with the unclassified Landsat 1989 and Sentinel 2018 Acacia sub-catchment-clipped images, each of the random points can be individually identified and given an appropriate classification. Random points for both 1989 and 2018 will be produced. These two random point sets will then be combined with the 1989 and 2018 supervised and unsupervised classified images to produce extracted points by making use of the ArcMap System Toolboxes>Spatial Analyst Tools>Extract by points tool. Four individual extracted shape files will then have been created from the random points, these being supervised and unsupervised 1989 files as well as supervised

and unsupervised 2018 files. The next step is to produce frequency tables which create a new table containing unique field values and the number of occurrences of each unique field value. The frequency table is created by making use of the following flow sequence in ArcMap System Toolboxes>Analysis Tools>Statistics>Frequency tool. The last step is to pivot the table into the required confusion matrix, which is obtained by making use System Toolboxes>Data Management Tools>Table>Pivot Table tool. The four confusion matrices can then be exported to Microsoft Excel and the accuracy indicators can then be calculated using the methods listed in section 2.8.

3.6 Research instruments

The following instruments were used during the river section field survey:

- Bushnell Yardage Pro Compact 800 laser (distance measuring device).

  The laser measuring device emits infrared energy pulses by making use of a sophisticated circuitry and a high-speed clock, to instantaneously calculate distance, by measuring the time it takes for each pulse to travel from the rangefinder to the target and back.

  The rangefinder was used to ascertain distances between river cross sections as well as distances along the longitudinal section of the river for slope calculations.

- Garmin eTrex 10 GPS: Is a rugged handheld navigator with preloaded worldwide base maps and a 2.2-inch monochrome display, featuring a WAAS-enabled GPS receiver with HotFix and GLONASS support. The GPS device was used to ascertain the geographic positions of the river cross sections as well as the positions where the dumpy level was set-up.

- A measuring staff was used to measure the length of the bridge columns during benchmarking as well as river cross section depth measurements.
- Shokkisha Tokyo 124624 B2 dumpy level. A dumpy level is an optical surveying levelling instrument consisting of a telescope tube firmly secured in two collars fixed by adjusting screws to a platform by a vertical spindle. The telescope can rotate only in the horizontal plane. The dumpy level was used to ascertain cross section depths as well as the relative elevation change along the river section.
- A spirit level. Is a device consisting of a sealed glass tube partially filled with alcohol or another liquid, containing an air bubble whose position reveals a perfectly level surface. The spirit level was used to make sure the levelling staff was positioned level and straight.
- A notebook was used for jotting down field measurements, observations, data and comments. A camera was used to take pictures of all the important features and observations.

3.7 Statistical Analysis

Microsoft Excel was used to run the t-test which was used to prove/disprove the hypothesis listed in section 1.4. The t-test is defined as any statistical hypothesis test in which the test statistic follows a t distribution if the null hypothesis is supported. The t-test is used to measure the difference between two sets of data. It calculates the averages, variances and standard deviations of the two data sets then it does a test that determines whether or not the means of the two data sets are significantly different.

3.8 Research ethics

Research ethics have been ensured throughout every aspect of the research with regards to properly acknowledging and crediting cited works of other researchers and publishers, with the exception of making use of general knowledge. No animal or human participants were required in this research. Formal assistance and permission to conduct field measurements from the Acacia River have been obtained from City of Windhoek Municipality and Ministry of Agriculture, Water and Forestry. Permission from Aurecon Consulting Engineers as well as DHI (Institute for Water and Environment) Software Company was obtained to gain access to their consulting publications on hydraulic modelling.

4. RESULTS

The chapter covers the results of the calculations and model simulations conducted as described by the procedures in the previous chapter.

4.1 Catchment characteristics

Table 4-1 gives an overview of the catchment characteristics. Although Windhoek is described as being a City encased by steep hills [4], the sub-catchment is fairly flat as it can be deduced from the averaged channel slope of 0.086 m/m, indicating that for every 100 m of channel length the drop-in elevation is around 1 m for simplification. Furthermore, the sub-catchments bell/circular-shape coincides with the phenomena pointed out by Figure 2-2 as well as the hydrograph depicted in Figure 2-16, indicating that circular shaped catchments produce a shorter concentration time with a higher peak discharge in comparison with an elongated catchment.

Table 4-1: Summary of Acacia and Arebbusch catchment characteristics.

Catchment Parameter	Acacia Sub-Catchment	Arebbusch Catchment
Area (km^2)	93	141
Length of Longest Watercourse (km)	17.3	26.3
Length of Centroid (km)	9.5	12.8
Average Channel Slope (m/m)	0.086	N/A
Time of Concentration (hr)	3.00	N/A

4.2 Image classification and area determination

Figures 4-1 and 4-2 depict the supervised and unsupervised classified images of the Acacia sub-catchment. Some conclusions can be drawn from the images, these being the doubling of urban land cover coverage, a more stratified coverage in the supervised classification while a more sectioned/grouped coverage in the unsupervised images and the most prevalent land cover in all images being grasslands followed by trees and shrubs.

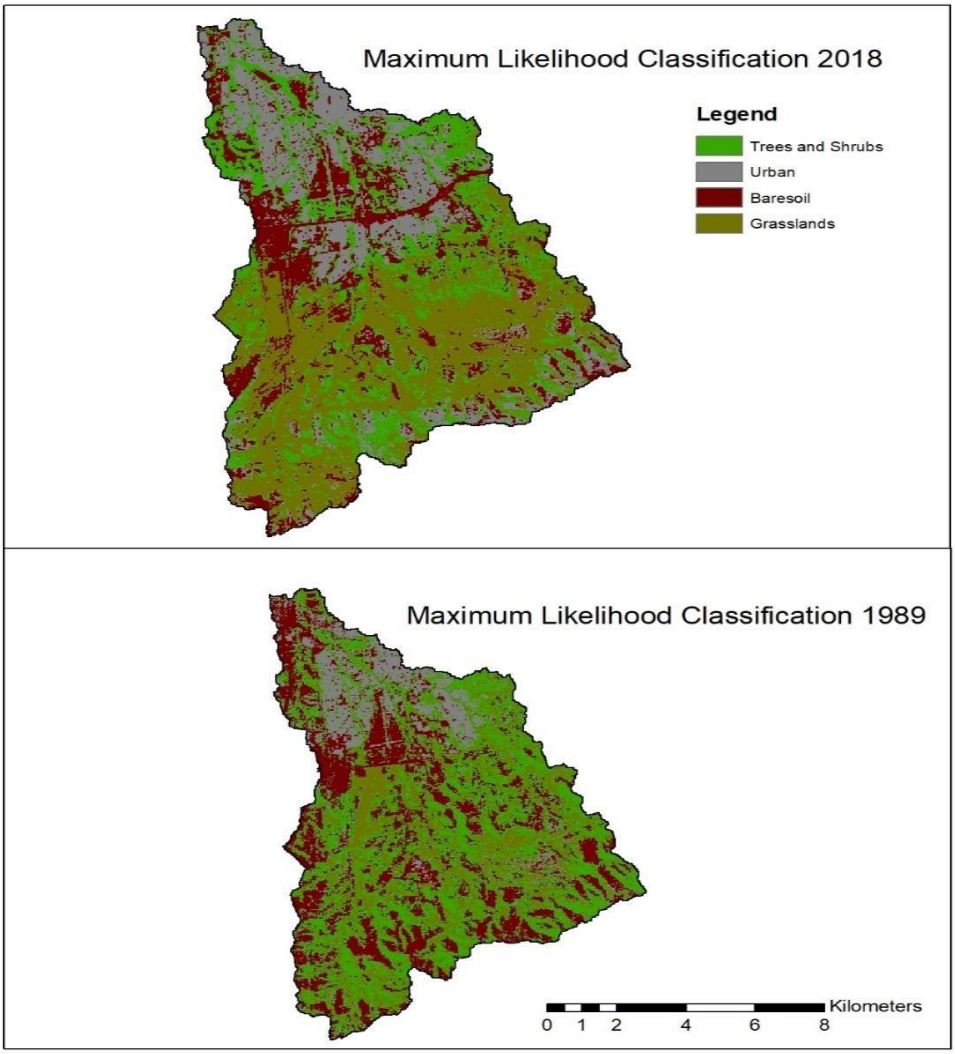

Figure 4-1: Supervised classification 1989 and 2018 land cover, Acacia sub-catchment.

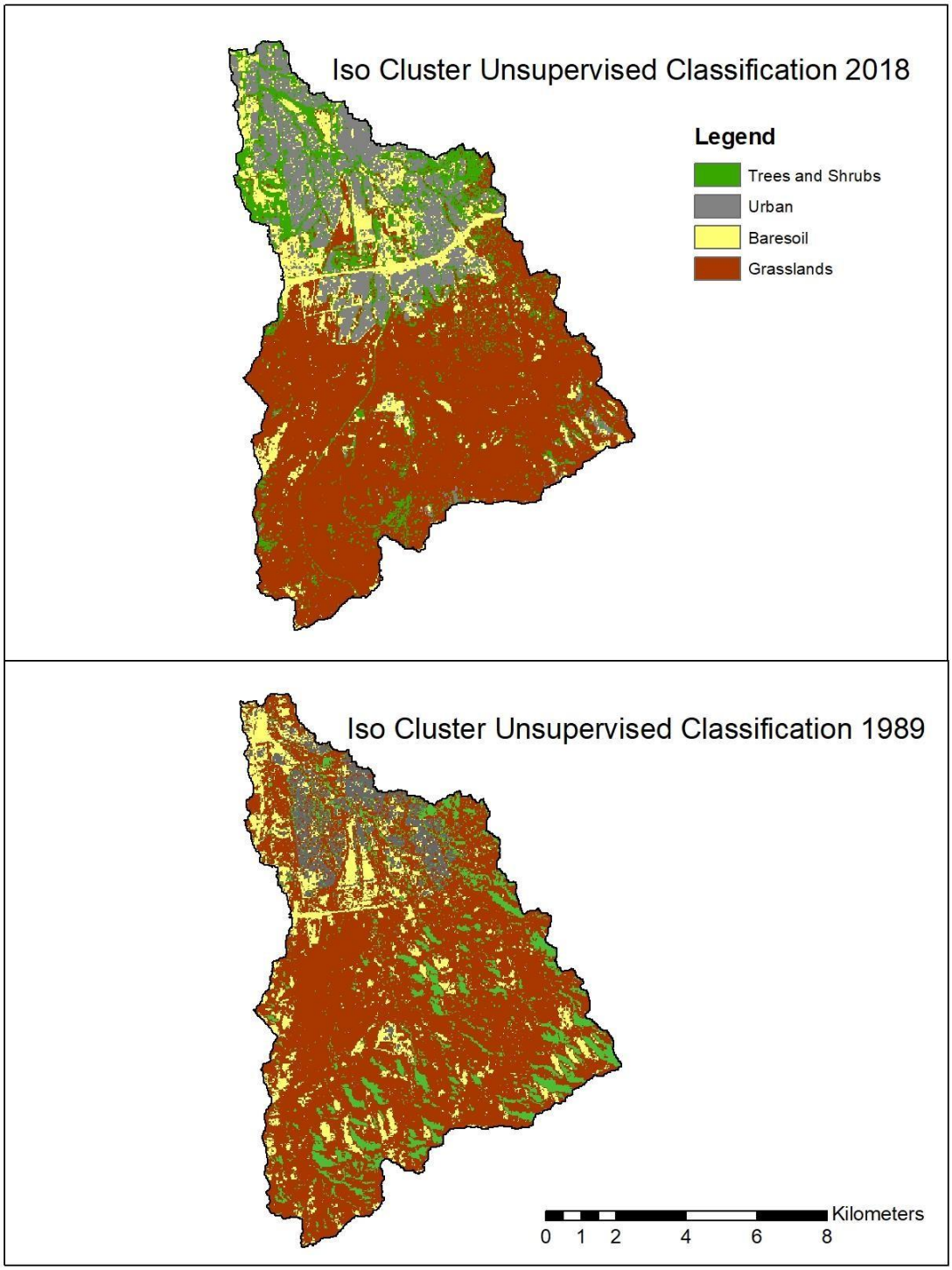

Figure 4-2: Unsupervised classification 1989 and 2018 land cover, Acacia sub-catchment.

Table 4-2 gives a summary of the land cover results. The important values required were the percentage of urban coverage to that of rural coverage.

Supervised: Rural coverage for the 2018 supervised image consisted of 100% Grasslands (53 km^2) and 100% Trees and shrubs (11 km^2) land cover, while urban coverage was attributed by 100% Urban (22 km^2) and 100% Baresoil (6 km^2) land cover. In the 1989 supervised image, Rural coverage was attributed by 100% Grasslands (42 km^2), 100% Trees and shrubs (24 km^2) and 50% Baresoil (6 km^2), while urban coverage was attributed by 100% Urban (11 km^2) and 50% Baresoil (6 km^2).

Unsupervised: Rural coverage for the 2018 unsupervised image consisted of 100% Grasslands (47 km^2) and 100% Trees and shrubs (17 km^2) land cover, while urban coverage was attributed by 100% Urban (18 km^2) and 100% Baresoil (11 km^2) land cover. In the 1989 unsupervised image, Rural coverage was attributed by 100% Grasslands (48 km^2), 100% Trees and shrubs (21 km^2) and 50% Baresoil (7 km^2), while urban coverage was attributed by 100% Urban (9 km^2) and 50% Baresoil (7 km^2).

Table 4-2: Urban and rural land cover summary table.

	Supervised Classification				**Unsupervised Classification**			
Class	1989 (Area km^2)	2018 (Area km^2)	1989 (Area %)	2018 (Area %)	1989 (Area km^2)	2018 (Area km^2)	1989 (Area %)	2018 (Area %)
Baresoil	16.358	6.362	17.65	6.86	14.612	11.024	15.76	11.89
Grassland	42.035	52.889	45.34	57.05	48.198	46.921	51.99	50.61
Trees and Shrubs	23.518	11.477	25.37	12.38	21.263	16.536	22.94	17.84
Urban	10.795	21.978	11.64	23.71	8.633	18.225	9.31	19.66
Total Area	**92.706**	**92.706**	**100**	**100**	**92.706**	**92.706**	**100**	**100**
Total Rural	**73.732**	**64.366**	**79.53**	**69.43**	**76.767**	**63.457**	**82.81**	**68.45**
Total Urban	**18.974**	**28.340**	**20.47**	**30.57**	**15.939**	**29.249**	**17.19**	**31.55**

Supervised classification runoff coefficient, peak flow calculation results:

2018: Q_{50} = 211 m^3/s 1989: Q_{50} = 189m^3/s

Unsupervised classification runoff coefficient, peak flow calculation results:

2018: Q_{50} = 221 m^3/s 1989: Q_{50} = 190m^3/s

Mean 2018: Q_{50} = 216 m^3/s Mean 1989: Q_{50} = 190m^3/s

Image calculation accuracy assessment:

By making use of the steps outlined in section 3.5 as well as the equations mentioned in section 2.8 the following accuracy assessment results and tables were obtained.

- Sample size calculated using Eq. 15 with:

  p = expected percent accuracy 85%

  q = 100 – p = 15%

  e = allowable error of 10%

  z = 2 (from the standard normal deviate of 1.96 for the 95% two-sided confidence level)

  Therefore, samples size is equal to 51.
- Stratified random sampling is chosen as it is related to land cover imagery.
- Confusion matrices:

The 1989 supervised image achieved an overall accuracy of 74%. Grasslands was the best classified class (81%), followed closely by trees and shrubs (79%) and then baresoil with 73%. Urban had the least user's accuracy (66%), where a third of its area was commissioned to other classes (Table 4-3). A similar trend for the supervised image classification was achieved in 2018 for the overall accuracy of 80% as shown in Table 4-4. Baresoil was the best classified class in 2018 (86%), while urban cover improved to nearly 80%. Trees and shrubs had a decreased accuracy of 76%, while grasslands increased minutely to 82% from the 1989 classification.

Table 4-3: Confusion Matrix – Supervised classification – 1989 results.

CM-ML-1989								
	Ground Truth/Reference data						Accuracy Indicator	
Classified data		Trees and Shrubs	Urban	Bairsoil	Grasslands	Row Total	Commision Error	User's Accuracy
	Trees and Shrubs	37	6	2	2	47	21.28%	78.72%
	Urban	5	35	7	6	53	33.96%	66.04%
	Baresoil	4	7	41	4	56	26.79%	73.21%
	Grasslands	5	3	1	39	48	18.75%	81.25%
	Column Total	51	51	51	51	204	Overall Accuracy	Kappa
Accu/Ind	Ommision Error	27.45%	31.37%	19.61%	23.53%		74.51%	0.660
	Producer's Accuracy	72.55%	68.63%	80.39%	76.47%			

Table 4-4: Confusion Matrix – Supervised classification – 2018 results.

CM-ML-2018								
	Ground Truth/Reference data						Accuracy Indicator	
Classified data		Trees and Shrubs	Urban	Bairsoil	Grasslands	Row Total	Commision Error	User's Accuracy
	Trees and Shrubs	42	3	4	6	55	23.64%	76.36%
	Urban	2	45	7	3	57	21.05%	78.95%
	Baresoil	2	2	37	2	43	13.95%	86.05%
	Grasslands	5	1	3	40	49	18.37%	81.63%
	Column Total	51	51	51	51	204	Overall Accuracy	Kappa
Accu/Ind	Ommision Error	17.65%	11.76%	27.45%	21.57%		80.39%	0.739
	Producer's Accuracy	82.35%	88.24%	72.55%	78.43%			

There was no significant difference for the unsupervised classifications in both the 1989 and 2018 images (Tables 4-5 and 4-6). Both images achieved a slightly lower overall accuracy of 72% and 79% in 1989 and 2018, respectively. The same trend of increased user's accuracy values was obtained for three of the 2018 unsupervised image classes, with the exception being trees and shrubs which had a decreased accuracy of 70%.

Table 4-5: Confusion Matrix – Unsupervised classification – 1989 results.

CM-ISO-1989								
	Ground Truth/Reference data						Accuracy Indicator	
Classified data		Trees and Shrubs	Urban	Bairsoil	Grasslands	Row Total	Commision Error	User's Accuracy
	Trees and Shrubs	34	0	0	4	38	10.53%	89.47%
	Urban	3	38	7	2	50	24.00%	76.00%
	Baresoil	8	5	35	5	53	33.96%	66.04%
	Grasslands	6	8	9	40	63	36.51%	63.49%
	Column Total	51	51	51	51	204	Overall Accuracy	Kappa
Accu/Ind	Ommision Error	33.33%	25.49%	31.37%	21.57%		72.06%	0.627
	Producer's Accuracy	66.67%	74.51%	68.63%	78.43%			

Table 4-6: Confusion Matrix – Unsupervised classification – 2018 results.

CM-ISO-2018								
	Ground Truth/Reference data						Accuracy Indicator	
Classified data		Trees and Shrubs	Urban	Bairsoil	Grasslands	Row Total	Commision Error	User's Accuracy
	Trees and Shrubs	40	4	7	6	57	29.82%	70.18%
	Urban	5	42	5	0	52	19.23%	80.77%
	Baresoil	4	2	38	2	46	17.39%	82.61%
	Grasslands	2	3	1	43	49	12.24%	87.76%
	Column Total	51	51	51	51	204	Overall Accuracy	Kappa
Accu/Ind	Ommision Error	21.57%	17.65%	25.49%	15.69%		79.90%	0.732
	Producer's Accuracy	78.43%	82.35%	74.51%	84.31%			

4.3 Alternative Rational Method Calculation

Following the steps listed in section 3.2 obtained from the SANRAL and Namibian Drainage manuals, Table 4-7 was produced, which gives a summary of the results obtained. In summary the peak flow values increased by 13.8% from 190 m^3/s in 1989 to 216 m^3/s 2018 resulting from the increased urban area in the Capital.

Table 4-7: Summary of Rational Method calculation steps and results.

STEP	Descriptio	Required Input/Parameters	Result/s	Units
1	Catchment Area	ArcGIS software	93	km2
		Landsat or Sentinel Images		
		1:50 000 and 1:10 000 scale maps and		
2	Length of Longest Watercourse	ALOS 30m DEM	17.3	km
		ArcMap software		
3	Average Slope	1085-Slope Method	0.086	m/m
	of Longest Watercourse	Length of longest watercourse		
		Elevation @ 85% of LLW		
		Elevation @ 10% of LLW		
4	Time of Concentration	Kirpich Formula	3	hrs
		Average slope		
		Hydraulic length of catchment		
5	Run-off coefficient	Weighted average equation	2018=0.419	N/A
		Runoff coefficient for rural area (C1)		
		Runoff coefficient for urban area (C2)	1989=0.375	N/A
		% of catchment defined as rural (α)		
		% of catchment defined as urban (β)		
		Tables [], [] and []		
6	Design Rainfall/	Depth-Duration-Frequency diagram	70	mm
	Point Rainfall Depth	Time of concentration		
		Specified return period (1:50 year)		
		Mean annual precipitation (MAP)		
7	Rainfall Point Intensity	Point rainfall depth	23.33	mm/hr
		Time of concentration		
8	Area Reduction Factor	UK Flood Studies Report ARF Equation	83.5	%
		ARF Alexander graph, Figure []		
9	Average Rainfall Intensity/	Area reduction factor as a percentage		
	Effective Catchment Precipitation	Rainfall point intensity	19.5	mm/hr
10	Averaged Peak Flow	Run-off coefficient	2018=216	m3/s
		Average rainfall intensity		
		Catchment area	1989=190	m3/s

4.4 Aurecon 2017 Flood line Analysis findings

Presented at the 2017 WaterNet conference and compiled by Mr. Nicholas Walker of Aurecon Consulting Engineers the following results were obtained from their 2017 flood line analysis in the Capital on a catchment similar in size to the Acacia sub- catchment. These results are compared with the results obtained in Table 4-7. Catchment two, as depicted in Figure 4-3 and summarized in Table 4-8 has an area of 38.42 km2 which is around 55 km2 smaller than the Acacia sub-catchment analysed in this report. The two catchments do share similar topographic similarities with both catchments split into urban and rural areas and both catchments having the Auas Mountain range in the south with urban development in the North. Further values comparable are the increased time of concentration, length of longest watercourse and length of centroid which are all attributed to the increased catchment size. The mean value of the flood peaks calculated is summarized in Table 4-9 from the three methods used in their study. This value of 145 m^3/s is comparable with the 216 m^3/s mean value generated in the Acacia sub-catchment, the added flow being attributed to the increased area coverage.

Table 4-8: Aurecon 2017 Flood line analysis catchment characteristics (Source: [30]).

Catchment Parameter	Catchment 1	Catchment 2	Catchment 3
Area (km^2)	2.31	38.42	0.50
Length of Longest Watercourse (km)	3.95	13.55	1.38
Length to Centroid (km)	1.93	7.90	0.60
Average Channel Slope (m/m)	0.0129	0.0175	0.0301
Average catchment slope (%)	6.2	16.0	7.62
Time of concentration (hrs)	1.05	2.41	0.33

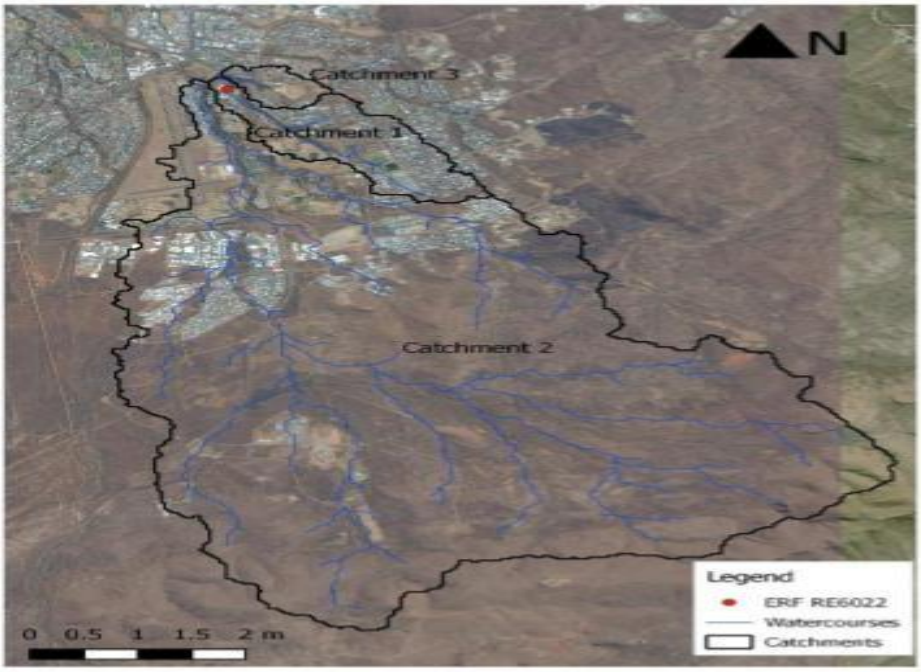

Figure 4-3: Aurecon 2017 Flood line analysis, catchment map (Source: [30]).

Table 4-9: Aurecon 2017 Flood line analysis, flood peak results (Source: [30]).

Flood Estimation Method	1: 50 Year Flood Peak (m^3/s)		
	Catchment 1	Catchment 2	Catchment 3
Rational Method	22.6	143.7	9.1
SCS	24.4	-	-
Unit Hydrograph	-	148	-
Recommended Peak	**23**	**145**	**9**

4.5 Statistical Analysis (t-Test)

Table 4-10 indicates the results of the statistical analysis done on the two peak flow values obtained from the two methods used in attaining the runoff coefficients for the two study years (1989 and 2018); as the runoff coefficient values were the determining variable in the Rational Method linear equation. The critical value to be observed is that of the P-value. The P-value for both tests are significantly lower than the 5% alpha value,

indicating a rejection of the Null Hypothesis and acceptance of the alternative hypothesis. As mentioned in section 1.4, the alternative hypothesis states that there is a significant difference in the flood peaks produced for the two varying urban developed catchments.

Table 4-10: Microsoft Excel peak flow t-Test results (1989 vs 2018).

2018.00		*1989.00*	
Mean	212.00	Mean	186.33
Standard Error	4.93	Standard Erro	3.18
Median	211.00	Median	189.00
Mode	#N/A	Mode	#N/A
Standard Deviation	8.54	Standard Dev	5.51
Sample Variance	73.00	Sample Varia	30.33
Kurtosis	#DIV/0!	Kurtosis	#DIV/0!
Skewness	0.52	Skewness	-1.67
Range	17.00	Range	10.00
Minimum	204.00	Minimum	180.00
Maximum	221.00	Maximum	190.00
Sum	636.00	Sum	559.00
Count	3.00	Count	3.00

t-Test: Two-Sample Assuming Equal Variances			
	2018.00	*1989.00*	
Mean	212.00	186.33	
Variance	73.00	30.33	
Observations	3.00	3.00	
Pooled Variance	51.67		
Hypothesized Mean Difference	0.00		
df	4.00		
t Stat	4.37		
P(T<=t) one-tail	0.01	<	0.05
t Critical one-tail	2.13		
P(T<=t) two-tail	0.01	<	0.05
t Critical two-tail	2.78		

t-Test: Two-Sample Assuming Unequal Variances			
	2018.00	*1989.00*	
Mean	212.00	186.33	
Variance	73.00	30.33	
Observations	3.00	3.00	
Hypothesized Mean Difference	0.00		
df	3.00		
t Stat	4.37		
P(T<=t) one-tail	0.01	<	0.05
t Critical one-tail	2.35		
P(T<=t) two-tail	0.02	<	0.05
t Critical two-tail	3.18		

4.6 HEC-RAS Model

Various input data has been fed into the HEC-RAS program and its simulation algorithms have been run and the following graphs and tables give an indication of the steady and unsteady flow (SF; USF) simulations.

Steady flow simulations:

In both steady and unsteady flow simulations the critical position in the longitudinal profile is at 618 m in the chainage, this is the position just upstream of the Acacia Bridge.

It should be noted that the profile plots have three critical lines indicating Energy grade (EG), Water surface (WS) and Critical depth (Crit) (related to Figure 2-5 in section 2); with each of the three having plots for both 2018 and 1989 simulations.

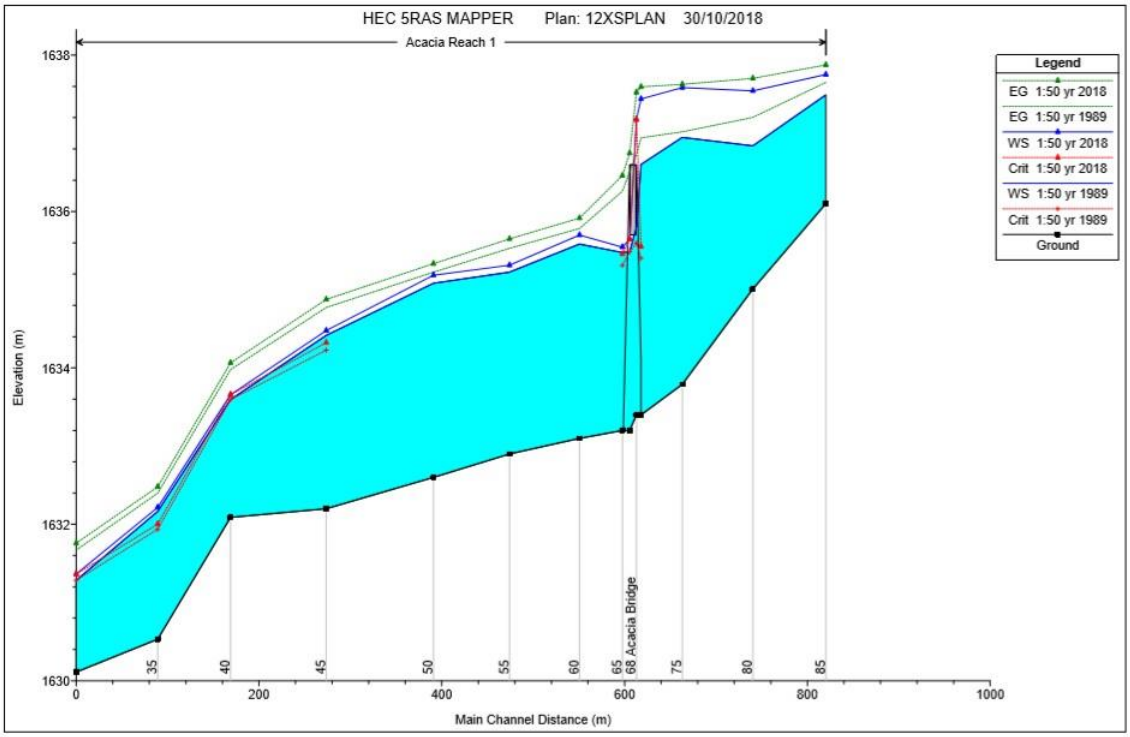

Figure 4-4: Acacia River longitudinal profile, 1989 and 2018 flood peak levels (SF).

Table 4-11 gives an overview of the elevations of the EG, WS and Crit for 2018 and 1989 steady flow simulations. The water surface elevation almost increases by a meter as it flows over the bridge for the 2018 flow (Figure 4-3), this indicates the consequence of the additional discharge accumulated in the catchment.

Table 4-11: Steady flow simulation profile-plot results (1989 vs 2018).

Chainage (m)	Variable	Year	Elevation (m)	Difference (2018-1989) (m)
618	E.G	2018	1637.6	
618	E.G	1989	1636.94	0.66
618	W.S	2018	1637.44	
618	W.S	1989	1636.6	0.84
613	Crit	2018	1637.18	
613	Crit	1989	1635.6	1.58

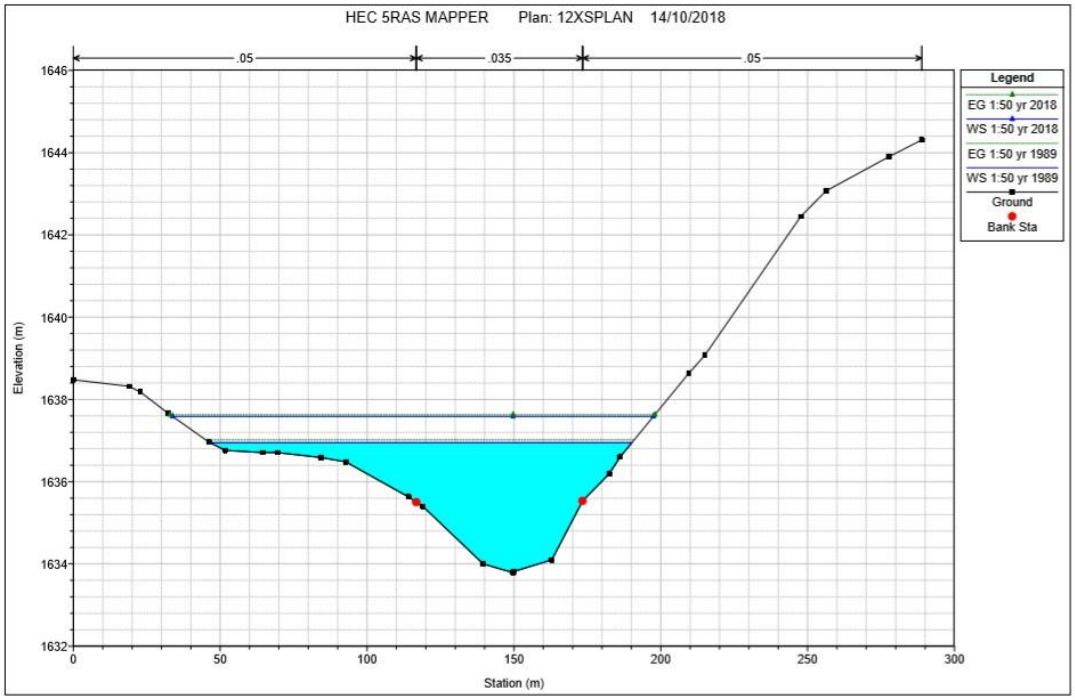

Figure 4-5: River station 75 cross section profile, 1989 and 2018 flood peak levels (SF).

In Figure 4-5 it can be deduced that both 1989 and 2018 1:50-year flood peak values manage to flow above the bank stations of the river, this value is calculated as 1.45 m as the WS elevation is 1636.95 m and the bank stations are at an elevation of 1635.5 m. Both

EG elevations share their positions with their corresponding WS elevations, which is constant with steady flow in open channel flow with few to no obstructions.

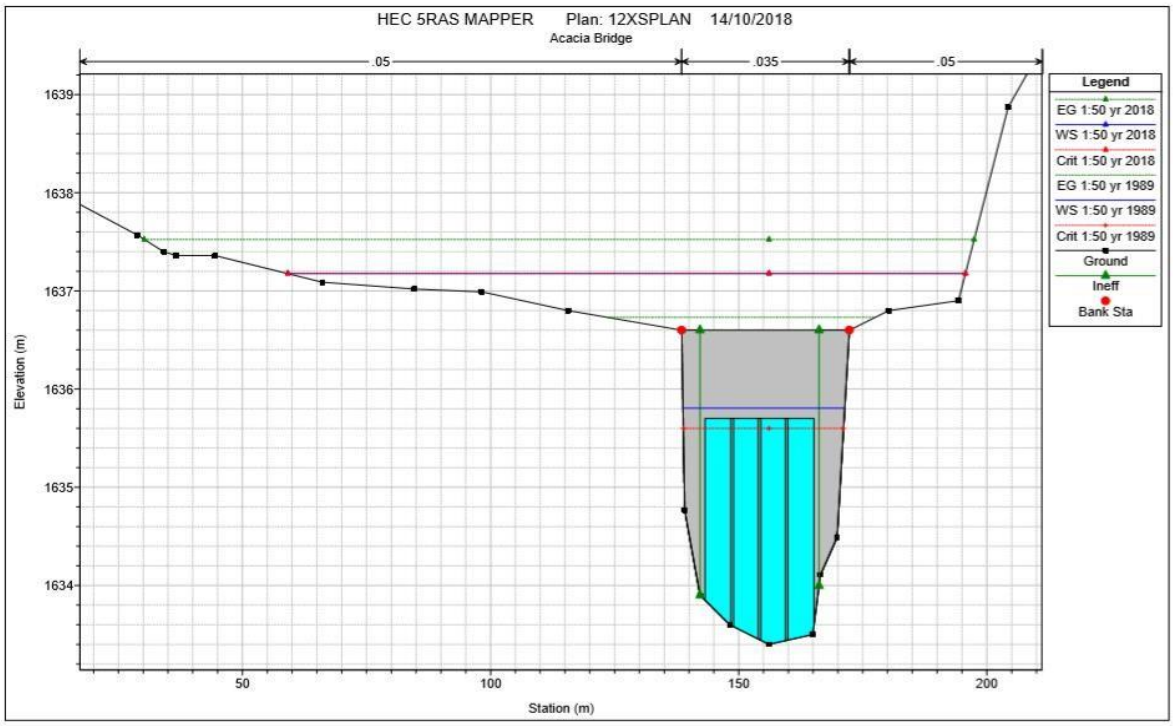

Figure 4-6: Bridge upstream cross section profile, 1989 and 2018 flood peak levels (SF).

The differences in elevation values for Figure 4-6 are identical to that of Table 4-11. Furthermore, the EG elevation difference between the 2018 and 1989 flow is 0.79 m with a critical flow observed above the bridge in the 2018 flow while the critical flow observed in 1989 is under the bridge which is reflected as well in the positions of the WS levels. The slight increase in water level directly after the bridge depicted in Figure 4-4 is consistent with a hydraulic jump observed after an obstruction like the bridge.

Table 4-12 list the critical values observed inside-upstream and downstream of the bridge for the 1989 and 2018 flow profiles. The important values are that of the flow area (44.39 m^2 upstream to 42.16 m^2 downstream), Froude number (upstream 0.88 and downstream 0.95) and the friction loss (upstream 0.19 m and 0.09 m downstream).

Table 4-12: Summary of bridge output steady flow, 1989 and 2018.

Plan: PL12XS Acacia Reach 1 RS: 68 Profile: 1:50 yr 1989

E.G. US. (m)	1636.94	Element	Inside BR US	Inside BR DS
W.S. US. (m)	1636.60	E.G. Elev (m)	1636.73	1636.51
Q Total (m3/s)	189.00	W.S. Elev (m)	1635.81	1635.49
Q Bridge (m3/s)	189.00	Crit W.S. (m)	1635.60	1635.49
Q Weir (m3/s)		Max Chl Dpth (m)	2.41	2.29
Weir Sta Lft (m)		Vel Total (m/s)	4.26	4.48
Weir Sta Rgt (m)		Flow Area (m2)	44.39	42.16
Weir Submerg		Froude # Chl	0.88	0.95
Weir Max Depth (m)		Specif Force (m3)	135.01	130.02
Min El Weir Flow (m)	1636.60	Hydr Depth (m)		2.06
Min El Prs (m)	1635.70	W.P. Total (m)	58.22	36.80
Delta EG (m)	0.68	Conv. Total (m3/s)	1058.6	1319.0
Delta WS (m)	1.12	Top Width (m)		20.50
BR Open Area (m2)	44.39	Frctn Loss (m)	0.19	0.09
BR Open Vel (m/s)	4.48	C & E Loss (m)	0.03	0.12
BR Sluice Coef		Shear Total (N/m2)	238.37	230.70
BR Sel Method	Energy only	Power Total (N/m s)	1014.94	1034.20

Plan: PL12XS Acacia Reach 1 RS: 68 Profile: 1:50 yr 2018

E.G. US. (m)	1637.60	Element	Inside BR US	Inside BR DS
W.S. US. (m)	1637.44	E.G. Elev (m)	1637.52	1636.75
Q Total (m3/s)	211.00	W.S. Elev (m)	1637.18	1635.65
Q Bridge (m3/s)	130.66	Crit W.S. (m)	1637.18	1635.65
Q Weir (m3/s)		Max Chl Dpth (m)	3.78	2.45
Weir Sta Lft (m)		Vel Total (m/s)	2.26	4.65
Weir Sta Rgt (m)		Flow Area (m2)	93.17	45.42
Weir Submerg		Froude # Chl	0.43	0.95
Weir Max Depth (m)		Specif Force (m3)	179.41	150.54
Min El Weir Flow (m)	1636.60	Hydr Depth (m)	0.68	2.22
Min El Prs (m)	1635.70	W.P. Total (m)	195.88	38.07
Delta EG (m)	1.14	Conv. Total (m3/s)	1676.9	1459.8
Delta WS (m)	1.89	Top Width (m)	136.54	20.50
BR Open Area (m2)	44.39	Frctn Loss (m)	0.14	0.10
BR Open Vel (m/s)	2.94	C & E Loss (m)	0.23	0.09
BR Sluice Coef		Shear Total (N/m2)	73.85	244.44
BR Sel Method	Energy only	Power Total (N/m s)	167.24	1135.56

Unsteady flow simulation:

The main difference between the steady and unsteady flow simulation cross section plot-results is that of the maintained WS elevation that is kept constant after the bridge up until station 40 where the water level starts to drop. This is due to the continuous recorded flow rate acquired from the Monravia gauging station upstream from the study area. Figure 3-16 gives an overview of the interpolated flow hydrograph. Figures 4-7 to 4-9 as well as Table 4-13 showcases similar results as the steady flow simulation.

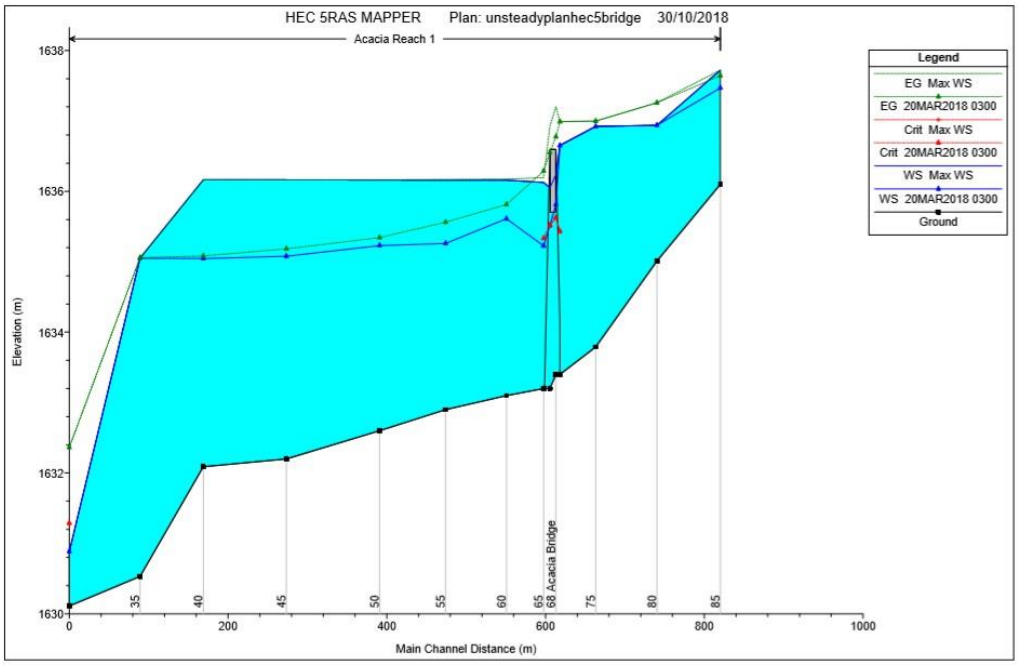

Figure 4-7: Acacia River longitudinal profile, 2018 flood peak levels (USF).

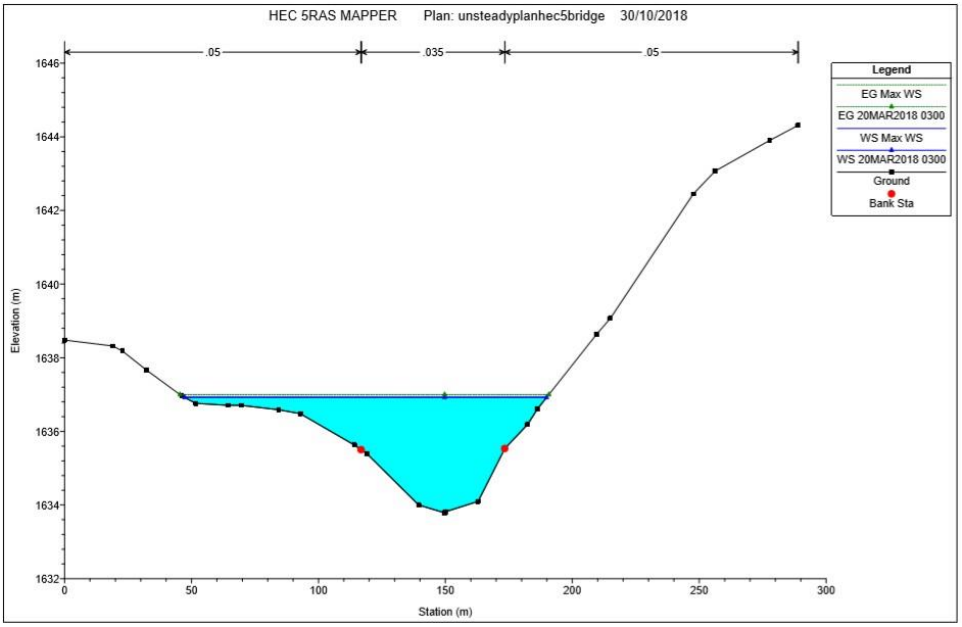

Figure 4-8: River station 75 cross section profile, 2018 flood peak levels (USF).

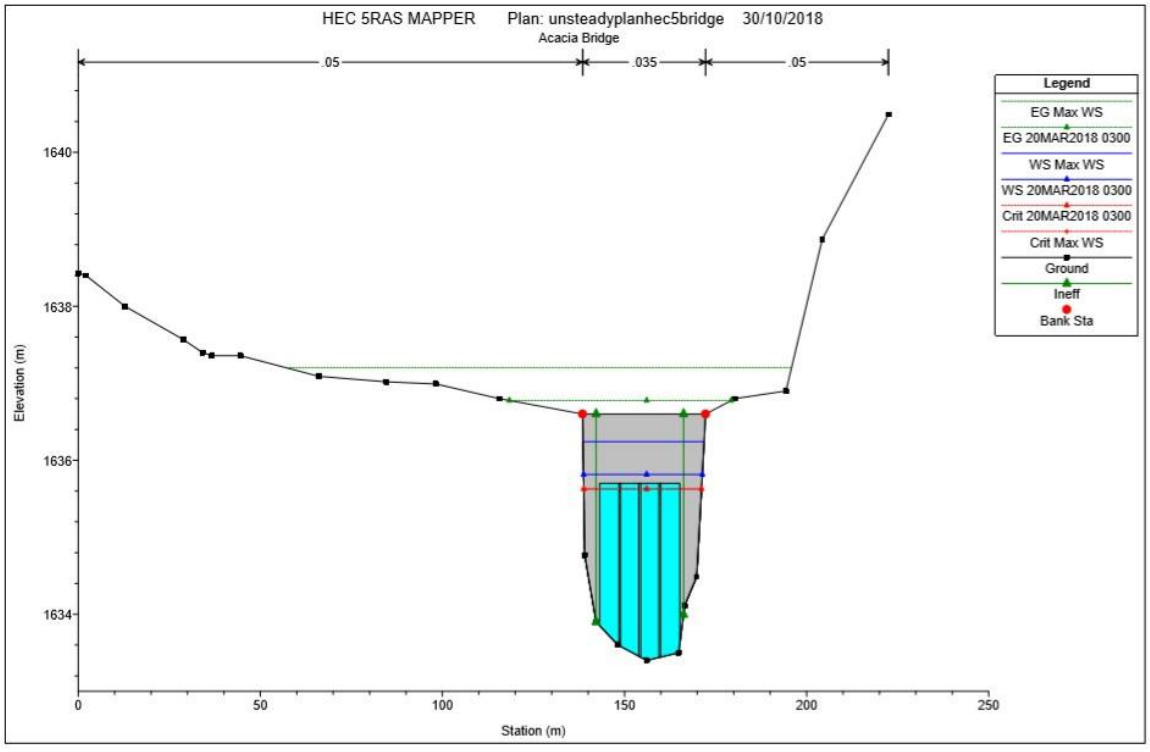

Figure 4-9: Bridge upstream cross section profile, 2018 flood peak levels (USF).

Table 4-13 lists the critical values observed inside-upstream and downstream of the bridge in the unsteady flow simulation. The important values are that of the flow area (44.39 m^2 upstream to 39.71 m^2 downstream), Froude number (upstream 0.80 and downstream 0.94) and the friction loss (upstream 0.18 m and 0.12 m downstream). These values can vindicate the aforementioned statement that the results of the steady and unsteady flow simulations do not differ by much. Both instances support the contraction and expansion phenomena described in section 3.3 and depicted in Figure 3-10.

Table 4-13: Summary of bridge output unsteady flow, 2018.

Plan: bridgeunsteady Acacia Reach 1 RS: 68 Profile: 16JAN2004 0320

E.G. US. (m)	1636.72	Element	Inside BR US	Inside BR DS
W.S. US. (m)	1636.39	E.G. Elev (m)	1636.57	1636.33
Q Total (m3/s)	172.79	W.S. Elev (m)	1635.79	1635.37
Q Bridge (m3/s)	172.79	Crit W.S. (m)	1635.48	1635.37
Q Weir (m3/s)		Max Chl Dpth (m)	2.39	2.17
Weir Sta Lft (m)		Vel Total (m/s)	3.89	4.35
Weir Sta Rgt (m)		Flow Area (m2)	44.39	39.71
Weir Submerg		Froude # Chl	0.80	0.94
Weir Max Depth (m)		Specif Force (m3)	120.96	115.41
Min El Weir Flow (m)	1636.60	Hydr Depth (m)		1.94
Min El Prs (m)	1635.70	W.P. Total (m)	58.22	35.84
Delta EG (m)	0.69	Conv. Total (m3/s)	1058.6	1214.8
Delta WS (m)	1.27	Top Width (m)		20.50
BR Open Area (m2)	44.39	Frctn Loss (m)	0.18	0.12
BR Open Vel (m/s)	4.35	C & E Loss (m)	0.06	0.04
BR Sluice Coef		Shear Total (N/m2)	199.25	219.84
BR Sel Method	Energy only	Power Total (N/m s)	775.61	956.68

Plan: bridgeunsteady Acacia Reach 1 RS: 68 Profile: 16JAN2004 0330

E.G. US. (m)	1636.28	Element	Inside BR US	Inside BR DS
W.S. US. (m)	1635.97	E.G. Elev (m)	1636.19	1635.99
Q Total (m3/s)	143.09	W.S. Elev (m)	1635.61	1635.14
Q Bridge (m3/s)	143.09	Crit W.S. (m)	1635.25	1635.14
Q Weir (m3/s)		Max Chl Dpth (m)	2.21	1.94
Weir Sta Lft (m)		Vel Total (m/s)	3.36	4.08
Weir Sta Rgt (m)		Flow Area (m2)	42.60	35.09
Weir Submerg		Froude # Chl	0.72	0.93
Weir Max Depth (m)		Specif Force (m3)	93.43	89.81
Min El Weir Flow (m)	1636.60	Hydr Depth (m)	2.08	1.71
Min El Prs (m)	1635.70	W.P. Total (m)	37.02	34.04
Delta EG (m)	0.52	Conv. Total (m3/s)	1336.9	1023.2
Delta WS (m)	0.88	Top Width (m)	20.50	20.50
BR Open Area (m2)	44.39	Frctn Loss (m)	0.12	0.11
BR Open Vel (m/s)	4.08	C & E Loss (m)	0.08	0.09
BR Sluice Coef		Shear Total (N/m2)	129.31	197.73
BR Sel Method	Energy only	Power Total (N/m s)	434.31	806.30

4.7 Flood-line

Figures 4-10 to 4-13 depict the 1:50-year flood inundation maps produced over the Acacia residential area for both steady and unsteady flows. Figure 4-14 is a clipped and stitched image of the 2014 COW flood line study, the image was initially split into two separate sections as obtained from COW offices. Roughly a third of the Acacia residential area (2.5 ha in 1989 flow and 2.8 ha in 2018 flow) can be seen to be inundated, this is in sharp contrast to the inundation coverage produced from the COW flood line study as indicated in Figure 4-14. Half of Umbrella Thorn Street as well as Three Thorn Street are the only areas flooded in the COW flood line study with combined area coverage of less than 1 ha for both their 1-50-year and 1-100-year flood lines. There are a few reasons for this discrepancy and will be elaborated on further in the discussions chapter.

Figures 4-12 and 4-13 were produced by exporting the inundation layers from RAS Mapper to ArcMap. These figures indicate the depth of inundation over the Acacia residential in the scenario of the calculated 1:50-year flood peak discharges. The difference in highest depth for the 2018 and 1989 flood peaks amounts to 0.75 m with both max depths occurring at the start of the river section. Most of the residential inundation depth is averaged around 0.5 m to a maximum of 0.9 m; any depth higher than this occurs in the river channel. The largest inundation coverage is observed at the downstream area with a total coverage of 1.8 ha and 2.1 ha for the 1989 and 2018 flows.

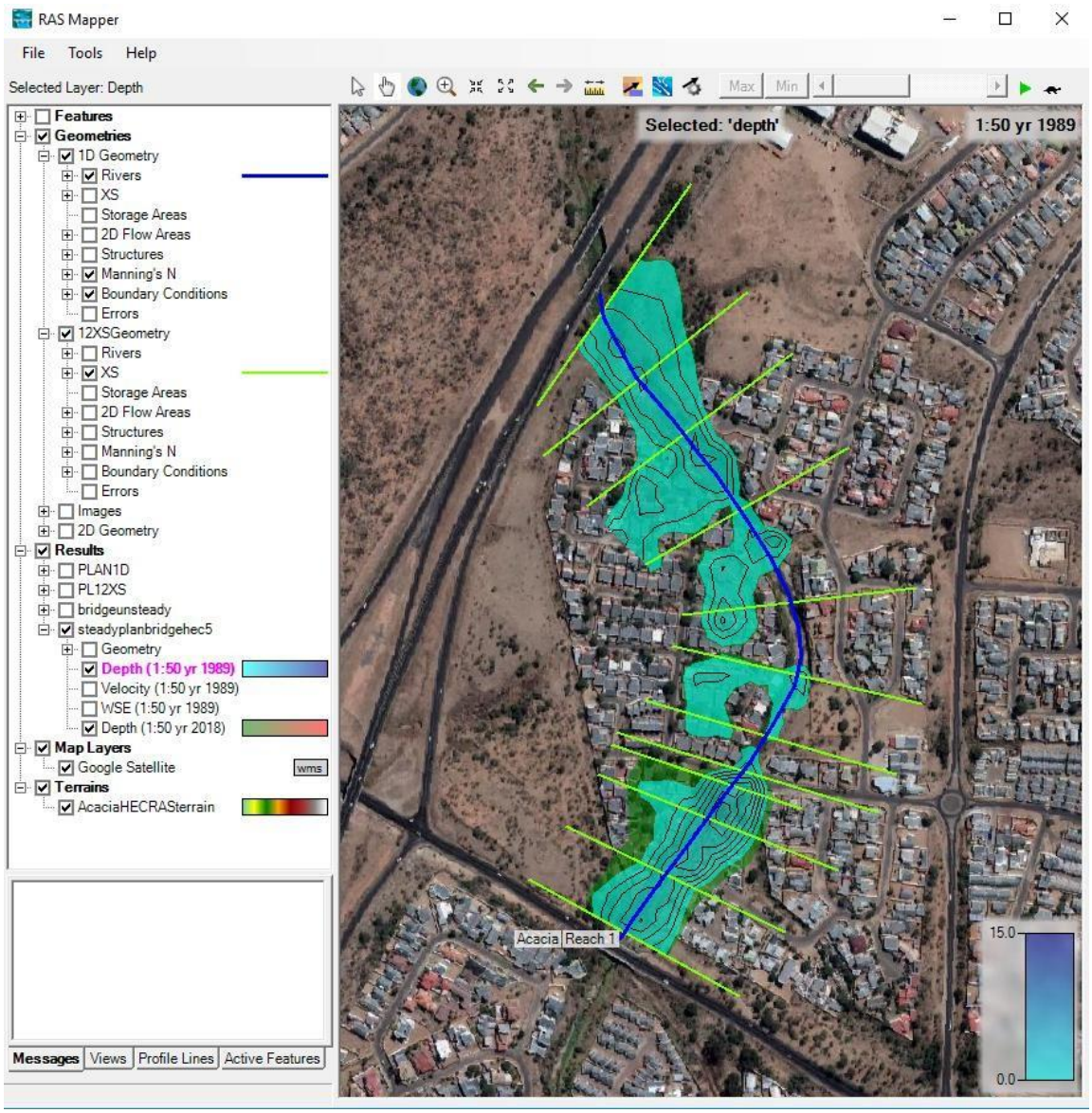

Figure 4-10: Steady flood plain mapping, 1989 and 2018 flood peaks.

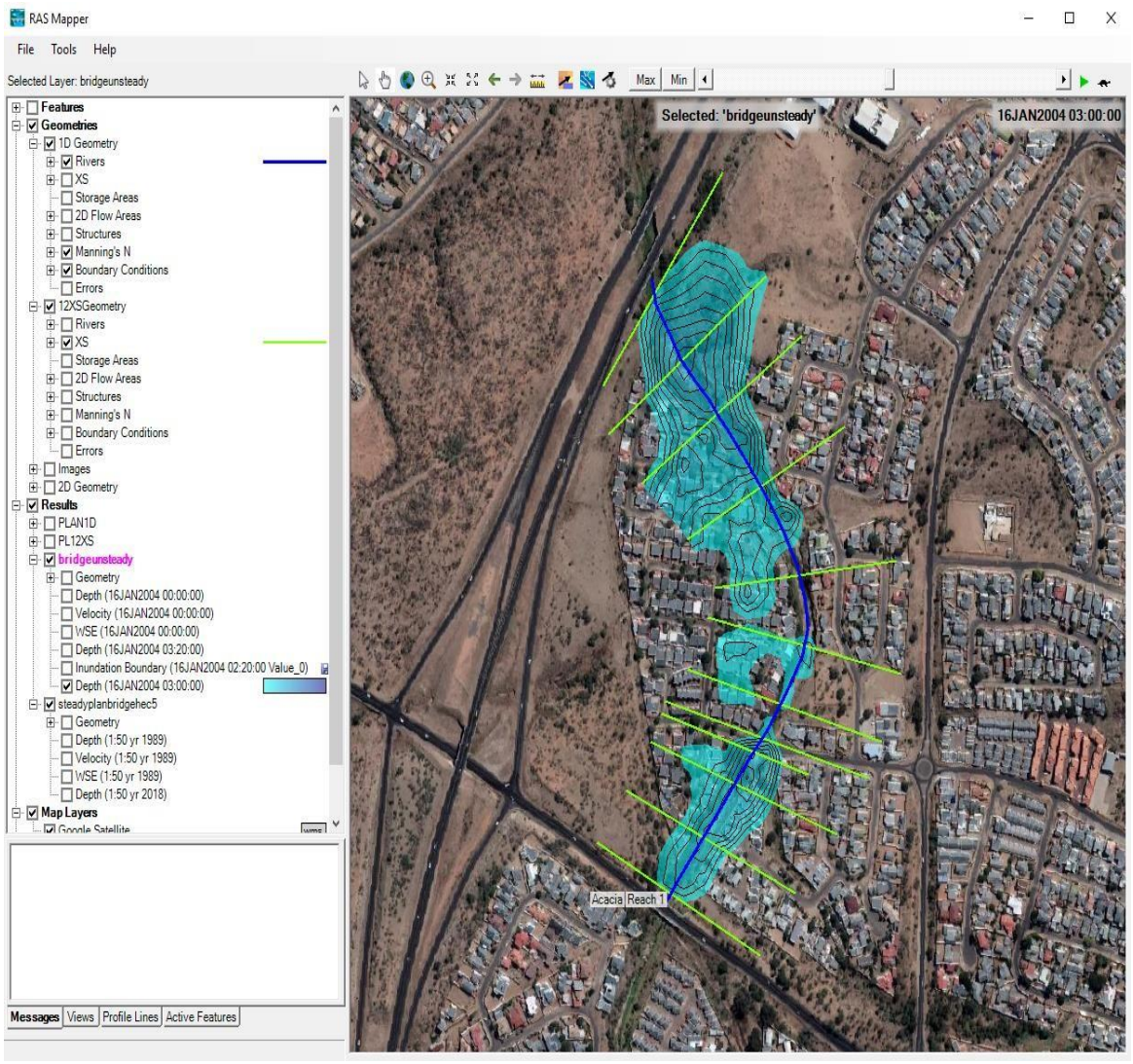

Figure 4-11: Unsteady flood plain mapping, 2018 flood peaks.

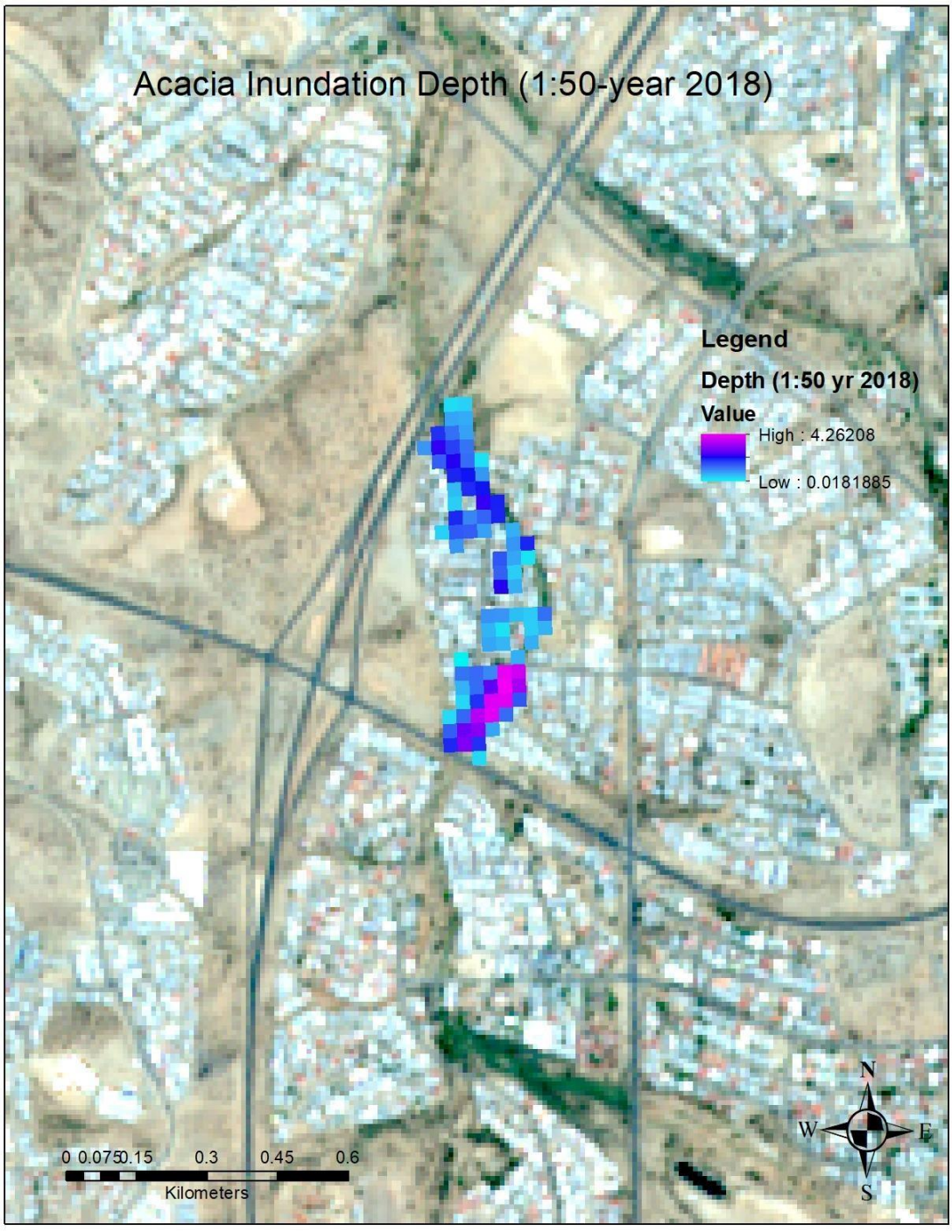

Figure 4-12: Acacia inundation map (1:50-year 2018 flood depth).

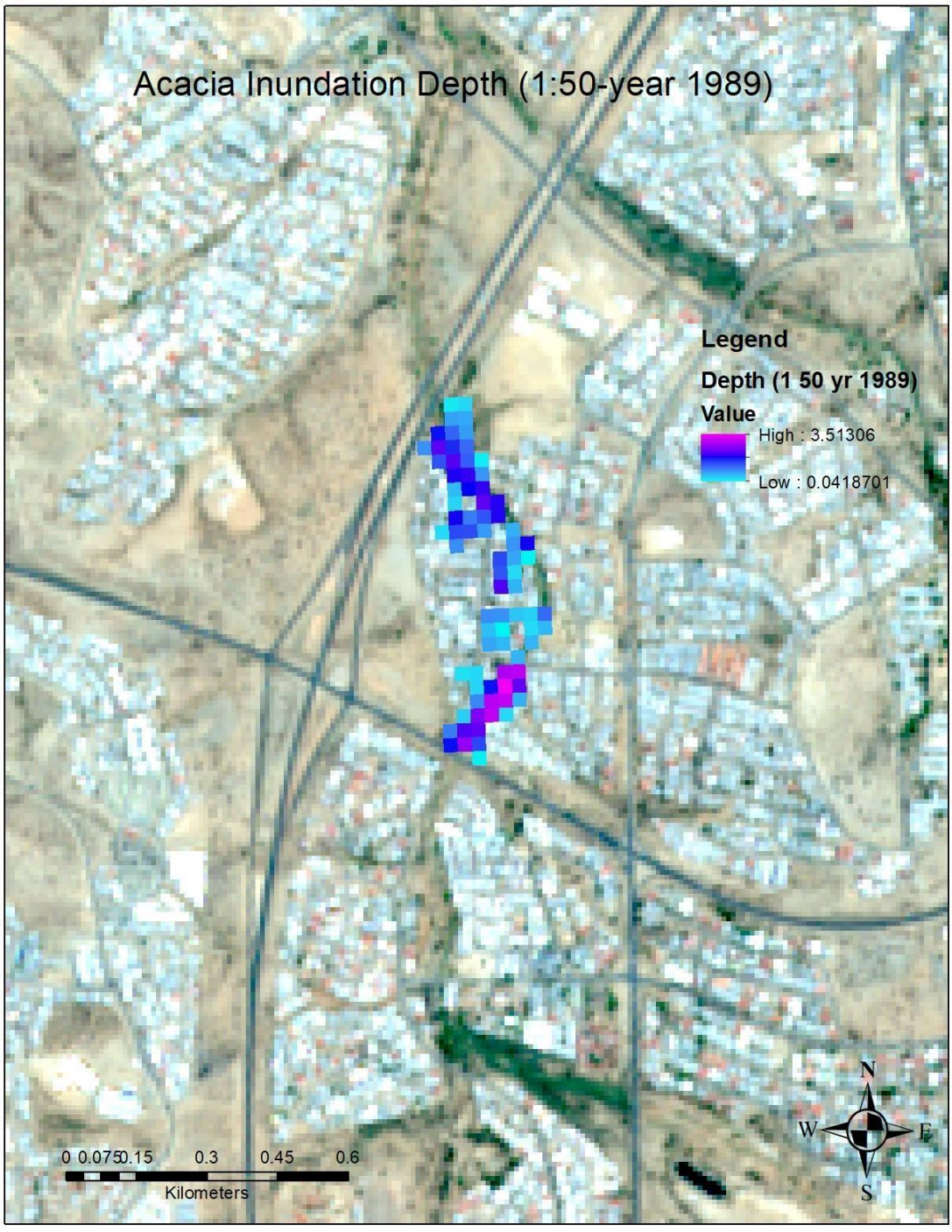

Figure 4-13: Acacia inundation map (1:50-year 1989 flood depth).

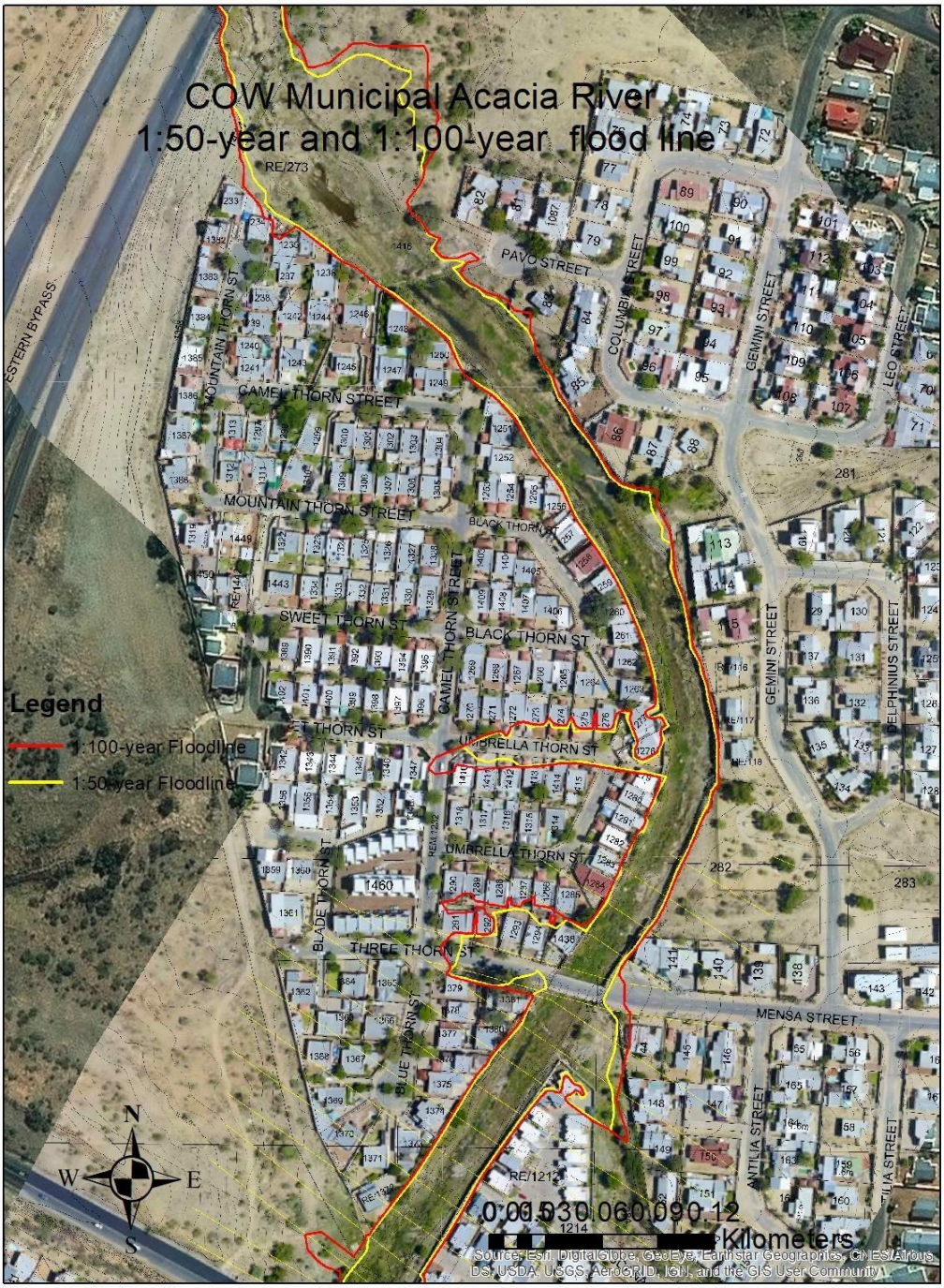

Figure 4-14: COW Municipal 1:50 year flood line mapping Acacia residential.

5. DISCUSSION

5.1 Image classification and area determination

The land-cover images classified from the 1989 and 2018 satellite images yielded satisfactory results, but commercial data with higher resolutions would have yielded results with better accuracy. There are new techniques being applied in the fields of remote sensing that are less expensive when compared to commercial satellite images. This is done by making use of areal photographic drones that can be remotely controlled with a flying radius of 2 km and an altitude of 200 m. In future field surveys this can be explored to gain images with higher resolutions, albeit archival data would still need to be accessed.

The Sentinel 2A images yielded more accurate classified images as was pointed out in section 4.2. This was observed with the unsupervised classified images as well. It was therefore necessary to adjust the rural and urban calculations to split some of the areas as it can be seen that the "*Baresoil"* area has a 50% percentage falling in the urban space of Windhoek while the other area is outside of town falling in the rural side. The land cover areas were then grouped into either rural or urban area so as to get the two main separators which are required for the use of Eq. 22.

From the accuracy assessment carried out on the classified images the confusion matrices in Tables 4-3 to 4-6 had a difference of nearly 0.2 of Kappa coefficient between the classified Landsat and Sentinel (Figures 4-1 and 4-2) images which reiterates the classification prowess higher resolution imagery has over the latter. Literature cited

indicated that Kappa values above 0.8 indicate good classified images, indicating that the classified images produced from this study can be categorized as average.

5.2 Alternative Rational Method

The run-off coefficient values used with the ARM equation gave the flood peak results which were fairly similar, with a mean value of 216 m^3/s for 2018 and 190 m^3/s for 1989. The average percentage increase from 1989 to 2018 in flood peak values of 13.8% is under the estimated increase that the SANRAL drainage manual advocates, as being in the range of 20 to 50%, but 13.8% is still a significant increase. The results obtained from the utilization of the ARM for determining the 1:50-year flood peak values for the Acacia sub-catchment have yielded satisfactory results as indicated by the comparison of results obtained in Tables 4-7, 4-8 and 4-9. The ARM provided relatively accurate results with comparatively fewer input requirements when compared to the other flood peak calculation methods. For the purpose of this mini thesis the use of only one flood peak calculation method was deemed sufficient as a comparative study or a study that made use of more than one method would have constricted the time, results and budget of the research.

5.3 Statistical Analysis (t-Test)

In this analysis, the critical value is the P-value. If the P-value obtained is larger than the alpha value (which in this case was chosen to be 5%), the Null Hypothesis is accepted. The opposite can be said if the P-value is smaller than the alpha value. It can be deduced from Table 4-8 that the P-values obtained for both tests (assuming equal and unequal

variances) are significantly smaller than the 5% alpha value; indicating that the Null Hypothesis is not accepted albeit the Alternative Hypothesis is accepted; which states that there is a significant difference in the flood peaks produced from the two varying urban developed catchments (1989 vs. 2018).

5.4 HEC-RAS Model

From Figure 4-3 it can be deduced that the 1:50-year 1989 flood peak does not overflow over the Acacia River, albeit the 2018 flood peak does which raises an increased risk factor associated with the bridges use during the rainy season. It should also be noted that these flood peaks are in relation to the effect of urbanization on the years specified and associated with the MAP of 360 mm/a and not in relation to the precipitation recorded in a particular year. HEC-RAS software provided a simple and easy to use interface for modelling the Acacia River section, the simulations yielded satisfactory results with the only limiting factor being the resolution of the DEM used. A higher resolution DEM would have been able to take into consideration the retaining walls that line the river watercourse. This would have assisted the simulation in containing the flow of the river in the river section with increased levels of accuracy. The inundation depth of 0.5 to almost a meter is still an alarming depth as this level would certainly coincide with the recorded depth observed during the 2004 flooding which in some cases where reported as being about 1.5 m in depth. The economic and social consequences of such flood risk needs to be assessed in greater detail as simple transfer of blame to acts of God be deemed as lacklustre as informed and analysed decision making can avert such events.

5.5 Flood-line

Both steady and unsteady state flow simulations yielded similar inundation maps. The 30x30 m resolution DEM downloaded from the ALOS website provides a land surface that is not as accurate as commercial products that have resolutions ranging from 1x1 m to 12x12 m which is a significant adjustment from the 30 m DEM. Hydraulic simulations usually require a resolution of less than 5 m, for commercial applications like municipal, consulting or governmental work. Nonetheless the ALOS DEM was utilized and rendered satisfactory results. Figures 4-10 to 4-13 can be compared with the COW 2014 flood line study (Figure 4-14); with the redlines indicating the 1:100-year flood line and the yellow lines indicating the 1:50-year flood lines. The inundation images produced in HEC-RAS and depicted in RAS-Mapper have a much larger coverage for both steady and unsteady flow simulations, more so for both simulation years (1989 and 2018) both have a larger inundation coverage as compared to the COW flood line study results. This can be attributed to the DEM used in the analysis as the COW used a higher resolution DEM; this is not to say that the inundation maps produced from this research be disregarded, it can just be classified as having a very conservative 1:50-year flood line; and the simple fact that Acacia residential area has been flooded 50 m inwards at a level of 0.5 m indicates that a more accurate reassessment of the 1:50-year and 1:100-year flood line be recommended.

6. CONCLUSIONS AND RECOMMENDATIONS

6.1 Conclusions

The calculated flood peak values for 2018 in comparison with that of 1989, has increased by 13% over the span of 3 decades. The flood inundation map produced from the 2014 COW flood line study is significantly smaller in size when compared with this study's findings for the same area. Obtaining written report/report-findings on the COW 2014 flood line study would have assisted the findings in this research by giving it an extra set of data to compare findings in terms of calibration, as only the flood maps were obtained from the COW offices. Data gathering from various institutions for research purposes is never a simple endeavour and more interconnection and data sharing between universities, research centres, consulting services and governmental institutions would assist the effectiveness of academic research tremendously.

The statistical analysis using the t-Test to compare the flood peak values of the 1989 and 2018 urban developed Acacia sub-catchment areas indicated that the proposed alternative hypothesis be accepted which vindicates the primary objective set forth by the research. This implies that there is a significant increase in flood peak values attributed from increased urban development. The specific objectives were all achieved; these include the use of ArcGIS and the national drainage manuals to calculate the flood peaks for the two comparative years (*Table 4-7*); the production of the river course model by utilising the surveyed cross section data (Appendices A and C); production of the river flow simulation in HEC-RAS to show the peak flow levels (*Figure 4-4*) as well as the establishment of the 1-50 year flood line and inundation maps (*Figure 4-10 to 4-13*).

These phenomena should be incorporated in the city planning design to cater for increased urban development and its potential effects on future developments undertaken in close proximity to the main rivers flowing through the City of Windhoek. With the looming effects of climate change fuelling the sporadic nature of our climate patterns it should be taken very seriously.

6.2 Recommendations

Legal mitigation of floods has proven to be a complicated issue as was witnessed during the 2004 flooding of Acacia residential. Not only concerned with the financial implications of floods but the fact that a family living in a house that has been flooded already makes it very difficult to sleep peacefully during the rainy seasons as history has shown to repeat itself countless times. This research finding recommends that more assessment be done on the hydraulic flow of the Acacia residential river section. The flood inundation maps ascertained from this research finding are in contrast with the flood lines provided from the COW 2014 study. Various reasons were elaborated on in the previous chapter with regards to these discrepancies. It should also be noted that the COW has introduced mitigation measures in the form of retaining walls constructed all along the river section so as to assist in channelling the river flow. Furthermore, it is recommended that further city development projects taking place close to the Windhoek's main rivers should take into consideration the accumulative effects of urban development on a catchments flood peak value. Further research can be conducted on this topic as a doctoral thesis where commercial software coupled with higher resolution DEM's and spatial data (satellite imagery) be utilized to give more accurate results.

7. REFERENCES

[1] W. J. R. Alexander, "Analytical Methods for Water Resource Development and Management", Handbook for Practitioners and Decision Makers, Univirsity of Pretoria, Pretoria, South Africa. 2012.

[2] Drainage Manual, 5th ed. SANRAL. The South African National Roads Agency Limited. Pretoria, South Africa, 2006.

[3] Drainage Manual, 1st ed. RA, the Roads Authority of Namibia. Windhoek, Namibia, 2014.

[4] J. Mendelsohn, A. Jarvis, C. Roberts, and T. Robertson, Atlas of Namibia. Cape Town: David Philip Publishers, 2002.

[5] L. Dentlinger, "Windhoek flooding not exceptional," *The Namibian*, January 10, 2006. [Online], Available: https://www.namibian.com.na/index.php?id=22732&page=archive-read [Accessed: October. 6, 2018].

[6] C. P. Konrad, "Effects of Urban Development on Floods," U.S. Geological Survey, November 2003, [Online], Available: https://pubs.usgs.gov/fs/fs07603/ [Accessed October. 6, 2018].

[7] A. Shanableh,"Effects of Land Cover Change on Urban Floods and Rainwater Harvesting: A case Study in Sharjah, UAE", *MDPI Water Journal*, vol. 10, May., pp. 631, 2018.

[8] E. Pedzisai,"Rainfall Runoff Modelling for Flash Floods in Cuong Thinh Catchment", M. S. thesis, The International Institute for Geo-information Science and Earth Observation, Enschede, Netherlands. 2010.

[9] U.S Department of Homeland Security, FEMA. (2018, 07, 25) *Types of Floods and Floodplains*. Retrieved from URL:https://training.fema.gov/hiedu/docs/fmc/chapter%202%20-%20types%20of%20floods%20and%20floodplains.pdf

[10] J. Lindeberg,"Locating Potential Flood Areas in an Urban Environment using Remote Sensing and GIS, Case Study Lund, Sweden", M. S. thesis, Lund University, Lund, Sweden. 2014.

[11] M. Wicht and K. Osinska-Shotak, "Identifying Urban Areas Prone to Flash Floods Using GIS - Preliminary Results," *Hydrology and Earth System Sciences – Discussions.* 2016.

[12] Z.P Kovacz, "Regional Maximum Flood peaks in South Africa," *Technical Report TR137,* Department of Water Affairs, Pretoria, South Africa, 1988.

[13] D. R. Maidment., "Handbook of Hydrology". *McGraw-Hill,* New York, USA. 1993

[14] K. J Beven, "Rainfall-Runoff Modelling," *The Primer. John Wiley and Sons,* Chichester, UK, pp. 360, 2000.

[15] Q. Weng, "Modelling Urban Growth Effects on Surface Runoff with the Integration of Remote Sensing and GIS," *Environmental Management*, vol. 28,

no. 6, pp. 737-748, 2001.

[16] C. Van Der Merwe, private communication, Mar. 2018.

[17] Rainfall Distribution in Namibia: Data Analysis and Mapping of Spatial, Temporal, and Southern Oscillation Index Aspects. MAWRD. Ministry of Agriculture, Water and Rural Development. Windhoek, Namibia, 1999.

[18] Weather Bureau. (1992). Climate tables of South Africa (WB42). SAWB, Pretoria.

[19] P.T Adamson, "Southern African Storm Rainfall," *Technical Report TR102*, Department of Water Affairs, Pretoria, South Africa, 1981.

[20] W.J.R Alexander, "The Standard Design Flood," *Journal of the South African Institution of Civil Engineers,* vol. 44, no. 1, pp. 26-31.

[21] D. McPherson., Comparison of annual flood peaks calculated by various methods. In: Maaren, H. (Ed.), South African National Hydrology Symposium. Technical Report TR119, *Department of Environment Affairs*, Pretoria, RSA., pp. 236-250, 1998.

[22] W. G. Strupczewski, V. P. Singh, and W. Feluch., "Non-stationary approach to at-site flood frequency modelling maximum likelihood estimation", *Journal of Hydrology*, vol. 248, pp.123-142, 2001.

[23] P. A. Longley, M. F. Goodchild, D. J. Maguire and D. W. Rhind, "New

Developments in Geographical Information Systems: Principles, Techniques, Management and Applications," *Preface to the Abridged Edition,* University of Edinburgh, Edinburgh, United Kingdom, 2001.

[24] ESRI - ArcGIS Desktop, "Image Classification Using the ArcGIS Spatial Analyst Extension," *ArcMap 10.6,* Chichester, 2018. [Online]. Available: http://desktop.arcgis.com/en/arcmap/latest/extensions/spatial-analyst/image-classification/image-classification-using-spatial-analyst.htm [Accessed: Oct. 6, 2018]

[25] ESRI - ArcGIS Desktop, "Resample," *ArcMap 10.3,* Chichester, 2018. [Online]. Available: http://desktop.arcgis.com/en/arcmap/10.3/tools/data-management-toolbox/resample.htm [Accessed: Oct. 30, 2018]

[26] A. Bogoliubova and P. Tymkow, "Accuracy Assessment of Automatic Image Processing For Land Cover Classification of St. Petersburg Protected Area," *Wroclaw University of Environmental and Life Sciences*. Wroclaw, Poland, 2014.

[27] J. R. Jenson, "Introductory Digital Image Processing: A Remote Sensing Perspective". 3rd Edition, Prentice Hall, Upper Saddle River, 2005.

[28] P. S Bharatkar and R. Patel, "Approach to Accuracy Assessment for RS Image Classification Techniques," *Internatioanl Journal of Scientific and Engineering Research,* vol. 4, no. 12, Dec, 2013.

[29] e-Pg Pathshala - Remote Sensing and GIS, "Classification Accuracy Assessment

and Errors," *National Mission on Education through ICT*, Gujarat, India, 2018. [Online]. Available: http://epgp.inflibnet.ac.in/epgpdata/uploads/epgp_content/S000448GO/P000602/M022472/ET/1505379618E-TextClassificationAccuracyAssessmentandErrors.pdf [Accessed: Nov. 10, 2018]

[30] N. Walker, "Flood line for Erf RE/6022 - Windhoek Flood line Analysis," Aurecon South Africa (Pty Ltd). Cape Town, South Africa, Tech. Report. 106853, 7 Apr. 2017.

[31] J. D. Fenton, "Calculating Resistance to Flow in Open Channels," *Altern. Hydraul. Pap. No. 2*, 2010.

[32] CivilGEO - Engineering Software, "HEC-RAS Contraction & Expansion Losses," *Knowledge Base*, Middleton, USA. 2018. [Online]. Available: https://www.civilgeo.com/knowledge-base/hec-ras-contraction-expansion-losses/

[33] X. Liu, "Open Channel hydraulics: From then to now and beyond," Handbook of Environmental Engineering., vol. 15, pp. 127–156, 2014.

[34] R. Congalton and K. Green, "Assessing the Accuracy of Remotely Sensed Data: Principles and Practices," Second Edition, CRC Press, Boca Raton, 2008.

[35] Food and Agriculture Organization of the United Nations, "Map Accuracy Assessment and Area Estimation - A Practical Guide," National Forest Monitoring Assessment Working Paper - No.46/E. Rome, Italy, 2016.

APPENDICES

Appendix A: Cross section profile plots for 12 stations

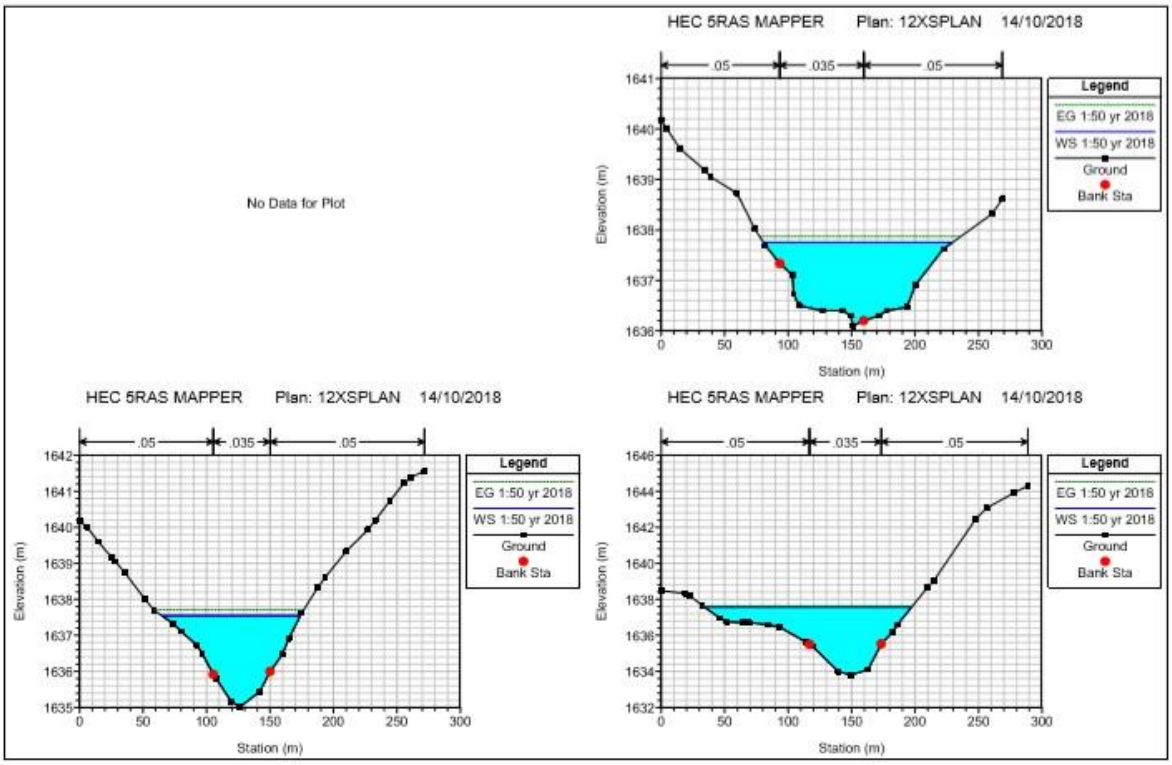

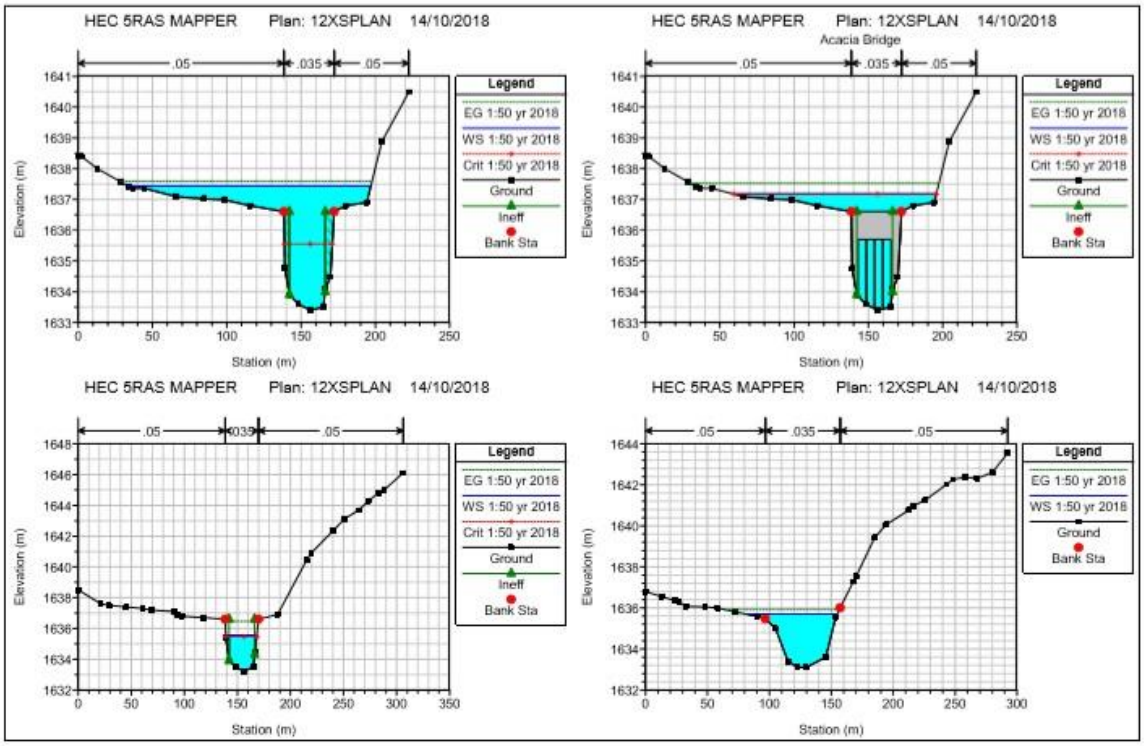
HEC 5RAS MAPPER Plan: 12XSPLAN 14/10/2018
Acacia Bridge
.05
.035
.05
Legend
EG 1:50 yr 2018
WS 1:50 yr 2018
Crit 1:50 yr 2018
Ground
Ineff
Bank Sta
Elevation (m)
Station (m)

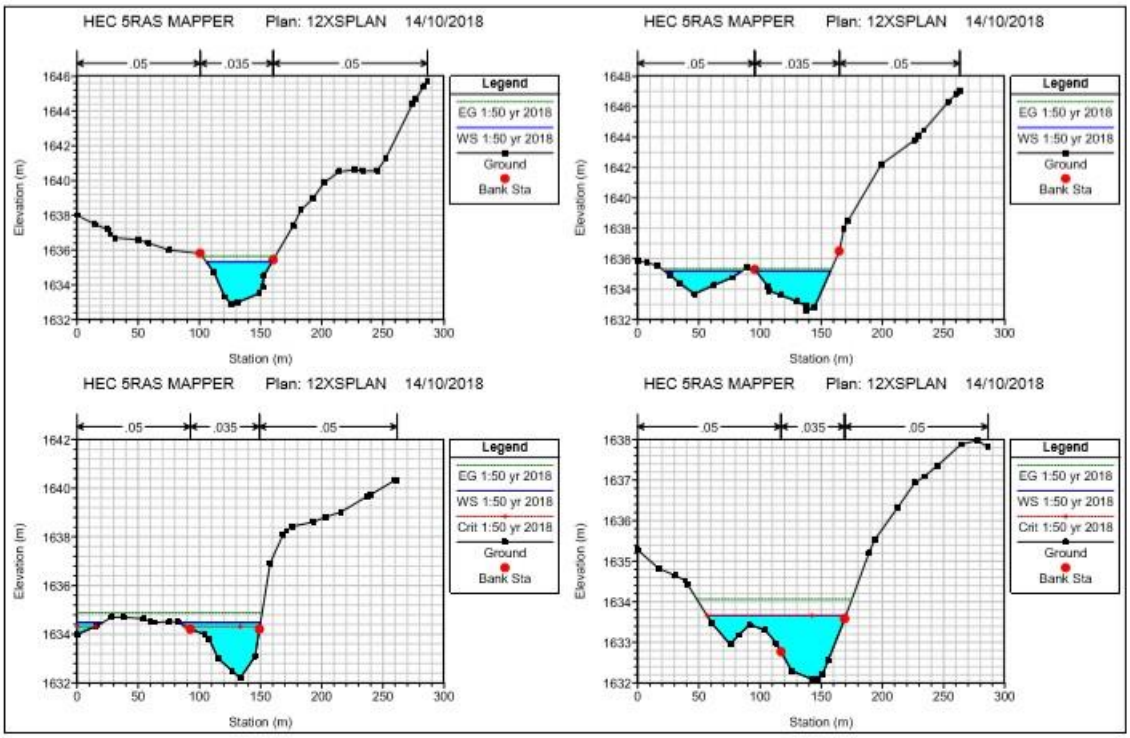
HEC 5RAS MAPPER Plan: 12XSPLAN 14/10/2018
.05
.035
.05
Legend
EG 1:50 yr 2018
WS 1:50 yr 2018
Crit 1:50 yr 2018
Ground
Ineff
Bank Sta
Elevation (m)
Station (m)

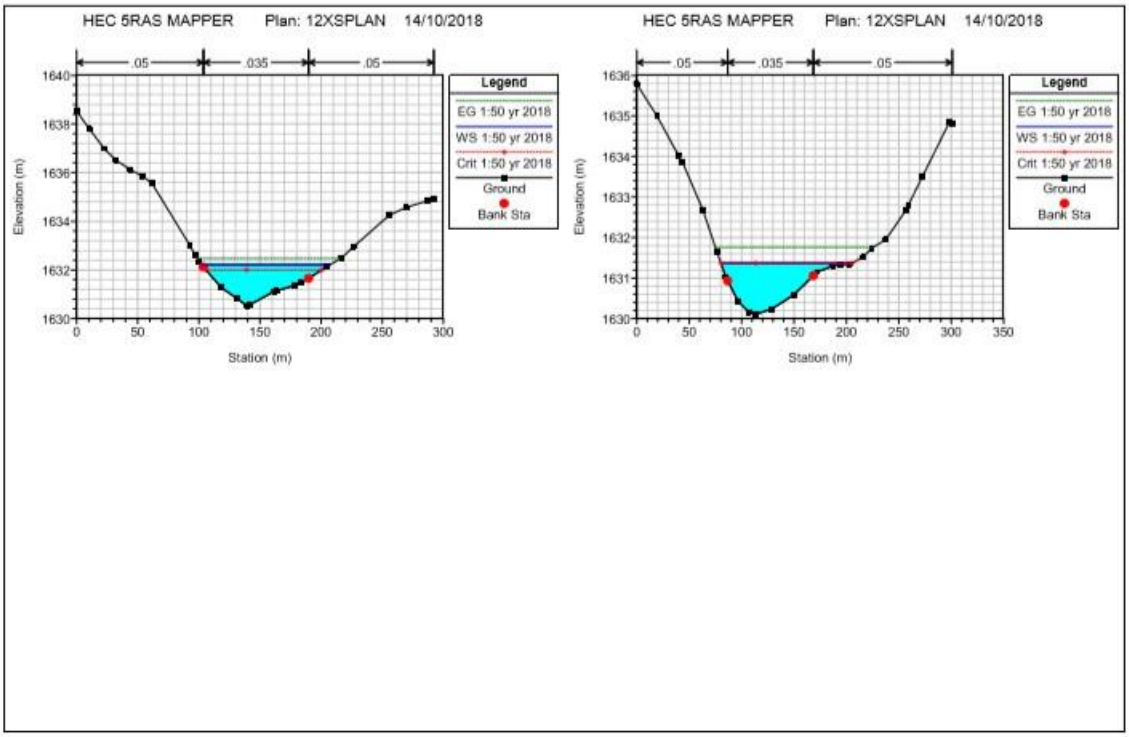
HEC 5RAS MAPPER Plan: 12XSPLAN 14/10/2018
.05
.035
.05
Elevation (m)
Station (m)
Legend
EG 1:50 yr 2018
WS 1:50 yr 2018
Crit 1:50 yr 2018
Ground
Bank Sta
HEC 5RAS MAPPER Plan: 12XSPLAN 14/10/2018
.05
.035
.05
Elevation (m)
Station (m)
Legend
EG 1:50 yr 2018
WS 1:50 yr 2018
Crit 1:50 yr 2018
Ground
Bank Sta

Appendix B: Cross section flow output summary

Plan: PL12XS Acacia Reach 1 RS: 80 Profile: 1:50 yr 2018

E.G. Elev (m)	1637.70	Element	Left OB	Channel	Right OB
Vel Head (m)	0.16	Wt. n-Val.	0.050	0.035	0.050
W.S. Elev (m)	1637.54	Reach Len. (m)	69.20	77.20	85.60
Crit W.S. (m)		Flow Area (m2)	26.31	96.08	19.78
E.G. Slope (m/m)	0.001577	Area (m2)	26.31	96.08	19.78
Q Total (m3/s)	211.00	Flow (m3/s)	15.70	181.43	13.87
Top Width (m)	108.82	Top Width (m)	40.33	44.70	23.79
Vel Total (m/s)	1.48	Avg. Vel. (m/s)	0.60	1.89	0.70
Max Chl Dpth (m)	2.53	Hydr. Depth (m)	0.65	2.15	0.83
Conv. Total (m3/s)	5314.0	Conv. (m3/s)	395.4	4569.2	349.3
Length Wtd. (m)	76.83	Wetted Per. (m)	40.37	44.75	23.84
Min Ch El (m)	1635.01	Shear (N/m2)	10.07	33.20	12.83
Alpha	1.42	Stream Power (N/m s)	6.01	62.69	9.00
Frctn Loss (m)	0.04	Cum Volume (1000 m3)	12.40	66.69	3.84
C & E Loss (m)	0.04	Cum SA (1000 m2)	21.30	43.13	7.87

Plan: PL12XS Acacia Reach 1 RS: 75 Profile: 1:50 yr 2018

E.G. Elev (m)	1637.63	Element	Left OB	Channel	Right OB
Vel Head (m)	0.04	Wt. n-Val.	0.050	0.035	0.050
W.S. Elev (m)	1637.59	Reach Len. (m)	38.70	45.20	51.00
Crit W.S. (m)		Flow Area (m2)	83.95	178.50	25.62
E.G. Slope (m/m)	0.000257	Area (m2)	83.95	178.50	25.62
Q Total (m3/s)	211.00	Flow (m3/s)	27.09	175.38	8.53
Top Width (m)	163.72	Top Width (m)	83.02	56.60	24.10
Vel Total (m/s)	0.73	Avg. Vel. (m/s)	0.32	0.98	0.33
Max Chl Dpth (m)	3.80	Hydr. Depth (m)	1.01	3.15	1.06
Conv. Total (m3/s)	13171.3	Conv. (m3/s)	1690.9	10947.9	532.4
Length Wtd. (m)	44.74	Wetted Per. (m)	83.06	56.75	24.19
Min Ch El (m)	1633.79	Shear (N/m2)	2.54	7.92	2.67
Alpha	1.53	Stream Power (N/m s)	0.82	7.78	0.89
Frctn Loss (m)	0.02	Cum Volume (1000 m3)	8.58	56.09	1.89
C & E Loss (m)	0.01	Cum SA (1000 m2)	17.03	39.22	5.82

Plan: PL12XS Acacia Reach 1 RS: 70 Profile: 1:50 yr 2018

E.G. Elev (m)	1637.60	Element	Left OB	Channel	Right OB
Vel Head (m)	0.16	Wt. n-Val.	0.050	0.035	0.050
W.S. Elev (m)	1637.44	Reach Len. (m)	5.00	5.00	5.00
Crit W.S. (m)	1635.55	Flow Area (m2)	44.78	101.37	14.89
E.G. Slope (m/m)	0.001062	Area (m2)	44.78	119.94	14.89
Q Total (m3/s)	211.00	Flow (m3/s)	16.47	187.62	6.91
Top Width (m)	164.14	Top Width (m)	105.61	33.80	24.73
Vel Total (m/s)	1.31	Avg. Vel. (m/s)	0.37	1.85	0.46
Max Chl Dpth (m)	4.04	Hydr. Depth (m)	0.42	3.00	0.60
Conv. Total (m3/s)	6475.4	Conv. (m3/s)	505.5	5757.9	211.9
Length Wtd. (m)	5.00	Wetted Per. (m)	105.61	36.16	24.79
Min Ch El (m)	1633.40	Shear (N/m2)	4.42	29.19	6.25
Alpha	1.78	Stream Power (N/m s)	1.62	54.02	2.90
Frctn Loss (m)	0.01	Cum Volume (1000 m3)	6.09	49.35	0.66
C & E Loss (m)	0.06	Cum SA (1000 m2)	13.38	37.17	4.58

Plan: PL12XS Acacia Reach 1 RS: 68 BR U Profile: 1:50 yr 2018

E.G. Elev (m)	1637.52	Element	Left OB	Channel	Right OB
Vel Head (m)	0.35	Wt. n-Val.	0.050	0.035	0.050
W.S. Elev (m)	1637.18	Reach Len. (m)	7.50	7.50	7.50
Crit W.S. (m)	1637.18	Flow Area (m2)	20.70	63.89	8.58
E.G. Slope (m/m)	0.015832	Area (m2)	20.70	63.90	8.58
Q Total (m3/s)	211.00	Flow (m3/s)	21.27	178.68	11.05
Top Width (m)	136.54	Top Width (m)	79.34	33.80	23.40
Vel Total (m/s)	2.26	Avg. Vel. (m/s)	1.03	2.80	1.29
Max Chl Dpth (m)	3.78	Hydr. Depth (m)	0.26	1.89	0.37
Conv. Total (m3/s)	1676.9	Conv. (m3/s)	169.1	1420.0	87.8
Length Wtd. (m)	7.50	Wetted Per. (m)	79.34	93.11	23.43
Min Ch El (m)	1633.40	Shear (N/m2)	40.51	106.53	56.84
Alpha	1.33	Stream Power (N/m s)	41.63	297.95	73.20
Frctn Loss (m)	0.14	Cum Volume (1000 m3)	5.93	48.89	0.80
C & E Loss (m)	0.23	Cum SA (1000 m2)	12.92	37.00	4.46

Plan: PL12XS Acacia Reach 1 RS: 68 BR D Profile: 1:50 yr 2018

E.G. Elev (m)	1636.75	Element	Left OB	Channel	Right OB
Vel Head (m)	1.10	Wt. n-Val.		0.035	
W.S. Elev (m)	1635.65	Reach Len. (m)	8.00	8.00	8.00
Crit W.S. (m)	1635.65	Flow Area (m2)		45.42	
E.G. Slope (m/m)	0.020892	Area (m2)		45.42	
Q Total (m3/s)	211.00	Flow (m3/s)		211.00	
Top Width (m)	20.50	Top Width (m)		20.50	
Vel Total (m/s)	4.65	Avg. Vel. (m/s)		4.65	
Max Chl Dpth (m)	2.45	Hydr. Depth (m)		2.22	
Conv. Total (m3/s)	1459.8	Conv. (m3/s)		1459.8	
Length Wtd. (m)	8.00	Wetted Per. (m)		38.07	
Min Ch El (m)	1633.20	Shear (N/m2)		244.44	
Alpha	1.00	Stream Power (N/m s)		1135.56	
Frctn Loss (m)	0.10	Cum Volume (1000 m3)	5.85	48.48	0.77
C & E Loss (m)	0.09	Cum SA (1000 m2)	12.62	36.80	4.37

Plan: PL12XS Acacia Reach 1 RS: 65 Profile: 1:50 yr 2018

E.G. Elev (m)	1636.46	Element	Left OB	Channel	Right OB
Vel Head (m)	0.91	Wt. n-Val.		0.035	
W.S. Elev (m)	1635.55	Reach Len. (m)	45.50	46.80	46.90
Crit W.S. (m)	1635.46	Flow Area (m2)		49.86	
E.G. Slope (m/m)	0.008396	Area (m2)		53.84	
Q Total (m3/s)	211.00	Flow (m3/s)		211.00	
Top Width (m)	29.11	Top Width (m)		29.11	
Vel Total (m/s)	4.23	Avg. Vel. (m/s)		4.23	
Max Chl Dpth (m)	2.34	Hydr. Depth (m)		2.08	
Conv. Total (m3/s)	2302.8	Conv. (m3/s)		2302.8	
Length Wtd. (m)	46.80	Wetted Per. (m)		24.26	
Min Ch El (m)	1633.20	Shear (N/m2)		169.22	
Alpha	1.00	Stream Power (N/m s)		716.15	
Frctn Loss (m)	0.19	Cum Volume (1000 m3)	5.85	48.08	0.77
C & E Loss (m)	0.35	Cum SA (1000 m2)	12.62	36.60	4.37

Plan: PL12XS Acacia Reach 1 RS: 60 Profile: 1:50 yr 2018

E.G. Elev (m)	1635.92	Element	Left OB	Channel	Right OB
Vel Head (m)	0.22	Wt. n-Val.	0.050	0.035	
W.S. Elev (m)	1635.70	Reach Len. (m)	70.70	76.60	84.00
Crit W.S. (m)		Flow Area (m2)	1.53	102.10	
E.G. Slope (m/m)	0.002472	Area (m2)	1.53	102.10	
Q Total (m3/s)	211.00	Flow (m3/s)	0.33	210.67	
Top Width (m)	73.35	Top Width (m)	15.44	57.91	
Vel Total (m/s)	2.04	Avg. Vel. (m/s)	0.21	2.06	
Max Chl Dpth (m)	2.60	Hydr. Depth (m)	0.10	1.76	
Conv. Total (m3/s)	4243.9	Conv. (m3/s)	6.5	4237.4	
Length Wtd. (m)	76.60	Wetted Per. (m)	15.44	58.32	
Min Ch El (m)	1633.10	Shear (N/m2)	2.40	42.44	
Alpha	1.03	Stream Power (N/m s)	0.51	87.57	
Frctn Loss (m)	0.25	Cum Volume (1000 m3)	5.81	44.43	0.77
C & E Loss (m)	0.01	Cum SA (1000 m2)	12.27	34.56	4.37

Plan: PL12XS Acacia Reach 1 RS: 55 Profile: 1:50 yr 2018

E.G. Elev (m)	1635.65	Element	Left OB	Channel	Right OB
Vel Head (m)	0.34	Wt. n-Val.		0.035	
W.S. Elev (m)	1635.31	Reach Len. (m)	44.60	83.20	125.30
Crit W.S. (m)		Flow Area (m2)		82.07	
E.G. Slope (m/m)	0.004635	Area (m2)		82.07	
Q Total (m3/s)	211.00	Flow (m3/s)		211.00	
Top Width (m)	53.58	Top Width (m)		53.58	
Vel Total (m/s)	2.57	Avg. Vel. (m/s)		2.57	
Max Chl Dpth (m)	2.41	Hydr. Depth (m)		1.53	
Conv. Total (m3/s)	3099.2	Conv. (m3/s)		3099.2	
Length Wtd. (m)	79.38	Wetted Per. (m)		54.01	
Min Ch El (m)	1632.90	Shear (N/m2)		69.07	
Alpha	1.00	Stream Power (N/m s)		177.57	
Frctn Loss (m)	0.26	Cum Volume (1000 m3)	5.76	37.38	0.77
C & E Loss (m)	0.06	Cum SA (1000 m2)	11.72	30.29	4.37

Plan: PL12XS Acacia Reach 1 RS: 50 Profile: 1:50 yr 2018

E.G. Elev (m)	1635.33	Element	Left OB	Channel	Right OB
Vel Head (m)	0.15	Wt. n-Val.	0.050	0.035	
W.S. Elev (m)	1635.19	Reach Len. (m)	75.50	117.40	167.60
Crit W.S. (m)		Flow Area (m2)	49.69	91.64	
E.G. Slope (m/m)	0.002438	Area (m2)	49.69	91.64	
Q Total (m3/s)	211.00	Flow (m3/s)	41.79	169.21	
Top Width (m)	123.94	Top Width (m)	63.15	60.79	
Vel Total (m/s)	1.49	Avg. Vel. (m/s)	0.84	1.85	
Max Chl Dpth (m)	2.59	Hydr. Depth (m)	0.79	1.51	
Conv. Total (m3/s)	4273.1	Conv. (m3/s)	846.2	3426.8	
Length Wtd. (m)	112.85	Wetted Per. (m)	63.23	61.21	
Min Ch El (m)	1632.60	Shear (N/m2)	18.79	35.80	
Alpha	1.29	Stream Power (N/m s)	15.80	66.10	
Frctn Loss (m)	0.43	Cum Volume (1000 m3)	4.65	30.15	0.77
C & E Loss (m)	0.03	Cum SA (1000 m2)	10.31	25.54	4.37

Plan: PL12XS Acacia Reach 1 RS: 45 Profile: 1:50 yr 2018

E.G. Elev (m)	1634.88	Element	Left OB	Channel	Right OB
Vel Head (m)	0.40	Wt. n-Val.	0.050	0.035	0.050
W.S. Elev (m)	1634.48	Reach Len. (m)	93.70	104.60	119.30
Crit W.S. (m)	1634.32	Flow Area (m2)	6.66	73.44	0.13
E.G. Slope (m/m)	0.006879	Area (m2)	6.66	73.44	0.13
Q Total (m3/s)	211.00	Flow (m3/s)	4.12	206.82	0.05
Top Width (m)	87.43	Top Width (m)	30.12	56.40	0.90
Vel Total (m/s)	2.63	Avg. Vel. (m/s)	0.62	2.82	0.43
Max Chl Dpth (m)	2.28	Hydr. Depth (m)	0.22	1.30	0.14
Conv. Total (m3/s)	2544.1	Conv. (m3/s)	49.7	2493.7	0.7
Length Wtd. (m)	103.79	Wetted Per. (m)	30.62	56.68	0.94
Min Ch El (m)	1632.20	Shear (N/m2)	14.67	87.40	8.99
Alpha	1.12	Stream Power (N/m s)	9.08	246.16	3.89
Frctn Loss (m)	0.81	Cum Volume (1000 m3)	2.52	20.46	0.76
C & E Loss (m)	0.00	Cum SA (1000 m2)	6.79	18.66	4.29

Plan: PL12XS Acacia Reach 1 RS: 40 Profile: 1:50 yr 2018

E.G. Elev (m)	1634.07	Element	Left OB	Channel	Right OB
Vel Head (m)	0.41	Wt. n-Val.	0.050	0.035	0.050
W.S. Elev (m)	1633.66	Reach Len. (m)	75.60	79.70	85.30
Crit W.S. (m)	1633.66	Flow Area (m2)	25.62	61.16	0.04
E.G. Slope (m/m)	0.008934	Area (m2)	25.62	61.16	0.04
Q Total (m3/s)	211.00	Flow (m3/s)	27.35	183.64	0.01
Top Width (m)	113.36	Top Width (m)	60.31	52.10	0.94
Vel Total (m/s)	2.43	Avg. Vel. (m/s)	1.07	3.00	0.22
Max Chl Dpth (m)	1.57	Hydr. Depth (m)	0.42	1.17	0.04
Conv. Total (m3/s)	2232.4	Conv. (m3/s)	289.4	1942.9	0.1
Length Wtd. (m)	79.48	Wetted Per. (m)	60.34	52.17	0.95
Min Ch El (m)	1632.09	Shear (N/m2)	37.19	102.71	3.39
Alpha	1.35	Stream Power (N/m s)	39.71	308.40	0.73
Frctn Loss (m)	0.57	Cum Volume (1000 m3)	1.01	13.42	0.75
C & E Loss (m)	0.04	Cum SA (1000 m2)	2.55	12.98	4.18

Plan: PL12XS Acacia Reach 1 RS: 35 Profile: 1:50 yr 2018

E.G. Elev (m)	1632.48	Element	Left OB	Channel	Right OB
Vel Head (m)	0.26	Wt. n-Val.	0.050	0.035	0.050
W.S. Elev (m)	1632.22	Reach Len. (m)	52.10	89.20	125.90
Crit W.S. (m)	1632.00	Flow Area (m2)	0.08	90.79	4.91
E.G. Slope (m/m)	0.005962	Area (m2)	0.08	90.79	4.91
Q Total (m3/s)	211.00	Flow (m3/s)	0.02	207.74	3.25
Top Width (m)	105.11	Top Width (m)	1.65	85.90	17.56
Vel Total (m/s)	2.20	Avg. Vel. (m/s)	0.20	2.29	0.66
Max Chl Dpth (m)	1.69	Hydr. Depth (m)	0.05	1.06	0.28
Conv. Total (m3/s)	2732.7	Conv. (m3/s)	0.2	2690.5	42.0
Length Wtd. (m)	89.52	Wetted Per. (m)	1.65	85.95	17.57
Min Ch El (m)	1630.53	Shear (N/m2)	2.80	61.75	16.35
Alpha	1.06	Stream Power (N/m s)	0.57	141.30	10.80
Frctn Loss (m)	0.71	Cum Volume (1000 m3)	0.04	7.37	0.54
C & E Loss (m)	0.01	Cum SA (1000 m2)	0.21	7.48	3.39

Plan: PL12XS Acacia Reach 1 RS: 30 Profile: 1:50 yr 2018

E.G. Elev (m)	1631.76	Element	Left OB	Channel	Right OB
Vel Head (m)	0.39	Wt. n-Val.	0.050	0.035	0.050
W.S. Elev (m)	1631.37	Reach Len. (m)			
Crit W.S. (m)	1631.37	Flow Area (m2)	1.50	74.38	3.65
E.G. Slope (m/m)	0.010916	Area (m2)	1.50	74.38	3.65
Q Total (m3/s)	211.00	Flow (m3/s)	1.18	208.17	1.65
Top Width (m)	124.76	Top Width (m)	6.52	81.90	36.35
Vel Total (m/s)	2.65	Avg. Vel. (m/s)	0.78	2.80	0.45
Max Chl Dpth (m)	1.26	Hydr. Depth (m)	0.23	0.91	0.10
Conv. Total (m3/s)	2019.5	Conv. (m3/s)	11.3	1992.4	15.8
Length Wtd. (m)		Wetted Per. (m)	6.53	81.93	36.35
Min Ch El (m)	1630.11	Shear (N/m2)	24.63	97.19	10.75
Alpha	1.10	Stream Power (N/m s)	19.32	272.01	4.85
Frctn Loss (m)		Cum Volume (1000 m3)			
C & E Loss (m)		Cum SA (1000 m2)			

Appendix C: 1989 and 2018 XYZ River Reach Plot

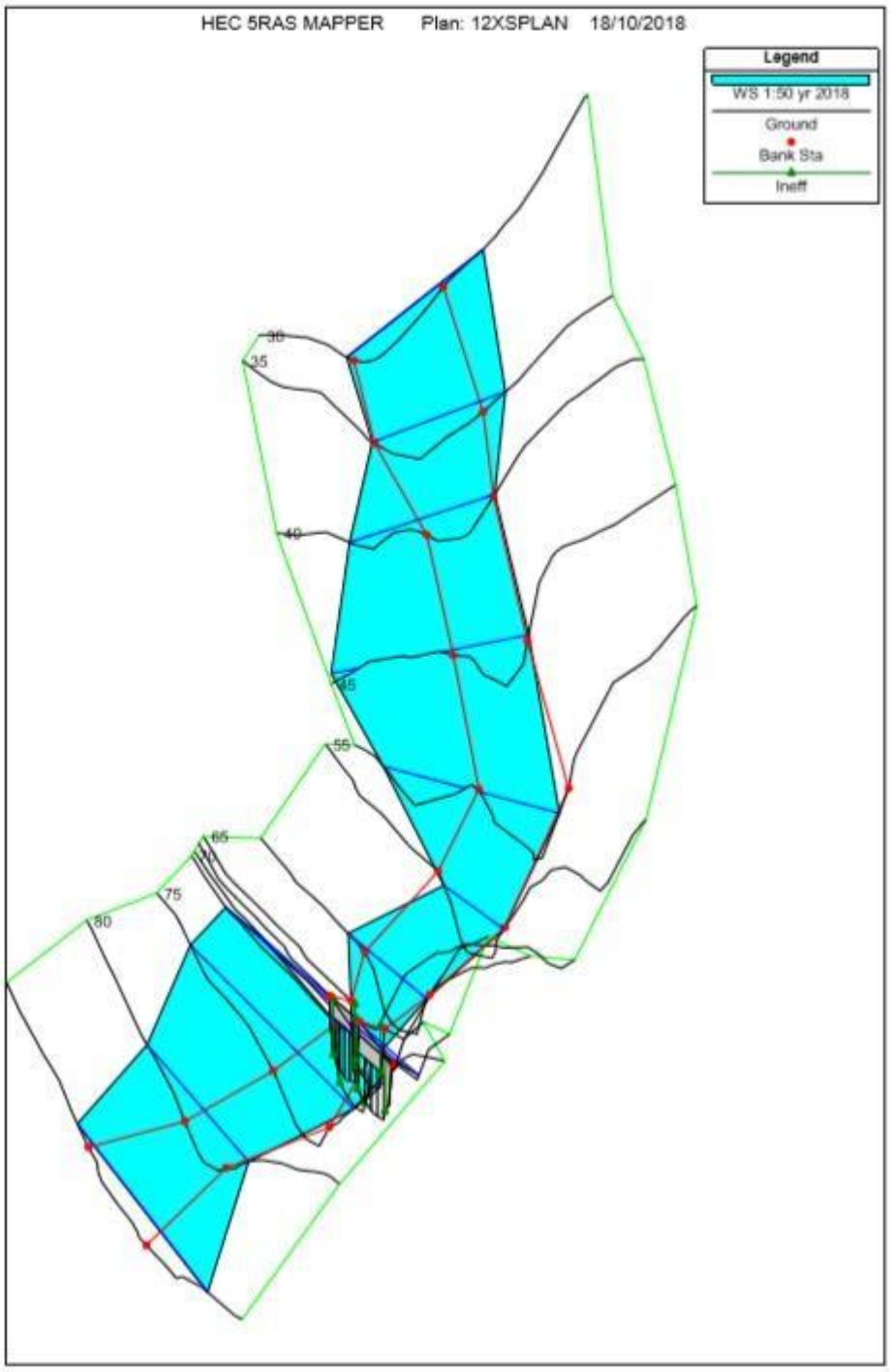

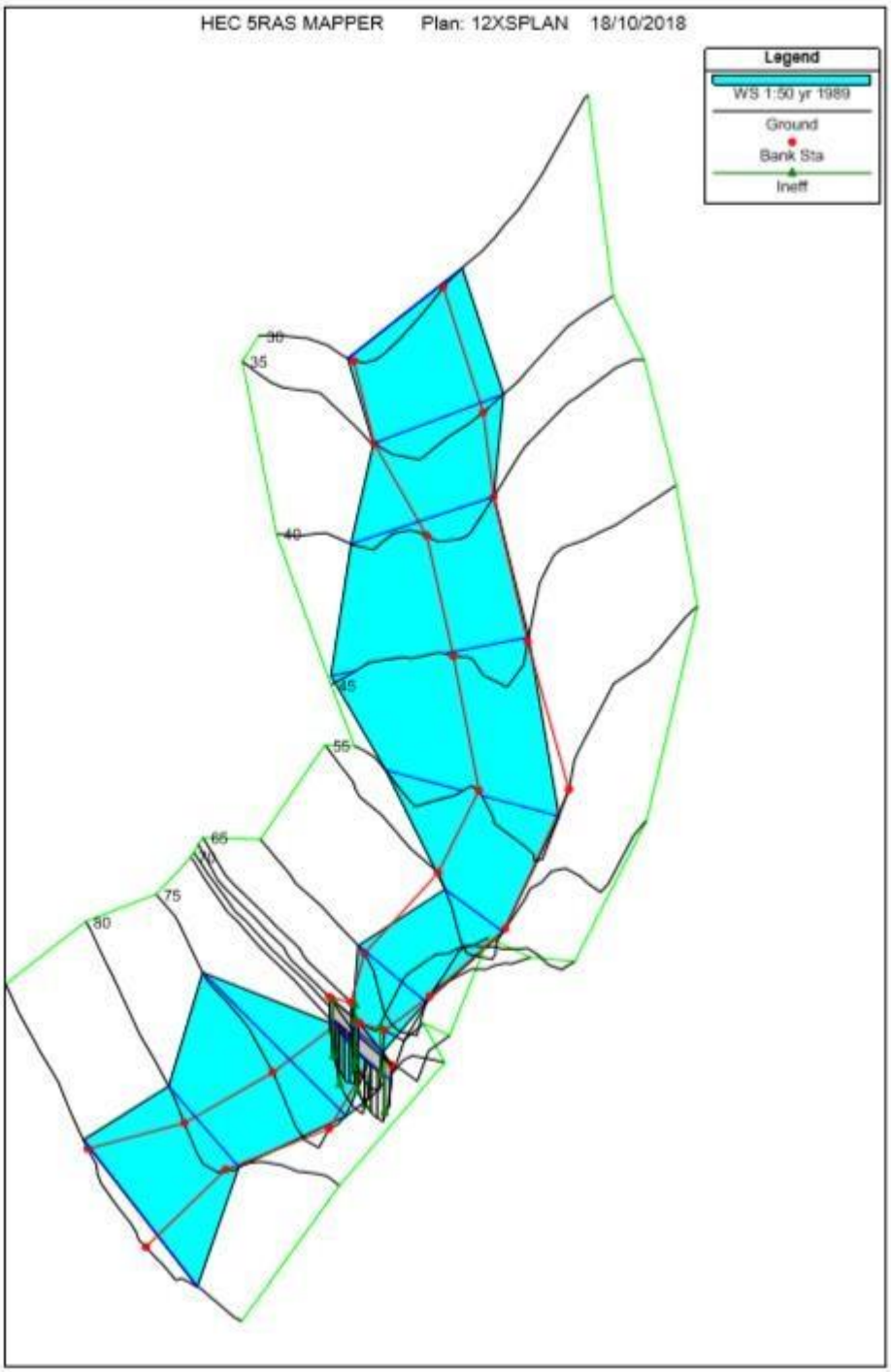
HEC 5RAS MAPPER Plan: 12XSPLAN 18/10/2018
Legend
WS 1:50 yr 1989
Ground
Bank Sta
Ineff
30
35
40
45
55
65
75
80

Appendix D: Surveying Images